Utrecht University

High resolution paleoclimatic study linking the Aegean Sea to Eastern Mediterranean Holocene records

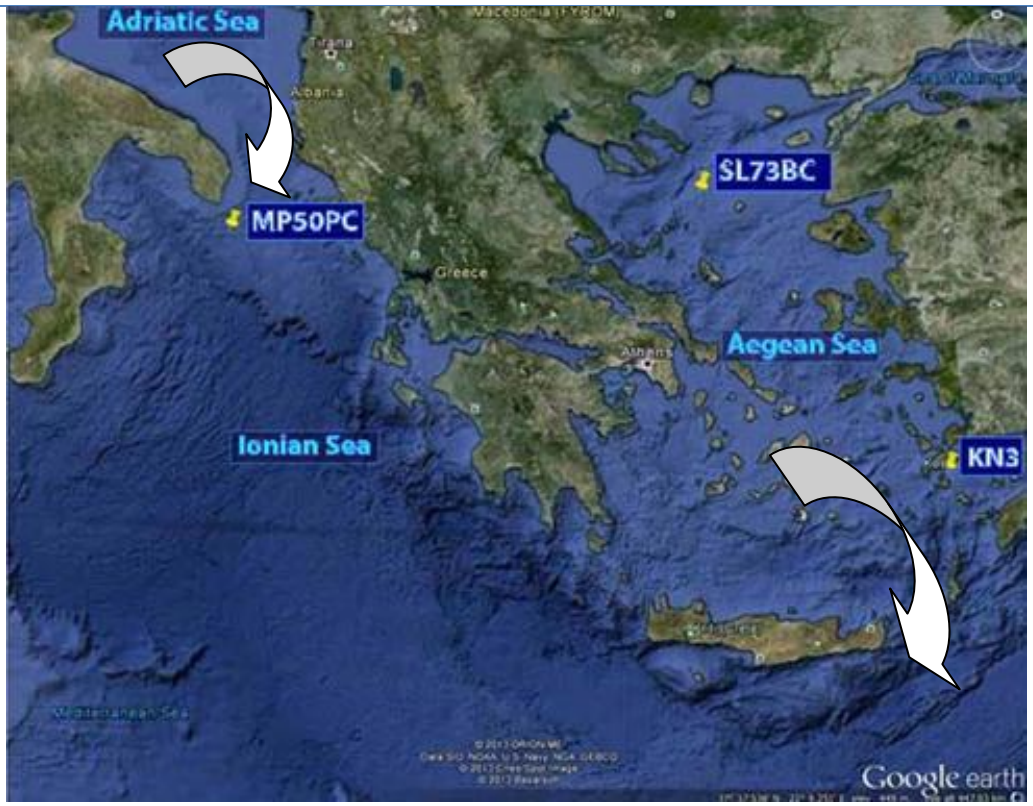

Amalia Filippidi* 3719669
Supervisor: Prof. Gert J. de Lange
60 ECTS

*Institute of Earth Sciences-Geosciences Utrecht University - a.filippidi@students.uu.nl

Figure in the cover page: Map of the Central Mediterranean Sea; the location of the cores used in this study are indicated in the areas of known Mediterranean deep water formation (white arrows), i.e. Aegean Sea and Adriatic Sea.

Table of Contents

ABSTRACT

Sapropel formation is thought to be strongly related to deep-water formation. The latter is known to take place in Adriatic and Aegean basins. In this study, therefore, high resolution geochemical analyses have been performed on three marine cores, collected from the South Aegean (KN3 core), North Aegean (SL73BC) and South Adriatic (MP50PC) Seas. Data on Total Organic Carbon (%) (TOC), stable carbon and nitrogen isotopes, elemental concentrations and foraminifera stable isotopes analyses have been used to unravel in detail the conditions established during the Holocene and the processes responsible for S1 deposition and preservation in particular. The sedimentary records show that during sapropel S1 deposition bottom-water conditions have been oxic to suboxic for the South Aegean Sea and suboxic to anoxic for the South Adriatic and North Aegean Sea, and that sedimentary conditions ranged from suboxic to anoxic. Significant variations within this interval are promiment, implying that at such shallow depths sapropel formation did not take place under stable conditions. Differences that are observed between the studied sites highlight the influence of water depths and sedimentation rates. In both studied basins distinct episodes of re-ventilation of the water column have been observed, whilst there is no evidence that fully anoxic conditions have maintained during S1 formation. In addition to the 8.2 cal ka BP event, an abrupt event at ca 7.5 cal ka BP has been identified in the south Adriatic core, which is thought to be related to a temporary cessation of sapropel formation. Similarly, in the southern Aegean core, the S1 formation appears to have been interrupted at 7.5 cal ka BP, whereas sediments older than ~ 8 ka cal BP have not been recovered in this core. Fluctuations in C_{org} content coupled with Ba/Al ratios and changes in Mn/Al, V/Al and Mo/Al profiles underline variability in water-column properties. The observed repetitive episodes of re-ventilation of the water column and their obvious implications for sapropel formation not only suggest a relation to paleoclimate control but also to sensitive water-column hydrological conditions. The latter and in particular the bottom-water formation mechanisms determine deep-water oxygenation thus preservation and shallow-water nutrients supply thus primary productivity. Although several studies, mostly based on micropaleontological and terrestrial archives, mention additional episodes of climate cooling during sapropel S1 formation, so far these have not all been linked to marine records. In the South Adriatic core an additional event is observed at 9.3 cal ka BP that suggests the temporal cessation of sapropel S1 formation. As this interval is also containing enhanced levels of tephra, these observations may at least in part be attributed to a tephra layer originating from Somma – Vesuvius.

INTRODUCTION

1.1 The Mediterranean Sea

The Mediterranean Sea is an intercontinental, semi-enclosed sea whose only connection with the open Atlantic Ocean is through the narrow and shallow strait of Gibraltar. It is divided into a Western and Eastern part by the straits of Sicily.

The Mediterranean Sea is an important source of salty and relatively warm water to the intermediate water of the North Atlantic Ocean and by contributing to the formation of the North Atlantic Deep Water (NADW) (Schlitzer et al., 1991) plays a significant role to the global thermohaline circulation system (Bigg, 1994). Therefore, climate related changes to the hydrological setting of the Mediterranean Sea in present and past, especially during the Plio-Pleistocene, have drawn the attention of many researchers from various disciplines.

A two-way circulation pattern acts in the Mediterranean Sea. Firstly, surface water from Atlantic Ocean enters the Mediterranean Sea and flows eastwards where its salinity and temperature increases. Secondly, high salinity water sinks in the Levantine basin forming the Levantine Intermediate Water (LIW) which moves westwards. After mixing with Eastern Mediterranean Deep Water (EDMW) formed in Adriatic and Aegean Seas, and subsequently with Western Mediterranean Deep Water (WMDP), it transforms to the Mediterranean Intermediate Water (MIW). The latter flows out into the Atlantic Ocean through the straits of Gibraltar (Béthoux, 1989; Pinardi & Masetti, 2000; Rohling et al., 2008). This

anti-estuarine circulation pattern is responsible for the constant removal of nutrients from the Mediterranean Sea to the Atlantic Ocean and hence creates an extremely oligotrophic system (Bethoux, 1989).

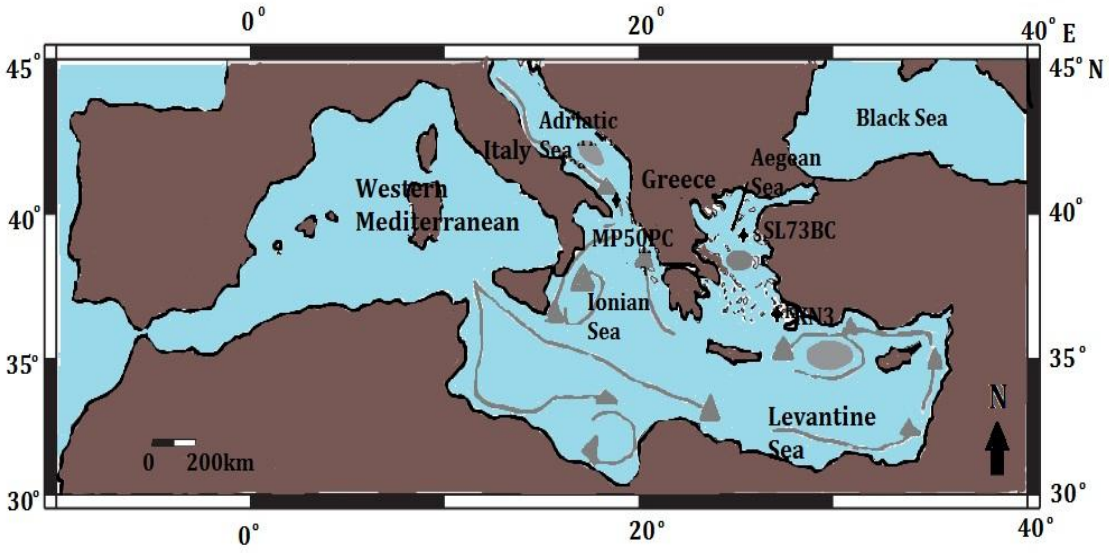

figure 1. Map of the Mediterranean Sea. Grey arrows show the surface water circulation patterns. Black crosses indicate the location where from the cores for this study have been collected (map modified from Marino 2008).

1.2 Sapropels

Sapropels have been described as organic-rich, dark-colored layers already in 1952 by Kullenberg, whilst in 1960 Olausson referred to these layers as sapropelic layers (Kidd et al., 1978). Kidd et al. (1978) studied sapropel layers present in cores recovered from the Eastern Mediterranean and gave the first definition of these layers: "a discrete layer more than 1cm thickness, set in open marine pelagic sediments and containing greater that 2% organic carbon by weight". A less restrictive definition for sapropels was given by Hilgen (1991): brownish, often laminated deposits that are interbedded with more marly sediments.

In the latter definition, sapropels have been deposited cyclically throughout the Mediterranean basin during the last 13.5 million years (Hilgen et al, 2003). Despite the different mechanisms and processes described to be responsible for the formation of sapropels, elevated productivity as well as conditions favorable for the preservation of organic matter are widely accepted to prevail during sapropel deposition (e.g. Calvert 1983; De Lange & Ten Haven, 1983; Emeis et al, 1996). Significant modifications in circulation and environmental conditions appear to have occurred repeatedly, in close association to global climate changes (e.g. Cita et al., 1977; Bethoux & Pierre, 1999; Rohling & Palike, 2005). The paleoceanographic records suggest that during the time of sapropels deposition, increased river input and precipitation led to sluggish circulation and cessation of bottom-water formation in the Mediterranean Sea. Such stagnation of the water column is thought to have resulted in the deposition of higher amounts of organic matter (De Lange & Ten Haven, 1983; Emeis et al., 1991; Bianchi et al., 2006). Rossignol-Strick (1985) has correlated sapropel formation with orbital forcing by linking their formation to the monsoonal index. Their (quasi) periodic pattern has been associated with Earth's precession and eccentricity cycles (fig.2. Hilgen, 1991), in particular with precession minima/insolation maxima.

The increased humidity is considered to have played a decisive role in the formation of the sapropels by changing the hydrological conditions of the basin. The elevated fresh water input in the basin has caused the lowering of the surface-water salinity, which subsequently led to intense stratification of the water column (Calvert 1983; Mangini & Schlosser, 1986) and the cessation of bottom water formation. Additionally, the higher riverine discharge increased the amount of nutrients, thus enhancing the primary production. The combination of high primary productivity, sluggish circulation and low oxygen concentrations in the water column enhanced the preservation of the organic matter by preventing its oxic degradation. The formation of sapropels is not only restricted to interglacial periods but have also –but less frequently- occurred during glacial times (e.g. Thunell et al., 1984), as can be observed in figure 2 for sapropel S6.

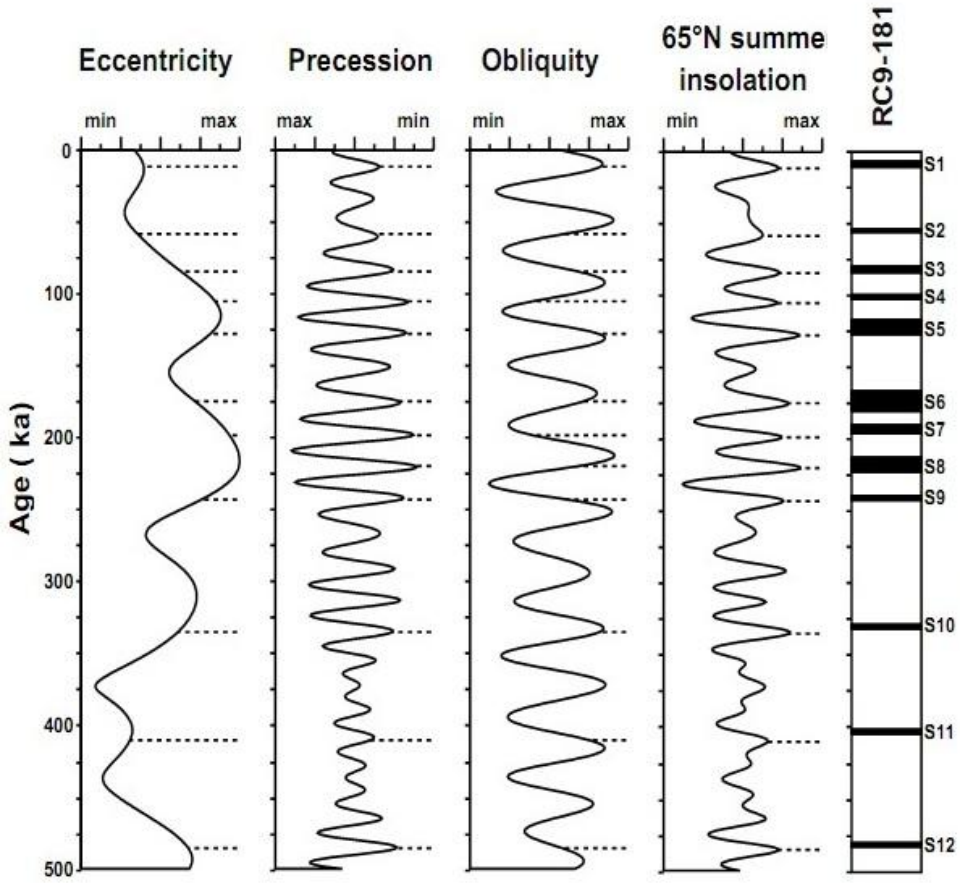

figure 2. Astronomical phase relationships for the late Pleistocene sapropel record of a core from the Eastern Mediterranean (right panel). From left to the right the orbital parameters of eccentricity, precession and obliquity are shown. The right panel shows the 65° N insolation for the last 500ka. All the astronomical parameters are computed by the La 93 solution (by Tuenter 2004).

Sapropel deposition has been accompanied by changes in isotopic composition of foraminifera as well as in that of organic matter (e.g. Thunell et al., 1977; Cita et al., 1977; Vergnaud – Grazzini et al., 1986; Ganssen et al., 1987; Parisi, 1987; Rohling et al., 1977; Rijk et al., 1999; Struck et al., 2001; Arnaboldi & Meyers, 2006; Meyers et al., 2008). Changes in the faunal abundances and assemblages have been identified and correlated with terrestrial records and specifically with pollen records and isotopes from speleothems (e.g. William & Thunell., 1979; Muerdter & Kenett, 1984; Nolet et al., 1990; Artzegui et al., 2000; Bar-Matthews et al., 2000; Principato et al., 2000; Zanchetta et al., 2007; Kuhnt et al., 2007; 2008, Abu-Zied et al., 2008; Kotthoff et al., 2008; Avramidis et al., 2012). Geochemical studies have shown that these layers were significantly enriched in trace metals and redox-sensitive elements often used as indicators for reduced oxygen conditions in the water column and/or the sediment/water interface (e.g. Calvert et al., 1983, Sutherland et al., 1984; Ten Haven et al., 1987; Pruysers et al., 1991; van Os et al., 1991; Fontugne & Calvert, 1992; Cheddadi & Rossignol-Strick, 1995; Wehausen & Brumsack, 1999; Nijenhuis et al., 1999; Thomson et al., 1999; Wehausen & Brumsack, 2000; Warning & Brumsack, 2000; Murat & Got, 2000; Nijenhuis & de Lange, 2000; Rinna et al., 2002; Larrasoaña et al., 2003; Slomp et al., 2004; Reitz et al., 2006b; Arnaboldi & Meyers, 2007; de Lange et al., 2008; Gennari et al., 2009; Moller et al., 2012). Additional studies were carried out focusing on post-depositional diagenetic processes that have taken place after the burial of these organic rich deposits due to the re-oxygenation of the water column (e.g. Pruysers et al., 1993; Passier et al., 1996; 1999; 2001; Zonneveld et al., 2001; Reitz et al., 2005). In many studies it has been identified that diagenetic processes have changed the geochemical signal of the sedimentary records or has removed partially or completely (e.g. S2, and "ghost" sapropel) the sapropelic layer (e.g. van Santvoort et al, 1996; de Lange et al., 2008). Lastly, many studies were focused on changes on the ocean circulation patterns whilst many attempts to correlate these fluctuations to North Hemisphere climate changes and North Atlantic oscillation have been made (Thunell et al., 1984; Jenkins & Williams., 1984; Rossignol-Strick 1985, Rohling & Hilgen, 1991; Emeis et al., 1991; Rohling, 1991; 1994; Aksu et al., 1995; Myers et al., 1998; 2002; Cramp & O'Sullivan, 1999; Bethoux & Pierre, 1999; Pinardi & Masetti, 2000; Myers & Rohling, 2000; Rohling et al 2000; Stratford et al., 2000; Meyers & Arnaboldi, 2005; Capozzi et al., 2009, Siani et al., 2013).

Thus, the general features and observations associated to sapropel formation are clear, yet the exact mechanisms for their deposition and preservation are still under debate. There are two most prevalent theories. One suggests that environmental changes (e.g. in evaporation, temperature, salinity) due to increased precipitation/river input weakened the thermohaline circulation which subsequently caused reduced deep-water oxygen conditions enhancing preservation of organic matter, whilst the second one attributes the high organic matter accumulation to elevated primary productivity due to increased nutrient input, which subsequently led to reduced oxygen levels in the deep-water column.

Sapropel S1

Sapropel 1 is the most recent sapropel, deposited during the Holocene and hence the most easily retrieved and accurately dated. Therefore it has been studied in great detail and its features have been linked directly or indirectly to processes taking place in the water column, as well as in the sediments. Its deposition has been dated between 9.8-5.7 ^{14}C kyr. (10.8–6.1 cal ka. BP) (De Lange et al., 2008). Sapropel S1 exhibits the same characteristics as the older sapropels and therefore it has been used as diagnostic for other sapropels

The increased fluvial discharge in the Mediterranean Sea during the sapropel deposition resulted in enhanced nutrient supply and thus higher primary productivity, whilst it also caused a decrease in surface water salinity, thus enhanced density gradient versus depth, resulting in the subsequent stagnation of the water column. The restriction or even temporary cessation of the deep water formation led to a rather sluggish water circulation which in turn progressively lowered the bottom-water oxygen concentrations resulting in the development of conditions favorable to the preservation of the organic matter (Emeis et al., 2000, Martinez-Ruiz et al., 2000). In addition, the anoxic bottom-water conditions which progressively developed have been reported to have resulted in enhanced regeneration of sedimentary phosphate (Slomp et al., 2002). This resupply of P in combination with the more efficient recycling of released P to the water column is thought to have been an important contribution to sustain high primary production during sapropel S1 formation (Kraal et al., 2010). Furthermore, the TOC content has been reported to vary with respect to depth as a result of more reduced conditions prevailing at greater depths (Murat and Got, 1988, 2000; De Lange et al., 1989; 2008).

The Ba/Al ratio is commonly used as an indicator for paleoproductivity, as Ba concentrations has been linked to organic matter export (Dymond et al., 1992; Paytan et al., 2004). Ba precipitates as biogenic barite and its accumulation in sediments is thought to be related to surface water primary production (van Os et al., 1991; van Santvoort et al, 1996). Moreover, Ba/Al ratio has retained its high levels even while the initial C_{org} content has been decreased due to post-depositional oxic degradation. Thus Ba/Al ratio can be used to define the original boundaries of sapropel deposition (fig. 3) (van Santvoort et al., 1996; Thomson et al., 1999; Paytan et al., 2004; De Lange et al., 2008). In addition, from a potential difference between Ba/Al (i.e. initial C_{org} deposited) and observed C_{org} (i.e. remaining C_{org}) a possible 'burn-down zone can be evaluated in particular for the top of sapropel S1. Furthermore, indirectly it can be used to determine the precessional period of increased precipitation and run off and thus increased nutrient supply that is considered to have promoted the elevated high primary production. As a consequence, the reported deep water conditions, below 1800m, have been fully anoxic and with enhanced levels of dissolved Mn (Mn^{2+}) (de Lange et al., 2008). By the end of the period of high humidity, the fresh water input has been significantly reduced and as a result sea-surface salinity increased, and bottom-water formation restarted and thus the re-oxygenation of the water column. The latter has resulted in the rapid basin-wide precipitation of dissolved Mn ($Mn^{2+} + O_2 \rightarrow MnO_2\downarrow$). This process has created the upper high Mn peak recorded at the end of sapropel formation (fig. 4). This change in hydrological conditions also resulted in reduced primary productivity and subsequently to low organic matter fluxes. Subsequently, the deep water remained permanently oxic. After the resumption of normal oxygen levels in the water column, oxygen has penetrated into the sediments while decomposing the organic matter. This has created an oxidation front which moves downwards progressively adding a diagenetic geochemical signal in the sediments (fig. 3). The development and downward migration of the oxidation front is underscored by the second sedimentary Mn peak that is immediately overlying the remaining organic rich unit. (De Lange et al., 1989; Pruysers et al., 1993; De Lange et al., 2008). This process depends primarily on the accumulation rates and to a lesser extent on the bioturbation depth (van Santvoort et al., 1996; Reed et al., 2011). The resulting distinct two lobe Mn/Al peaks have been recognized in Mediterranean marine records at the end of sapropel deposition across the basin. Hence, the Mn-rich layers are used as indicators for the end of S1 re-ventilation and the subsequent downward oxidation of S1. In addition, it is the combination of TOC, Ba/Al and Mn/Al profiles that can be used as a diagnostic tool to assess re-ventilation of the water column, and the development of such a downward oxidation.

Shifts in the general composition of the organic matter deposited in sapropel layers have been traced and studied in terms of its origin and nature. Changes in C/N and δ^{13}Corg have been reported to indicate changes in its origin

(Fontugne et al, 1989; Nijenhuis & De Lange, 1999; Kuhnt et al., 2008; Schmiedl et al., 2010) comparing to the background values. Although, usually the C/N ratio in low organic carbon sediments cannot be used as an indicator for the origin of the organic matter, in sapropels it has been reported as a useful tool to distinguish between marine and terrestrial sources (Meyers & Doose, 1999). The stable carbon isotope ratios exhibit different values between terrestrial and marine originated organic matter; marine organic matter is heavier isotopically ($\delta^{13}C$ values around -20 to -22‰). Hence, relatively low C/N values (around 10) in combination with less negative $\delta^{13}C_{org}$ values have been suggested to indicate that the terrestrial component only represents a small fraction of the organic matter in sapropels (Nijenhuis & De Lange, 2000). Therefore, the source of the high organic matter accumulated in sapropels is considered to be primarily marine. Shifts have been recorded in nitrogen isotopes ($\delta^{15}N$ values) as well; these have been attributed to increased N_2 fixation by cyanobacteria as a result of the intense stratification and low oxygen levels in the water column that expanded up to the euphotic zone (Sachs & Repeta, 1999; Struck et al., 2001). Due to possible diagenetic alteration these two bulk parameters should be used only indicatively although it has been suggested that the oxygen depleted bottom water promoted the preservation of the nitrogen isotopic signal (Sachs & Repeta 1999; Robinson et al., 2012). Thus, during sapropel formation and high organic matter accumulation, the lighter $\delta^{15}N$ values can be used as a proxy for the changes in the biogeochemical cycle of N as well as the oxygen condition in the bottom waters (Robinson et al., 2012).

The organic rich sediment layers are accompanied with sulfur (S) enrichments which have been attributed to pyrite formation (e.g. Passier et al., 1999 and refs therein). Pyrite forms in anoxic conditions where iron reacts with reduced sulfur species (Passier et al, 1996; Paytan et al., 2004; Mercone et al., 2001). Therefore, the formation of pyrite is strictly dependent on the iron available and hence enrichments in Fe/Al are also commonly observed in sapropelic layers.

Sapropel formation has been linked to humid conditions due to the intensification of the monsoonal activity (Rossignol-Strick, 1985), which subsequently has caused higher riverine input and limited aeolian dust influx. Geochemical data confirm that the origin of the detrital input in sapropels has been more riverine. Zr/Al and Ti/Al ratios are widely used as proxies for aeolian input in marine sediments and during sapropel formation they appear to be significantly lower (Martinez-Ruiz et al., 2000; Calvert and Fontugne, 2001; Larrasoaña et al., 2003; Gallego-Torres et al., 2007;). K/Al and Mg/Al ratios are used as proxies of higher riverine input and thus indicating more humid conditions, since they are more abundant in different minerals such illite and chlorite respectively (Krom et al., 1999; Rutten & de Lange, 2003; Martinez-Ruiz et al., 2003). Nonetheless, changes in the mineralogical composition have also been correlated to the different origin of the sediments (Wehausen & Brumsack, 1999).

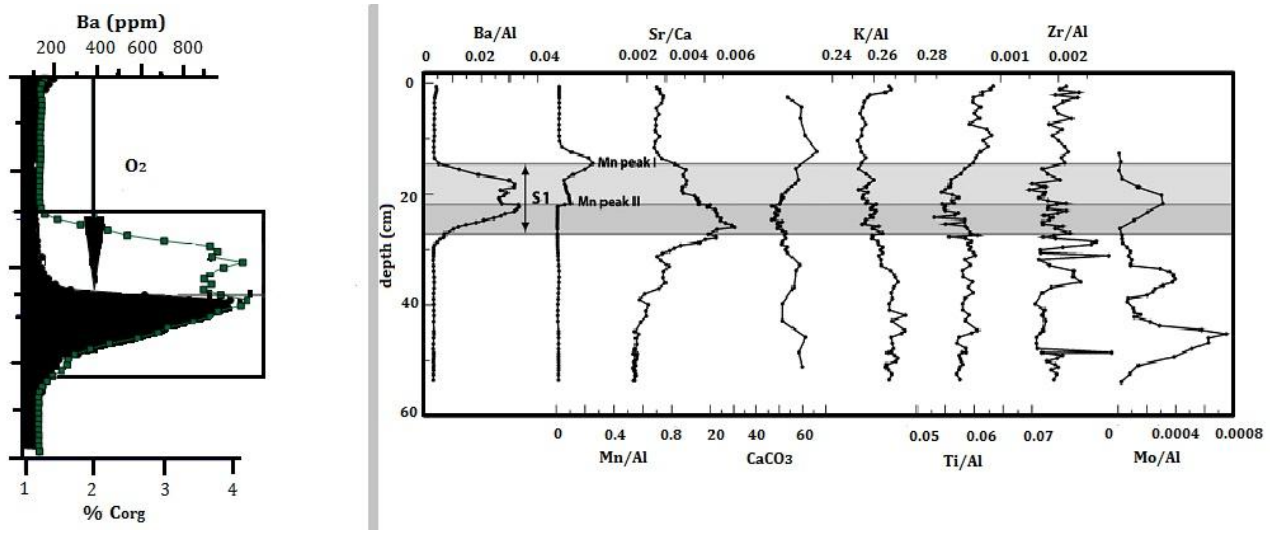

figure 3. Left panel: example of upper oxidized and lower unoxidized sapropel S1,; the Ba profile is thought to indicate the initial %Corg profile (from De Lange et al., 2008). Right panel: Main patterns of elemental concentrations in sapropel (S1) from core MC12 (2211m water depth) from the Eastern Mediterranean Sea (from Reitz et al., 2006b).

Sapropel sediments are often enriched in redox sensitive elements and trace metals such as Mo, V, Cr, Ni, Co and Zn. Their behavior and relation to reduced bottom-water conditions, as well as their sensitivity to diagenetic re-

mobilization have been studied thoroughly (e.g. Calvert, 1983; Calvert & Pedersen, 1993; Thomson et al., 1995; Martinez-Ruiz et al., 2000; Wehausen & Brumsack, 2000; Mercone et al., 2001; Fontugne & Calvert, 2001; Gallego-Torres et al., 2007; Jilbert et al., 2010). Enrichments in these elements cannot be attributed solely to riverine input and thus they are widely used as proxies for anoxic/ dysoxic conditions, whereas at the same time their high accumulation rates impose a continuation of the water circulation and do not permit a complete stagnation of the basin (Nijenhuis et al., 1998). Their precipitation may be related to the formation of sulfides and co-precipitation with pyrite, or in the absence of oxygen they may transform to a less soluble phase (Warning & Brumsack, 2000). Mo/Al and V/Al ratios have been reported to be good indicators for anoxia. Mo is largely conservative in sea water and its precipitation is mainly controlled by the presence of authigenic sulfides (Crusius et el., 1996; Reitz et al., 2006b) and its removal from the water column requires strongly reducing or sulfidic conditions (Calvert & Pedersen, 1993). V shows similar behavior and its precipitation demands strongly reduced conditions, whilst its deposition is associated with increased organic carbon accumulation (Calvert & Pedersen, 1993; Morford & Emerson, 1999). Redox sensitive elements such as Mo and V tend also to precipitate with Mn-hydroxides at the terminal-S1 reventilation event, and with Fe and Mn oxyhydroxides at the postdepositional oxidation front. Consequently, enrichments may occur at the upper Mn peak and at the current oxidation front, thus the lower Mn peak (Thomson et al., 1995; Reitz et al., 2006b). Elevated Cr and Ni concentrations, although thought to be indicative for low-oxygen conditions, for the Eastern and Central regions in Mediterranean Sea in particular can also be due to the fluvial discharge of Greek rivers enriched in these elements (Wehausen & Brumsack, 2000). Similarly, Co, Cu and Zn may redistribute in the absence of oxygen and diffuse downwards into the sediments (Nijenhuis & De Lange, 2000). Additional ratios have been proposed in the literature (e.g. (V/Cr, V/(V+Ni), Ni/Co, V/Mo) for determining the intensity of anoxia (Hatch & Leventhal, 1992; Gallego-Torres et al., 2007).

Another distinguishable feature in sapropel layers is the calcium carbonate ($CaCO_3$) content that is usually low compared to the background sediments. The lower carbonate content observed for sapropel sediments can be caused by carbonate dissolution, lower carbonate production, or by its dilution with other sedimentary components. Van Os et al., (1994) showed that the low content of calcium carbonate cannot be explained solely from dissolution processes. Therefore, an overturn in fauna flourishing during sapropel formation was proposed as possible explanation of diminished carbonate production (Van Os et al., 1991; 1994; Wehausen & Brumsack, 1999; Meyers & Arnaboldi, 2005). This may also be related to the reported enhanced diatom production during sapropel formation (e.g. Kemp et al., 1999). Significantly higher Sr/Ca levels have been observed during sapropel deposition, which has been reported to be related to enhanced fluxes of near-coastal Sr-rich aragonite and to the diagenetic, in-situ formation of Sr-rich aragonite during sulfate reducing conditions (Thomson et al., 2004; Reitz & De Lange, 2006).

The restricted circulation of the Mediterranean Sea makes it very vulnerable to small changes such as those induced by climate variability. Prominent changes in the ocean circulation patterns during sapropel formation initiated a whole group of studies focusing on these changes aiming to link sapropel deposition to alterations in hydrological conditions (circulation reversal) of the basin based on planktonic foraminifera, oxygen isotopes or temperature and salinity gradients. (Sarmiento et al., 1988; Thunell & Williams, 1989). The decrease in salinity and high riverine input in the basin implies a weakened anti-estuarine circulation comparing to the present, rather than an estuarine circulation (Rohling, 1994; Meyers et al., 1998). The weakened anti-estuarine circulation hypothesis accompanied by a significant increase in nutrient supply was also confirmed by the models suggested by Stratford et al. (2002) especially for the youngest sapropel, which exhibits a relatively low enrichment in organic carbon. Additionally, a sluggish circulation would also reduce the export of deep-water thus would contribute to the increased primary production. Budget calculations for accumulation rates of trace and redox sensitive elements have shown that complete stagnation cannot have been established in the basin. In fact, a weakened but still continuous circulation must have persisted even during the very organic-rich sapropel formation (Nijenhuis et al., 1999). More recently, analyses were performed in much higher resolution and reconstructions of past conditions illustrate that the oxygenation state of the water column and changes therein have been variable throughout the sapropel S1 formation. (e.g. Mercone et al., 2000; Crasford et al., 2003; Kuhnt et al., 2007; 2008). All of this advocates that a reversal in water column circulation cannot have occurred during sapropel S1 formation.

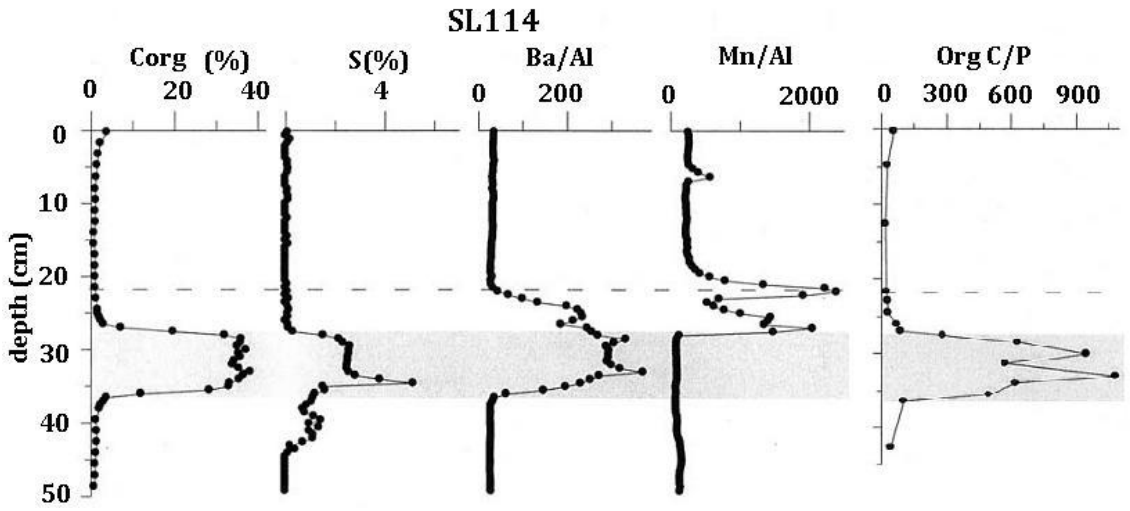

figure 4. Corg (%), S(%), Ba.Al, Mn/Al and Org C/P vs depth profiles for core SL114 (depth 3390m from the central part of Eastern Mediterranean Sea) (from Slomp et al., 2002).

Interruption of Sapropel S1 formation: "8.2ka event"

Some of the most recent studies have shown that sapropel S1 formation did not take place under a stable, persistently anoxic environment but fluctuations in the oceanographic regime as a whole occurred repeatedly, interrupting the accumulation of high amounts of organic matter. Brief episodes of re-ventilation of the water column and thus cessation of high accumulation of organic matter on the sea bottom have been identified during the deposition of sapropels. During sapropel S1 formation a vigorous episode interrupted the formation of the organic-rich layer across the whole basin. Its development has been linked to cold and dry air masses acting from Northeast Europe (Rohling et al., 1997; 2002; Mercone et al., 2000; Rohling & Palike, 2005) Despite its short duration of 200 years, this 8.2 cal. ka BP event , has been preserved explicitly in marine and terrestrial records. The significant lowering of the organic matter content manifests the resumption of bottom-water formation in both Aegean and Adriatic Seas (e.g. Rohling et al., 1999; De Rijk et al., 1999; Ariztegui et al., 2000; Crasford et al., 2003 Kuhnt, et al., 2007; Kothoff et al., 2008; Schmiedl et al., 2010; Siani et al., 2010). The re-oxygenation of the water column is also attested by the repopulation of the seafloor by oxic benthic fauna (e.g. Siani, 1999; Abu-Zied et al., 2008) and sharp drops in the trace metals and redox sensitive elements concentrations. The rapid cooling of the climate is expressed by the re-occurrence of subpolar planktonic species, as well as their isotopic composition on the one hand and a conspicuous turnover in terrestrial ecosystems on the other (Pross et al., 2009; Geraga et al., 2010). The intensity and distribution of this event underlines the direct link of the Mediterranean Sea to the Northern Hemisphere Climate and its sensitivity to changes thereof (Rohling & Palike, 2005).

1.3 Holocene Climate Variability

The onset of the Holocene marks the end of the last glacial period when low temperatures, low sea levels and dry conditions were prevailing also in the Eastern Mediterranean Sea (Gvirtzman & Wieder, 1999). The Holocene era started approximately at 11.6 cal ka BP and is characterized by intense climate variability.

Numerous studies have been carried out in the Eastern Mediterranean Sea focusing on the climate variability expressed in the Holocene sedimentological and faunal records. The prominent climate amelioration in the Eastern Mediterranean Sea was followed by the warmer and more humid period which is linked to insolation maxima/precession minima, when the most recent sapropel (S1) was deposited (Rossignol-Strick, 1985, Rohling & Hilgen, 1991). Despite the significant improvement of the climate with the Holocene Climate Optimum (Rossignol-Strick, 1999; Peyron et al 2011), additional cooling/warming events occurred during the Holocene, varying in duration and intensity. The most pronounced one has been the so-called "8.2 cal ka BP event", during which sapropel formation has been disrupted (Rohling & Palike, 2005).

Moreover, the Mediterranean basin appears to have a more distinct history compared to the open ocean due to its relatively restricted exchange of seawater with the Atlantic Ocean. Consequently, processes driving the deep water formation from Adriatic and Aegean sources are more sensitive even to smaller changes related to climate, which in turn

affect the thermohaline circulation of the basin. Spatial and temporal differences have been traced throughout the sedimentary records that can be partially explained by regional conditions that themselves have a more general climatic control. Especially, proxies based on micropalaeontological assemblages are strongly influenced by local paleoceanographic conditions (Capotondi et al., 1999; Geraga et al., 2010). Nonetheless, the most recent studies with high resolution results illustrate that most of these events have occurred nearly simultaneously across the Eastern Mediterranean Sea, and are associated with global climatic variability.

These studies are mostly using planktic and benthic foraminiferal assemblages and their isotopic composition, as well as organic geochemical proxies, pollen and nannoplankton data focusing on the reconstruction of the paleonvironmental, paleoceanographic and hydrological conditions in the Adriatic (e.g. Rohling et al., 1997; Capotondi et al., 1999; Ariztegui et al., 2000; Asioli et al., 2001; Giunta et al., 2003; Siani et al., 2013), Ionian (e.g. Geraga et al., 2008), Aegean (e.g Aksu et al., 1995; Geraga et al., 2000; 2010; Casford et al., 2003; Gogou et al., 2007; Triantaphyllou et al., 2009; Katsouras et al., 2010; Kouli et al., 2012) and Levantine basins (e.g. Emeis et al., 2000; Principato et al., 2003; Kuhnt et al., 2007; Schmiedl et al., 2010). These high-resolution paleoclimatic reconstructions have shown that short and longer lasting cooling events occurred throughout the Holocene and are linked to the high latitude climate forcing mechanisms that are also expressed in the North Atlantic Ocean archives (Asioli et al., 2001).

All records used for paleoclimatic reconstructions indicate warm climate conditions starting at ~11.5ka and prevailing during the Holocene throughout the Eastern Mediterranean. Dinoflagellate assemblages dominated by warm water indicators together with increased marine microfauna associations, depleted isotopic signal and higher abundance and diversity of steppic tree elements advocate for temperate/arid conditions prevailing almost permanently in the entire basin with cooling events of different intensity, resulting in high frequency climate fluctuations (Aksu et al., 1995; Triantaphyllou et al., 2009; Geraga et al., 2010; Kouli et al., 2012). More specifically, at ~10.5ka more arid and warm conditions are recorded in warm species of dinoflagellate cysts, marine and terrestrial pollen records, by lower surface water salinity and higher temperatures together with increased abundances of planktonic foraminifera and terrestrial biomarkers. In addition nannoplankton fluxes and benthic assemblages are characterized by a well-developed ecosystem and sufficient mixing in the water column (Aksu et al., 1995; Zonneveld, 1996; Rohling et al., 1997; Geraga et al., 2000; Principato et al., 2006; Abu-Zied et al., 2008; Geraga et al., 2008; Gogou et al., 2007; Geraga et al., 2008; Triantaphyllou et al., 2009; Katsouras et al., 2010; Kouli et al., 2012;). Immediately prior to sapropel S1 formation gradual changes in plaktonic foraminiferal assemblages indicate the progressive stratification in the water column as well as the transition towards more eutrophic conditions (Geraga et al., 2000). Concomitantly, all the records related to paleoclimate conditions show a decline in water-column oxygen concentration, an increase in sea surface temperatures (Jorissen et al., 1999; Emeis et al., 2000; Kuhnt et al., 2007; Gogou et al., 2007; Triantaphyllou el., 2009) as well as lowering of the sea surface salinities and the development of a pronounced Deep Chlorophyll maximum (Rohling & Gieskes, 1989; Castradori, 1996; Negri & Giunta, 2001; Triantaphyllou et al., 2009). These changes are also reflected in shifts in the stable isotopic composition of the planktic foraminifera whilst the elevated river discharges associated with higher precipitation have been linked to a the significantly higher content of terrestrial biomarkers (Casford et al., 2003; Geraga et al., 2010; Katsouras et al., 2010). However, the increased input of terrestrial and marine material during the S1 formation together with the prominent reduction of the oxygen levels in the water column as well as the water/sediments interface also have contributed to the higher preservation of this material and hence to the higher fluxes that have been identified in these records (e.g. Ten Haven et al., 1987; Cheddadi & Rossignol-Strick, 1995; de Rijk et al., 1997; Kothoff et al., 2008). Thus restricted circulation and deep-water formation cessation are amongst the factors that have contributed to the repetitive formation of distinct organic-rich units in eastern Mediterranean sediments during the last 13 Ma (e.g. Rohling & Grieskes, 1989; Pruysers et al., 1991; Sachs & Repeta, 1999; Wehausen & Brumsack, 1999).

As mentioned above an abrupt cooling event at 8.2 ka cal. BP which caused the re-oxygenation of the bottom waters and the complete cessation of the sapropel S1 formation has been conspicuously expressed in the marine and terrestrial records. The end of this event was marked by the reappearance of warm taxa both in pollen records as well as in foraminiferal assemblages and dinoflagellate cysts. Planktic foraminiferal thus surface water oxygen isotope values became lighter again as a result from increased fresh water input leading to higher nutrient supply and hence higher organic matter accumulation. The restoration of climate and oceanographic conditions allowed the continuation of the sapropel formation up to ~6ka BP. A small but prominent decline in warm taxa in pollen and faunal assemblages; proliferation of benthic taxa indicating oxygenation of the bottom waters, in combination with sharp shifts in isotopic composition was recognized between 7.5-7.2 cal. ka in the Aegean (Kothoff et al., 2008; Geraga et al., 2010) and Adriatic Seas (Siani, 1999; Siani et al., 2010) and at ~7.0 cal. ka in the Ionian Sea (Geraga et al., 2008)

The end of the sapropel formation in the Eastern Mediterranean is marked with the re-establishment of oligotrophic conditions, similar to those at present (Kuhnt et al., 2007; Abu-Zied et al., 2008, Kothoff et al., 2008). This shift is accompanied with a small decline in SST (Gogou et al., 2007), in foraminiferal assemblages as well as in the vegetation records. Several interruptions in the general trend of warm, normal salinity, well mixed oxygenated waters have been identified in the sediment records of the basin during late Holocene. These cool and dry events have been dated around 5.4 cal. ka and 4.3 cal. ka, practically resulting in a continuous alteration of the climate (de Rijk et al., 1999; Kuhnt et al., 2007; Triantaphyllou et al., 2009; Geraga et al., 2008; 2010; Katsouras et al., 2010) albeit with possible spatial and temporal variations in their amplitude.

1.4 Oceanographic setting and deep water formation

The Eastern Mediterranean sea is an almost isolated basin and its only connection to the open ocean is through the shallow and narrow strait of Sicily to Western Mediterranean Sea and to the Atlantic Ocean. Its restricted character and its location makes this basin suitable for studying (paleo) environmental and (paleo)oceanographic processes. Despite its small size Eastern Mediterranean exhibits all the features of the physical processes acting in the global ocean, like water formation, buoyancy and lateral mass exchange (Robinson et al., 1992).

The basin has been characterized as a concentration basin due to the high levels of evaporation, whilst fresh water input significantly influences its anti-estuarine circulation in combination with climate (Myers et al., 1998; Béthoux et al., 1999). The most important known sources of fresh water are the Po river, as well as the rivers flowing from Apennines in the central Mediterranean (Adriatic Sea), Eurasian rivers from Greece and Turkey in the Aegean Sea, and the predominant source of river water from the Nile (before the completion of Aswan Dam in 1964; Ross et al., 1979) in the Southeastern Mediterranean Sea. In addition, the Black Sea contributes with a riverine source through the Dardanelles strait (Theocharis et al, 1999). Another important source of nutrients is the aeolian dust transported to the Mediterranean Sea from the Saharan desert (Krom et al., 1999, Kocal et al., 2005)

The present Mediterranean Sea is a well-ventilated, oligotrophic basin with low productivity and low organic matter accumulation rates while its circulation is dominated by successive deep basins separated by narrow straits due to the numerous islands (Turley, 1999; Béthoux & Pierre, 1999; Tsimplis, 1999; Béthoux et al., 1999). Deep-water formation is taking place in three different areas, namely the Aegean (Theocharis et al., 1993; Laskaratos et al., 1999; Klein et al., 2003) the Adriatic , and the Levantine Intermediate Water from the Rhodes Gyre area (Lascaratos et al., 1993). Such formation is controlled by northerly cold air masses that force the cold and dense water to sink to greater depths (Lascaratos et al., 1999; Béthoux & Pierre, 1999), thus also transferring oxygen from surface to deep water.

Aegean Sea

The Aegean Sea is located in the Northern part of Eastern Mediterranean Sea, between Turkey and Greece. It is connected to the Black Sea through the Straits of Dardanelles and Bosporus and is divided to the North, Central and South Aegean Sea due to the different basins formed from the numerous islands that belong to Hellenic island arc and Aegean volcanic arc.

The hydrological setting of the Aegean Sea is controlled mainly by the high river discharge from Turkey and Greece (Hamann et al., 2008), the regional climate conditions and the water inflow from the Black Sea (Aksu et al., 1995). It is characterized by anti-clockwise circulation pattern (Lykousis, 2001). The increase in net evaporation and the water mass transformation under the influence of cold winds from the Balkan are responsible for deep water formation in the Aegean Sea (Boscolo & Bryden, 2001). Due to its elongated shape spatial and temporal variations have been identified from the North to the South of the basin (Zervakis et al., 2000).

Paleonvironmental reconstructions of the Aegean Sea have illustrated that due to its small volume and its geographical position, it responds immediately to climate forced changes and along with the high sedimentation rates contribute to the documentation of even the short term changes. These studies focusing on the last Glacial period and Holocene era have shown that the Aegean Sea has been subjected to many long and short term variations that are associated to variations in the Siberian High intensity and the Northern Hemisphere Climate (e.g. Rohling et al., 2002; Geraga et al., 2010). Alterations of cold and warm periods have been depicted in micropaleontological and geochemical records with the formation of sapropel S1 being the most prominent one. These events have been identified in the marine

records from the whole Mediterranean basin as well as in the terrestrial records from North East Africa, Middle East and Europe (see above in 1.3 Holocene Climate Variability).

Adriatic Sea

The Adriatic Sea is an elongated basin that expands from the coast of Venice, in the North, to the Gulf of Taranto, in the South. At present, surface water flows from the Adriatic to the Ionian whereas intermediate depth water (Levantine Intermediate Water) flows from the Ionian to the Adriatic Sea through the Otranto Strait. Deep-water formation takes place due to northern cool winter air masses, namely Bora, and flows to the Ionian Sea through the same Strait (Artegiani et al., 1997; Giunta et al., 2003). The Adriatic Sea exhibits the same characteristics as the Aegean Sea; namely having a relatively small volume, its geographical position between the subpolar and subtropical climate zones, and an important influence from riverine input resulting in high sedimentation rates. The Adriatic deep-water source has been reported to affect the Mediterranean circulation in present and past (e.g. Fontugne et al., 1989; Artigiani et al., 1997; Pinardi & Masetti, 2000; Assioli et al., 2001; Rohling et al., 2002; Giunta et al., 2003; Siani et al., 2013).

Objective

Most studies related to S1 formation and reconstruction of the Holocene variability use micropaleontological proxies and are confined to a single core or area. In this research high resolution geochemical proxies are used to determine paleoproductivity, redox conditions and preservation of organic matter. Therefore, high sedimentation rate cores have been selected near the areas where bottom-water formation is known to take place; the Aegean and Adriatic Sea.

The specific geochemical parameters of these cores are interpreted in association with palaeo-environmental conditions and variations thereof and are compared with information available from the literature. In this way, processes related to deep water formation can be linked to those that have resulted in the formation and preservation of sapropel S1.

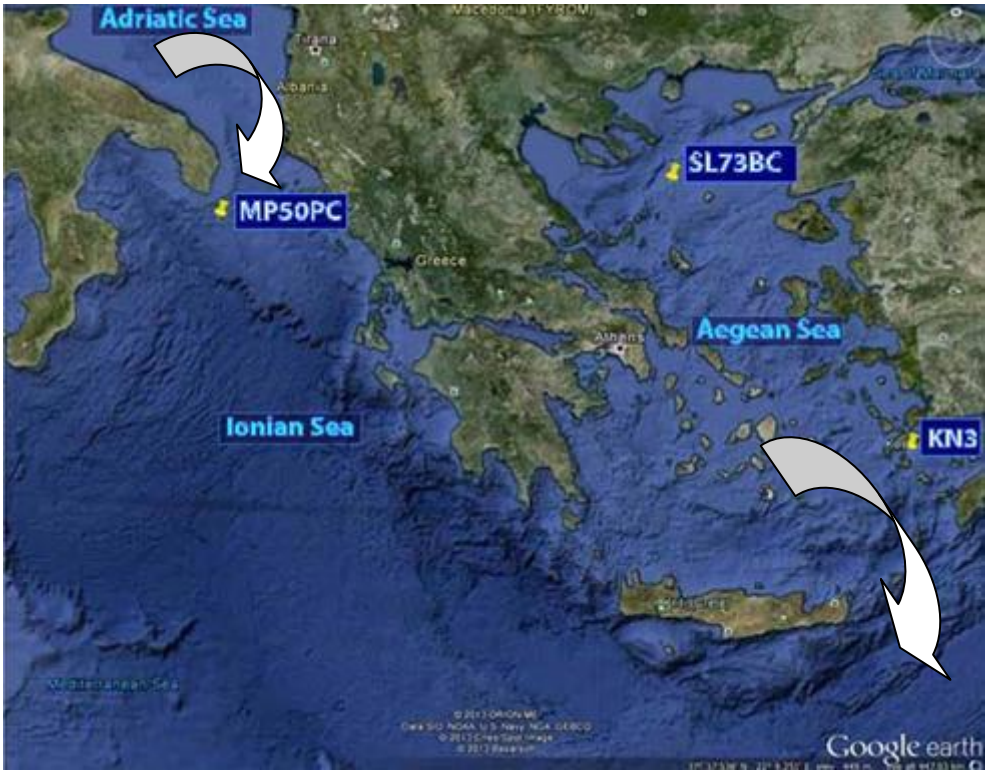

figure 5. Map of Central Mediterranean Sea; the location of the cores used in this study are indicated in the areas of known Mediterranean Deep Water formation, i.e. Aegean Sea and Adriatic Sea.

2. MATERIAL & METHODS

2.1 Material

In this study three relatively shallow cores have been analyzed; two from the Aegean Sea: KN3 gravity core (South Aegean Sea), SL73BC (North Aegean Sea) and one from a site immediately south of the Adriatic Sea, MP50PC (South Adriatic Sea) (fig. 5).

KN3 core

KN3 gravity core (73mm diameter) has been collected north of Nisyros island (South Aegean Sea) from a water depth of 607m (27°12.03' E, 36° 40.60' N) by the Hellenic Centre for Marine Research. Core KN-3 has a total length of 318cm and consists mostly of muds, rich in water, with an olive-grey unit occurring between 155 and 198 cm possibly representing the Sapropel S1 deposits (Rousakis personal communication)(fig. 6). It has been sampled and analysed at a 0.5 cm sample resolution.

The area surrounding the core site, i.e the margin of the Strongyli island (appendix figure A1) is characterized by a canyon-like topography with steep slopes. Probably, much of the thick sedimentary cover at the core site has been derived via turbidity gravity flows from the upper section of the Nisyros margin and/or Strogili Island margins (Rousakis pers.com) (appendix figure A2). However, the studied interval appears to represent regular sediment deposition.

SL73 BC

SL73 box core (sub core #5) has been collected west of Limnos island (North Aegean Sea) from a water depth of 339m (39N 40', 24E 31') during the Smilable cruise in 1999 and has a total length of 39 cm (fig. 7). The core had been sampled and analysed at a 0.5 cm sample resolution.

MP50PC

MP50 piston core has been collected from South Adriatic Sea from a water depth of 775m (39N29', 18E31') during the Macchiato cruise in 2009, and has a total length 473cm. In this study the top 175cm has been sampled and analyzed at 0.5 cm sample resolution (fig. 8).

2.2 Methods

The cores were sampled at 0.5cm resolution; samples were freeze-dried and ground in an agate mortar.

Choronological framework

Accelerator mass spectrometry (AMS) radiocarbon ^{14}C were performed at Poznan Radiocarbon Laboratory, Poland, from the size fraction >63 μm on clean, hand-picked planktonic foraminifera. Conventional ^{14}C ages have been calibrated using the program CALIB 6.0 (Marine 09) (Stuiver & Reimer, 1993; Stuiver et al., 1998) with a regional reservoir age correction (ΔR) for the Aegean Sea cores (KN3 & SL73BC) of 149±30 years for the sapropel interval (Facorellis et al., 1998) and 58±85 outside the sapropel (Reimer and McCormac, 2002) and 112±30 years for the Adriatic Sea core (MP50PC) (Siani et al., 2000; Reimer & McCormac, 2002). For the South Aegean Sea Core the Santorini Ash layer (Z2) was recognized from its geochemical signal (Reitz et al., 2006a) at depth 75.7cm. Hereafter all ages will be discussed as cal. ka BP.

TOC and C/N ratio

Organic C and N contents were measured on a Fisons NA 1500 CNS elemental analyser. Inorganic C was removed prior to the analysis by shaking the sample with 1 M HCl twice (4 h and 12 h). The samples were then rinsed with demineralized water twice, dried at ~60°C and ground in an agate mortar. N content was measured in untreated samples. In house standard nicotinamidae, calibrated with international standards was used. The average standard deviation for all measurements was < 1%.

$\delta^{13}C_{org}$ & $\delta^{15}N$

$\delta^{13}C_{org}$ & $\delta^{15}N$ isotopes were measured on a Fisons NA 1500 CNS elemental analyser connected to a Thermo Delta $^{+}$ IRMS in decarbonated samples. In house standards GQ (graphite-quartz) for carbon isotopes and ASS (ammonium sulphate) for nitrogen isotopes, calibrated with international standards were used. The standard deviation for all measurements of these standards was < 0.2‰.

Elemental concentrations

Total concentrations of elements were determined after digestion in a mixture of HF, HNO_3 and $HClO_4$ and final solution in HNO_3 using ICP-OES (Spectro Arcos) using radial view measurement. The accuracy of the measurements was monitored by including international and in house standards. The standard deviation was better than 3%.

The elements concentrations are normalized to Al concentration to minimize effects of dilution of sediments with variable amounts of biogenic carbonate(e.g Wehausen & Brumsack, 1999; Warning & Brumsack, 2000; Rinna et al., 2002), and because aluminum contents of sapropels are not influenced by biogenic activity, authigenic enrichment or diagenetic dissolution (Rinna et al., 2002).

Dry Bulk Densities

Dry bulk densities were calculated from the weight loss (W%) upon freeze-drying of sediment samples taken at 0.5 cm resolution, assuming a sediment density ($\rho_{sediment}$) of 2.65 gr/cm^3 and a density of seawater ($\rho_{sea\ water}$) of 1.028 gr/cm^3, according to the following equation:

$$DBD = (100 - \varphi\ \%\ ) \times 0.01 \times \rho_{seawater}$$

Where φ(%) porosity is : $$\varphi\ \% = \frac{W(\%)}{W\ \% + \frac{(100 - W\ \% \times \rho_{seawater}}{\rho_{sediment}}}$$

Paleoproductivity

The empirical equations of Sarnthein et al. (1992) (1) and Muller & Stuess (1979) (2) were used to calculate paleoproductivity (gC/m^2 yr).

$$PaP = 61.39 \times (C_{org} \times DBD \times \frac{SR}{10})^{0.25} \times SR_{cf}{}^{-0.049} \times z^{0.15} \quad (1)$$

$$PaP = 333 \times C_{org} \times DBD \times SR^{-0.3} \quad (2)$$

Where,

DBD: dry bulk densitiy,

SR: sedimentation rate(cm/kyr), SR_{cf}: C_{org}-free sedimentation rate (cm/kyr) = SR (1-C_{org} (%)/100),

z: water depth (m).

Fluxes

Selectively, the fluxes of TOC, major and trace elements were calculated using the DBD (dry Bulk Densities) and MAR (mass accumulation rates), according to the following equation:

MAR = sedimentation rate (cm/kyr)* DBD (g/cm^3)/1000

Flux = concentration * MAR

Enrichment factors

The normalization to Al easily expresses excesses or depletions of trace- metals with respect to background values, the enrichment factors (EFs) were calculated at each site with respect to average shale composition (Wedepohl, 1971). EFs for elemental ratios are calculated as: relative enrichments are expressed by an EF>1 (Brumsack, 2006).

$$EF = (element/Al)_{sample}/(element/Al)_{shale}$$

Micropaleontological content and isotopic composition of foraminifera

Samples from core MP50PC were washed and sieved by separating three fraction >350μm, 350-150μm and 150-63μm. Additionally, dry -sieving was applied and 25 *G.ruber* foraminifera white were hand-picked from the fraction 250-200μm, crashed and an average weight of 40μgr was used for measuring the $\delta^{18}O$ and $\delta^{13}C$ composition in a Kiel device connected to a Finnigan MAT 253 IRMS. In house and international standards were used (NBS-19) and the average standard deviation for all measurements was <0.1‰.

Data processing

Spectra analysis was performed for selected elements in order to define high-frequency cycles in the sedimentary record. The analyses were carried out in the concentration of certain elements versus Al ratios using Past (2.17c) software program and the cycles in 95% confidence level were determined (Hammer et al., 2001).

3. RESULTS

3.1 Age model

sample	depth interval (cm)	^{14}C age (BP) ±1σ error	ΔR	1σ age cal BP
KN3 75,5	*75.5-76.0*			*3563[a]*
KN3 119	*119-120*	*5213±40[b]*	*58±85*	*5404-5629*
KN3 149-152	*149-152*	*6070±40[c]*	*58±85*	*6315-6527*
KN3 163-165	*163-165*	*6760±40[c]*	*149±30*	*7078-7218*
KN3 181-184	*181-184*	*7040±50[c]*	*149±30*	*7342-7460*

Table 1. KN3 core a. Santorini ash layer (Friedrich et al., 2006), b. Maria Triantaphyllou (pers. comm.), c. this study. Regional reservoir age correction (ΔR) 149±30 years for sapropel interval (Facorellis et al., 1998) and 58±85 outside the sapropel (Reimer and McCormac, 2002).

Sample	depth interval (cm)	^{14}C age (BP) ± 1σ error	ΔR	1 σ cal age BP
HH00395-396	*3.4-4.4*	*3131±100[a]*	*58±85*	*2717-3027*
HH00406-407	*8.9-9.9*	*5056±100[a]*	*58±85*	*5203-5544*
HH00428-249	*19.9-20.9*	*8600±100[a]*	*149±30*	*8952-9241*
HH00440-441	*25.9-27.0*	*9349±100[a]*	*149±30*	*9858-10162*

Table 2. SL73BC. Regional reservoir age correction (ΔR) 149±30 years for sapropel interval (Facorellis et al., 1998) and 58±85 outside the sapropel (Reimer and McCormac, 2002).a. G. de Lange (pers. comm.)

sample	depth interval(cm)	^{14}C age (BP) ± 1σ error	ΔR	1σ age cal BP
MP50PC#5 5,0-5,5	*5.0-5.5*	*3700± 30[a]*	*112±30*	*3436-3532*
MP50PC#5 19,5-20,0	*19.5-20.0*	*6265±35[a]*	*112±30*	*6537-6641*
MP50PC#5 39,0-39,5	*39.0-39.5*	*8020±40[a]*	*112±30*	*8332-8406*
MP50PC#5 48,5-49,0	*48.5-49.0*	*8670±50[a]*	*112±30*	*9118-9281*
MP50PC#5 57,0-57,5	*57.0-57.5*	*9540±50[a]*	*112±30*	*10208-10336*
MP50PC#4 36,5-37,0	*115.5-112*	*17930±90[a]*	*112±30*	*20629-20974*

Table 3. MP50PC. Regional reservoir age correction (ΔR) 396±85 years (MP50PC) (Siani et al., 2001; Reimer & McCormac, 2002). a. this study.

KN3 core

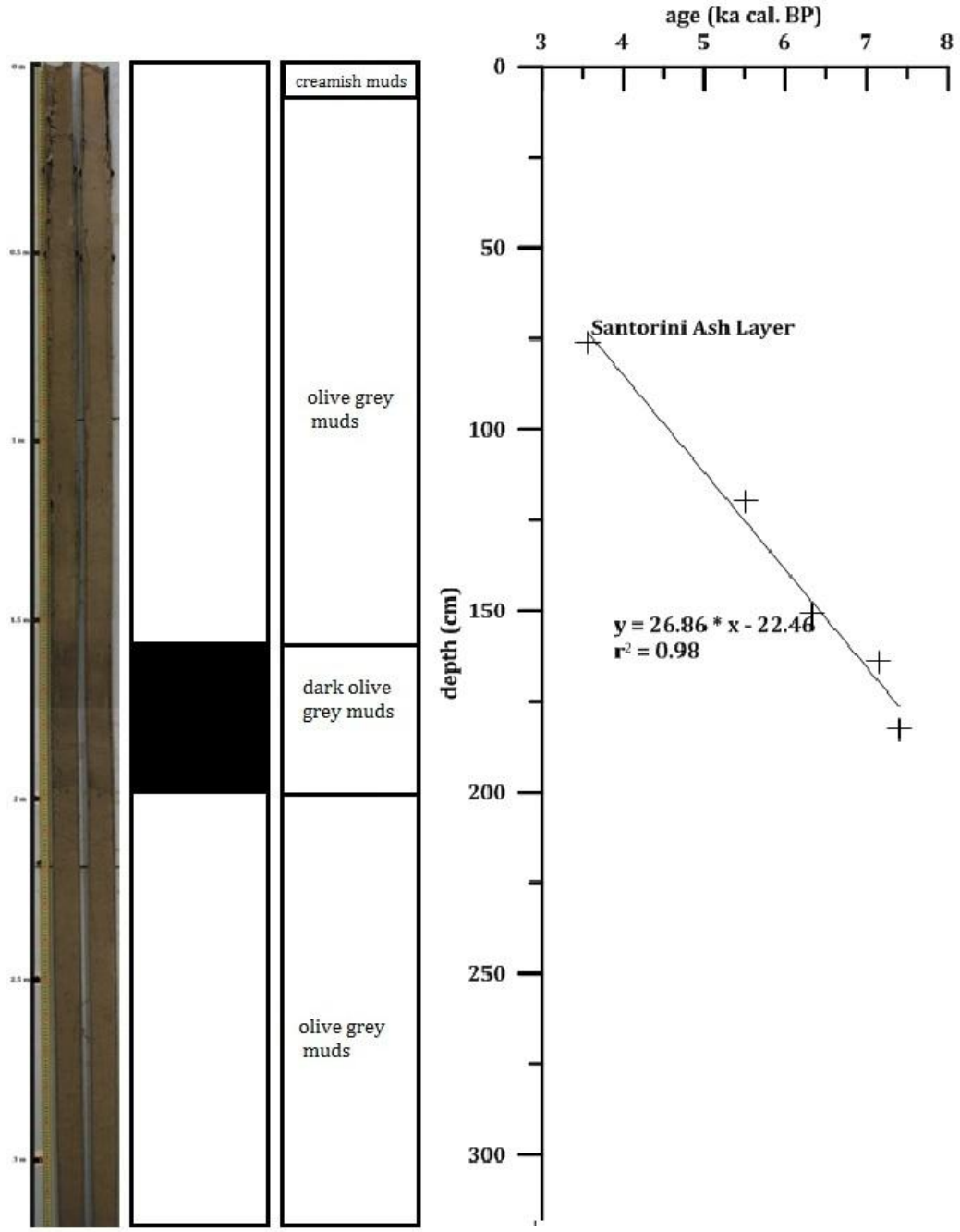

figure 6. KN3 core, left panel: It consists mostly of muds; the interval from 155-198cm is thought to represent the sapropel 1 (Triantaphyllou, pers.communication). Right panel: Age model as derived from the calibrated AMS ^{14}C dated points and the santorini ash layer after Friedrich et al. (2006) versus depth.

SL73BC

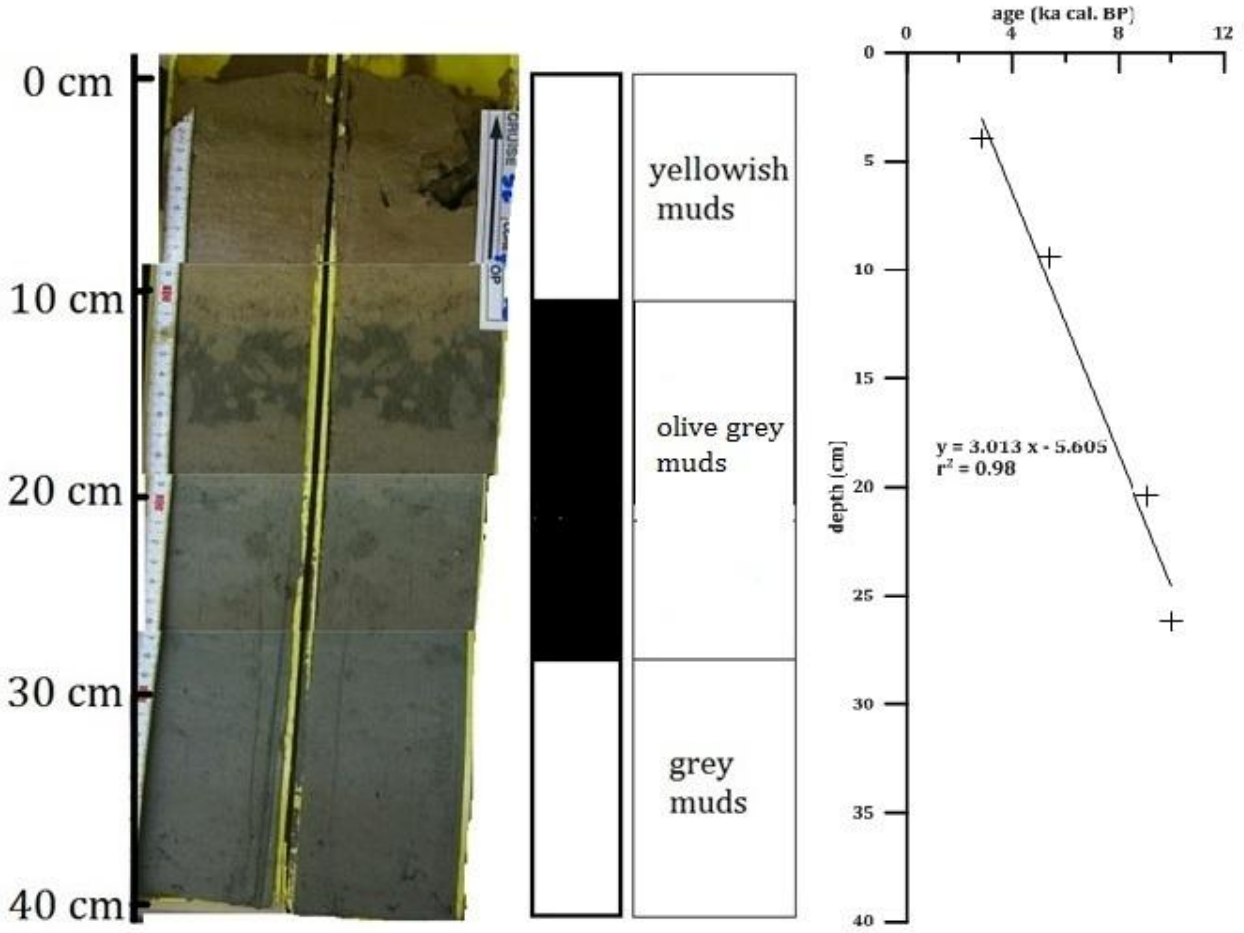

figure 7. Core SL73 BC, left panel: The upper part consists of creamish muds. The interval 11-27cm is thought to represent the sapropel S1 (de Lange, pers. communication). The lower part consists of grey muds. Right panel: Age model as derived from the calibrated AMS ^{14}C dated points versus depth.

MP50PC

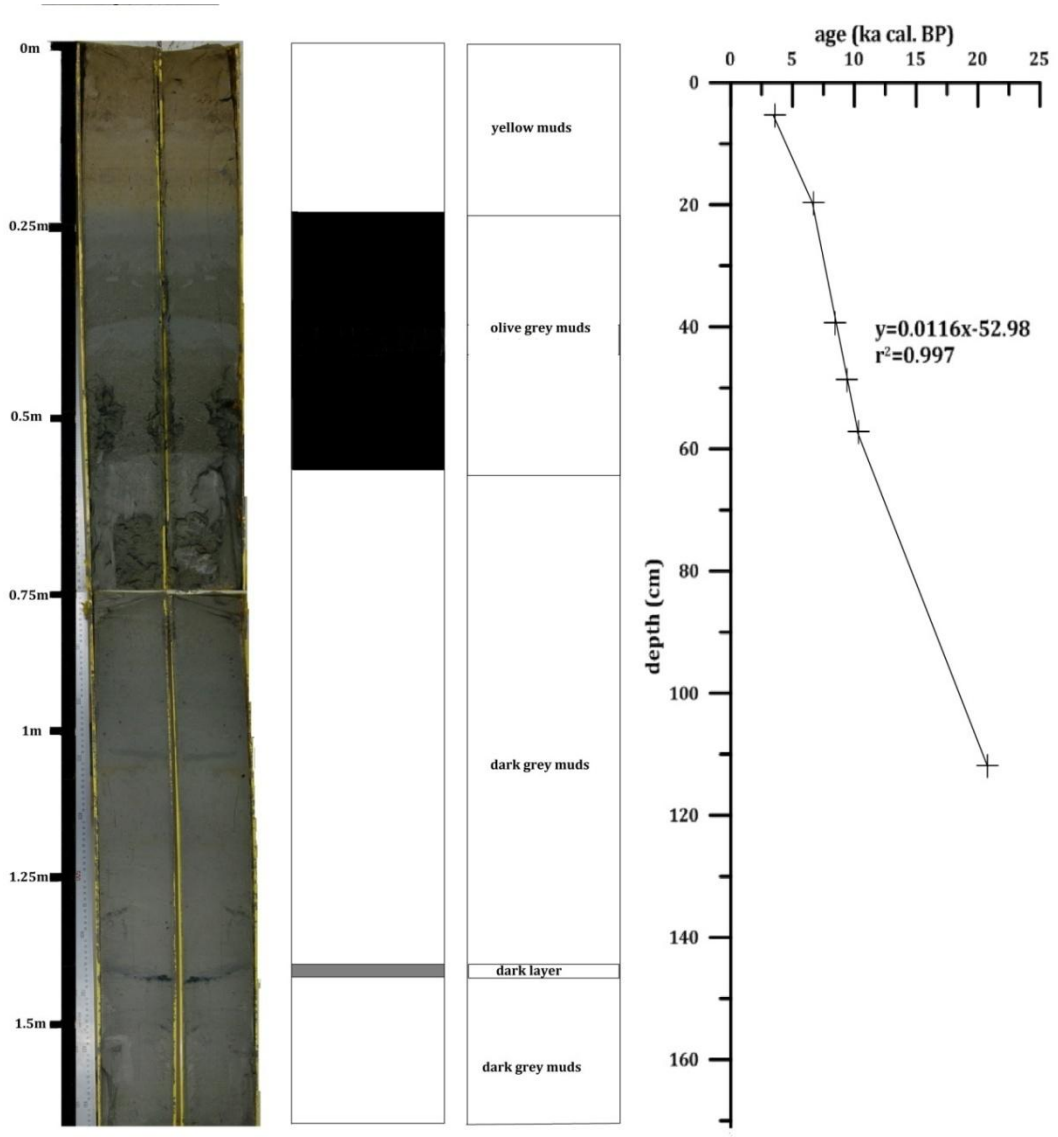

figure 8. MP50PC core, left panel: it consist of dark frey muds. The interval 19-60cm is thought to represent the sapropel S1. Right panel: Age model and the calibrated AMS ^{14}C dated points versus depth.

Age model and sedimentation rates

Age assessments for all three cores have been based on ^{14}Cage measurements and for KN3 core also Santorini tephra layer was used. The age of the sediments shows a linear relation with depth and thus the age model was established using linear interpolation. In KN3 core probable slumps have interrupted the sequence of the sediments below the depth of 200cm, as it can be observed in Appendix figure A3. This can be attributed to the physiography of the site where the core has been collected from (figures A1 and A2). The visual sapropel in this core represents the upper part of the sapropel, i.e. S1b, alone. Therefore, the records below 200 cm were not used for this study and in the figures are represented with fade lines only in order to easily visually determine the background values. Both cores of the Aegean Sea show constant sedimentation rate within, as well as before and after sapropel deposition. In the Adriatic core the sedimentation rate is rather different for the period during sapropel formation and for that prior to- and past- sapropel formation. Therefore, different equations were used to establish the age model. The sedimentation rates were calculated for the South Aegean site to be 27.3cm/kyr, for the North Aegean site to be 3.0cm/kyr and for Adriatic site to be ~4.5cm/kyr before and after the sapropel deposition and to be 10.2cm/kyr during this interval. The samle resolution is ~20 and 160yrs for South and North Aegean Sea sites respectively and for S. Adriatic Sea site that is~50yrs during S1 interval and 100yrs before and after this interval.

3.2 TOC, Ba/Al ratios and Mn/Al ratios

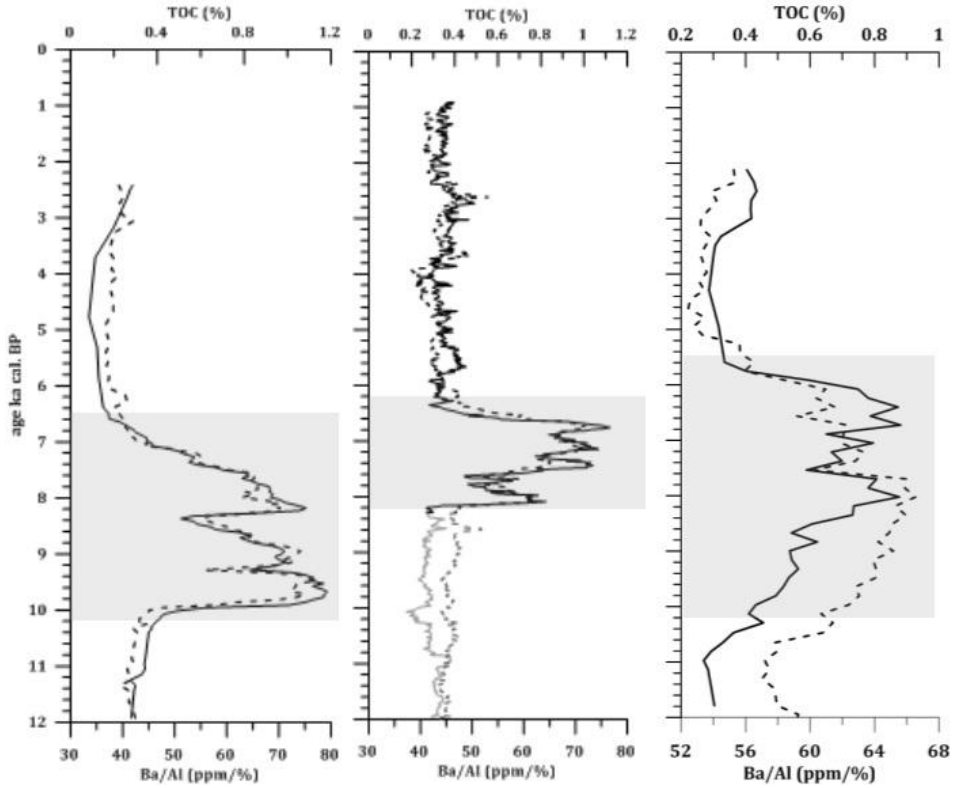

figure 9. TOC (%) (solid lines) and Ba/Al ratio (dashed lines) of the three cores. Prominent increase in both records can be distinguished during the sapropel formation, whilst additional fluctuation within this time interval from all sites can be observed. The grey shaded area indicates the sapropel S1 interval. Left MP50PC, middle KN3, right: SL73BC

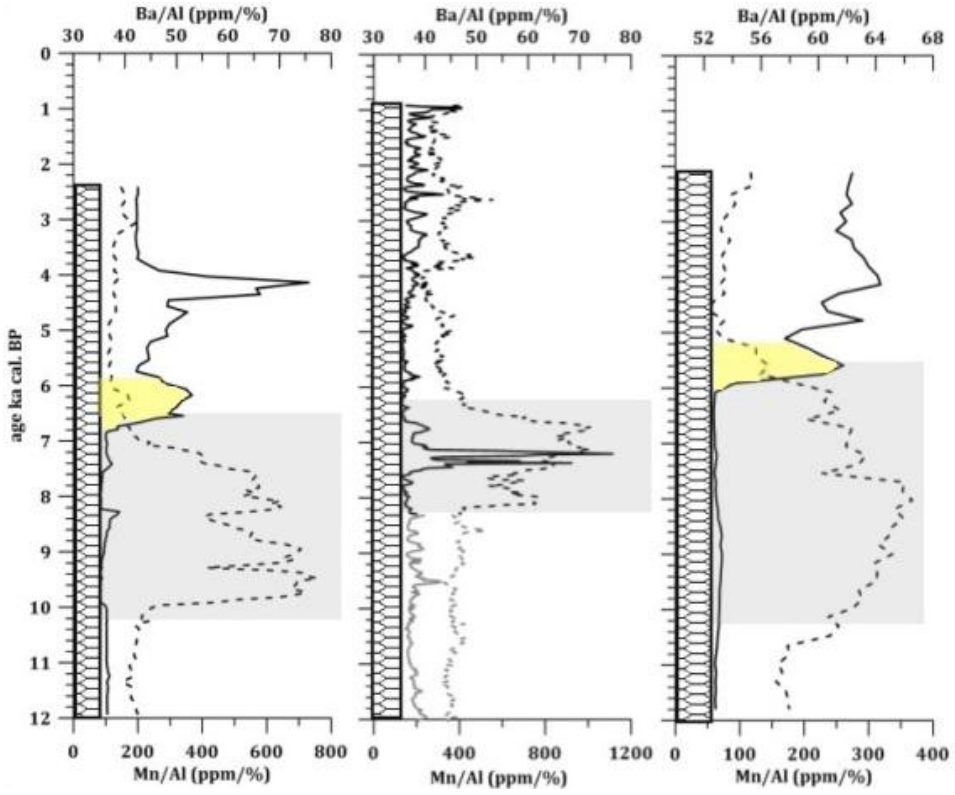

figure 10. Ba/Al (dashed lines) and Mn/Al (solid lines) (ppm/%) of the three cores The grey shaded area indicates the sapropel S1 interval. Note different scale for Mn/Al. The yellow shaded areas highlight the major manganese peak at the end of S1. Left MP50PC, middle KN3, right: SL73BC

3.3 $\delta^{13}C_{org}$ & $\delta^{15}N$

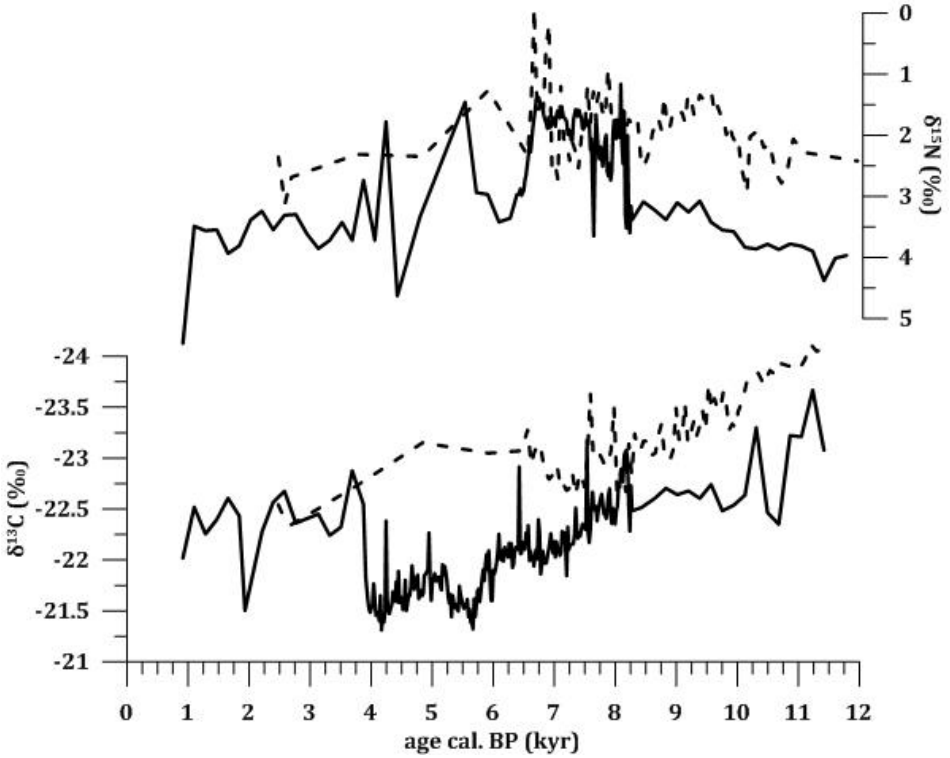

figure 11. Carbon and Nitrogen isotopes of organic matter from KN3 core (solid lines) and MP50PC (dashed lines). As it can be observed changes in isotopic composition of the sediments during the formation of S1 are prominent.

The average total organic carbon concentration during Holocene is 0.35% for South Aegean Sea site, 0.34% for the North Aegean Sea site and 0.24% for the South Adriatic Sea site. During sapropel deposition the average concentration of TOC is significantly higher and in particular for the South Aegean Sea is about 0.8%, the North Aegean Sea is 0.64% and the South Adriatic Sea is 0.76% whilst the highest concentrations for the different sites is 1.09%, 0.9% and 1.16% respectively (fig. 9 & A6). The sapropel S1 interval is determined as the interval with distinctly elevated TOC(%) and Ba/Al; (ppm/%); the two profiles appear to vary consistent in all three studied sites. The sapropel S1 interval in South Adriatic and North Aegean Sea sites start at 10.2 ± 0.3 to 0.5 cal ka BP ± 0.3/0.4 (no data available from South Aegean Sea site) and end at ~ 6.6 ± 0.3 cal ka BP on South Adriatic Sea and ~6.2 ± 0.3 and 5.6 ± 0.5 cal ka BP in South and North Aegean Sea, respectively.

The Ba/Al ratios in all three sites show a very strong correlation to organic carbon content and thus appear significantly enriched during the period of sapropel formation. The Mn/Al profiles from all three cores show slight enrichments at certain times within the sapropel interval and clearly increase above the sapropel layer. In South Aegean Site the Mn/Al ratio show a high peak much earlier that the end of sapropel layer (fig. 10). Mn/Al (ppm/%) ratios in South Aegean Sea site is much higher than the other two sites, during sapropel interval but also before and after S1.

The isotopic composition of the organic matter shows a gradual shift to heavier values both for carbon and nitrogen isotopes (fig. 11). The values of $\delta^{13}C$ from the south Adriatic site are lighter than the south Aegean site although from both site there is a general trend to values diagnostic to marine organic matter (~-21‰). $\delta^{1}5N$ values are similar and although they shift to lighter values, for the whole time they remain positive. In addition to the isotopic compositional variation the C/N ratios also show higher values around 8-10 (fig. A5), which are typical values for fresh algal derived organic matter (Meyers, 1997).

3.4 Elemental concentrations

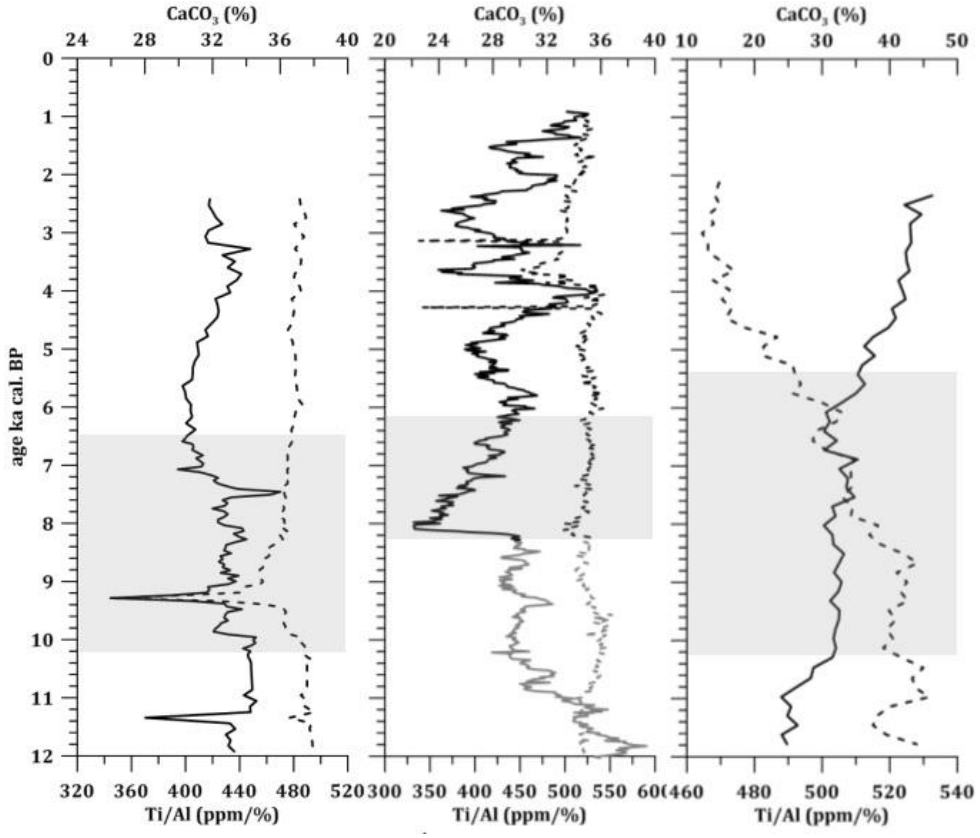

figure 12. CaCO3 (%) (solid lines) andTi/Al. (dashed lines) (ppm/%) profiles for the last 12kaBP for the the three cores. The grey shaded area indicates the sapropel S1 interval. Left MP50PC, middle KN3, right: SL73BC.

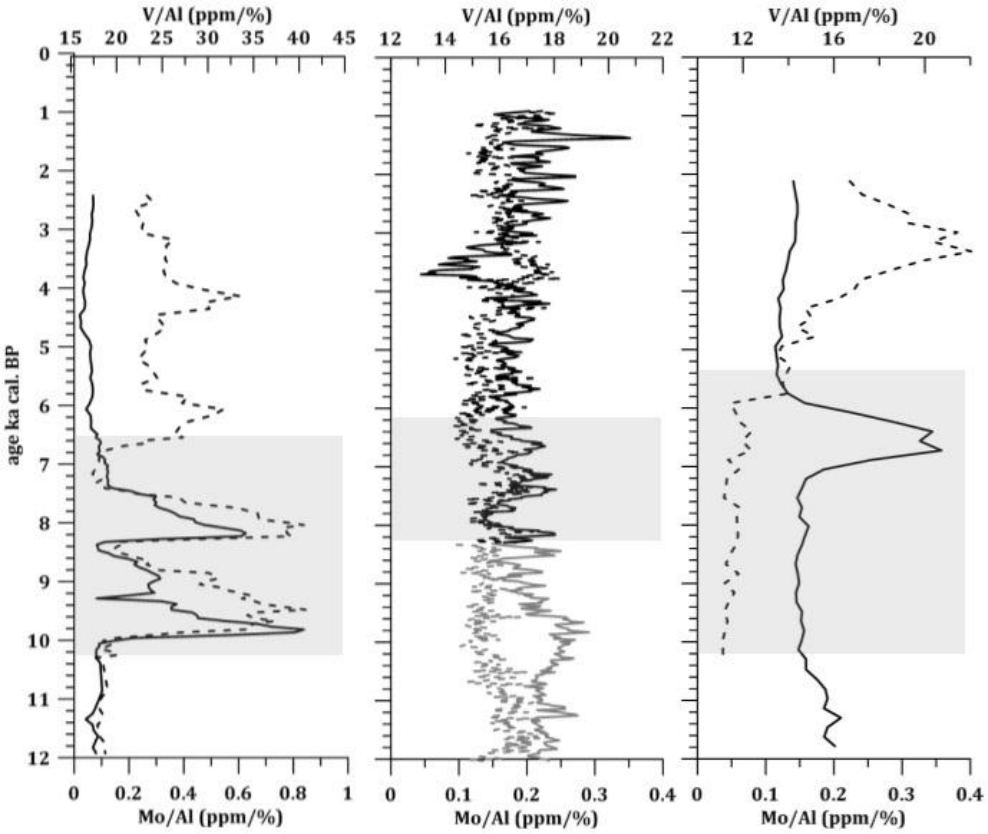

figure 13. V/Al (solid lines) and Mo/Al (dashed lines) (ppm/%) profiles for the last 12kaBP for the three cores. The grey shaded area indicates the sapropel S1 interval. Left MP50PC, middle KN3, right: SL73BC.

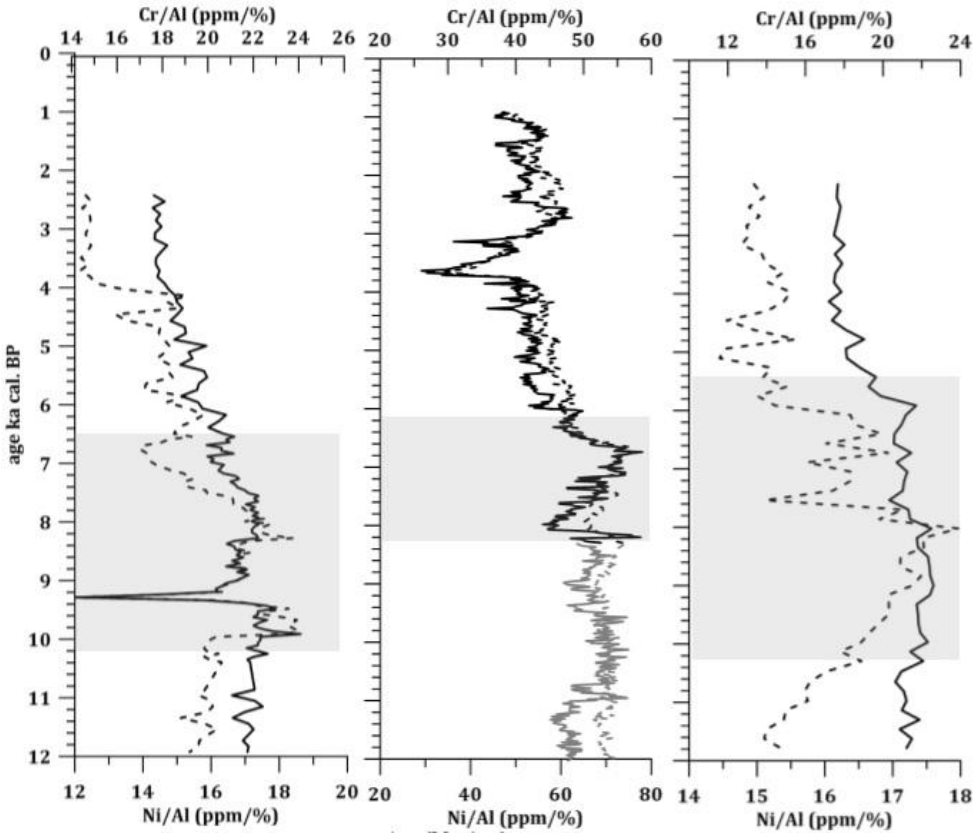

figure 14. Cr/Al (solid lines) and Ni/Al (dashed lines) (ppm/%) for the last 12ka for the three cores. The grey shaded area indicates the sapropel S1 interval Left MP50PC, middle KN3, right: SL73BC..

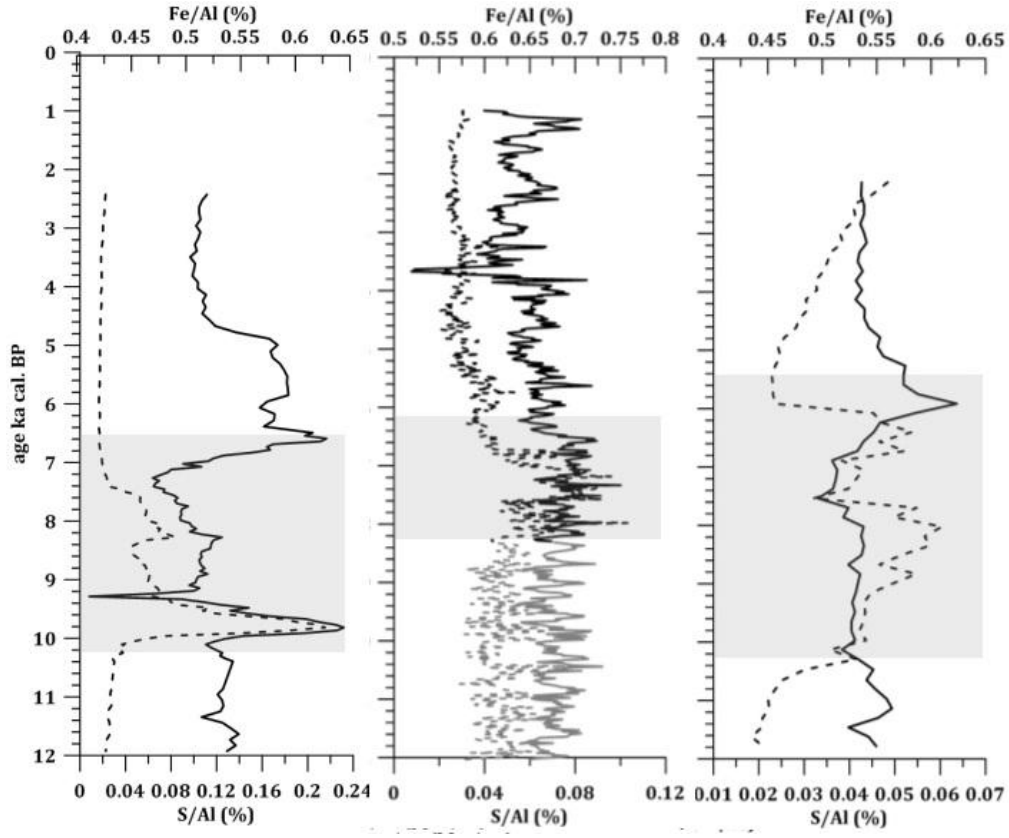

figure 15. Fe/Al (solid lines) and S/Al (dashed lines) (ppm/%) for the last 12 ka for the three cores. The grey shaded area indicates the sapropel S1 interval. Left MP50PC, middle KN3, right: SL73BC.

During the sapropel time interval $CaCO_3$ (%) although rather constant, shows a slight trend to higher values. The concentration for most of the elements show distinguishable responses to the environmental changes occurred during sapropel S1 deposition. Trace metals and redox sensitive elements appear enriched during sapropel S1 formation, such as V, Mo, Cr and Ni, for the south Adriatic and North Aegean Sites. The V/Al profile covary consistently with TOC(%) and Ba/Al ratios, whilst the rest of the elements show a closer relation ot S/Al (%). The profiles of these elements from south Aegean site show high frequency variability and an overall slight enrichment during S1. Lastly, in south Aegean Sea site the concentrations in redox sensitive elements are higher than at the other two sites, with exception of high peaks in certain time periods within the S1 layer. Ti/Al ratios from the South Aegean and Adriatic Sea sites show rather constant concentrations and no major shifts during sapropel S1 formation can be detected with the former exhibiting mich higher values in general. In North Adriatic Sea Ti/Al ratios show as high background values as the South Aegean sea records but gradually decreases during S1 (fig.12-15).

In South Adriatic Sea site a distinct event at 9.4 cal. ka can be observed with the redox sensitive elements as well as the Ti/Al ratios dropping dramatically. Sharp high peaks in K/Al, Cu/Al, Sr/Ca, Zn/Al, Zr/Al and Na/Al accompanied with low peaks in Co/Al, Mg/Al, Ni/Al and Cr/Al profiles. This event is also accompanied with lower TOC(%) and Ba/Al values (figures 9-15 and A7-A10).

3.5 Oxygen and carbon isotopes

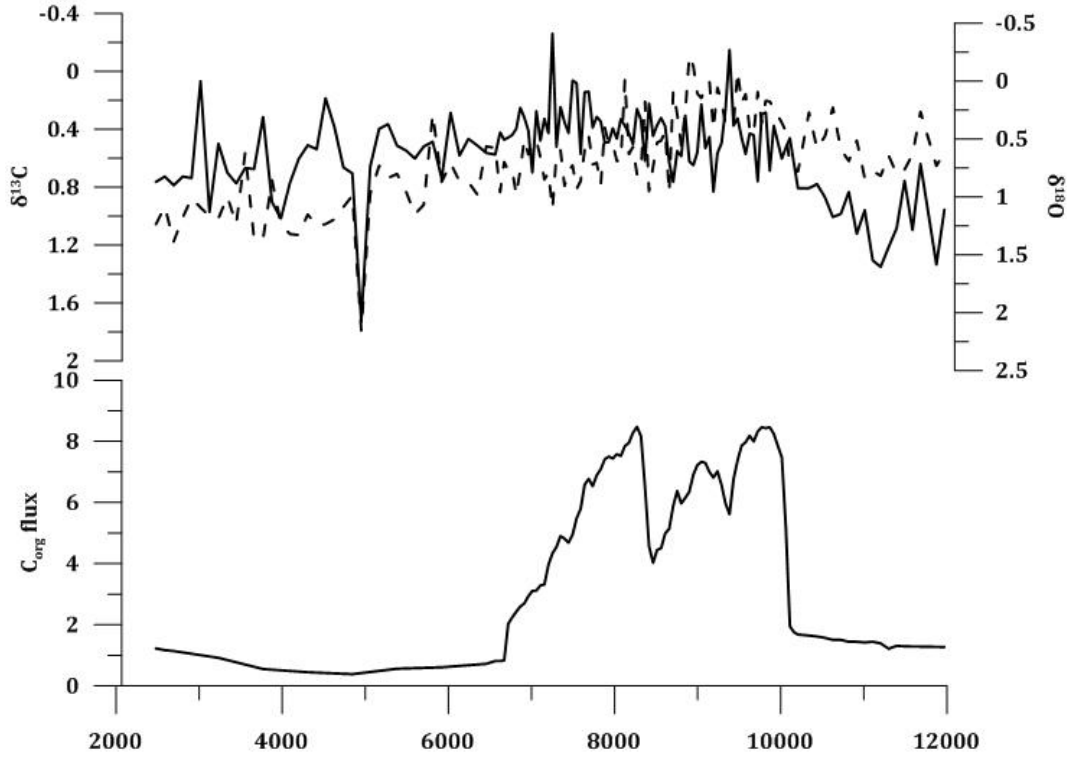

figure 16. MP50PC. Corg flux (gC/cm²/yr), $\delta^{13}C$ (dashed lines) and $\delta^{18}O$ (solid lines) (‰) for the last 12ka BP measured in G.ruber forams white.

The general trend in the oxygen and carbon isotopes of foraminifer *G.ruber* (white) is a shift to lighter values during the sapropel interval. Despite the considerable scatter in the data, $\delta^{13}C$ and $\delta^{18}O$ values during sapropel S1 is ~0.5‰, while before and after this period these values are ~0.6 and 0.9‰ and ~1.6 and 0.7‰ respectively.

3.6 Paleoproroductivity

		average PaP	
core	***pre S1***	***sapropel S1***	***post S1***
KN3	*131*	*159*	*133*
SL73BC	*76*	*90*	*80*
MP50PC	*98*	*126*	*78*

Table 4. Paleoprodutivity estimation for all three cores during sapropel S1 formation before and after this interval according to Saenthein et al. (1992).

		average PaP	
core	***pre S1***	***sapropel S1***	***post S1***
KN3	*39*	*89*	*43*
SL73BC	*73*	*146*	*89*
MP50PC	*65*	*95*	*31*

Table 5. Paleoprodutivity estimation for all three cores during sapropel S1 formation before and after this interval according to Müller & Suess (1979).

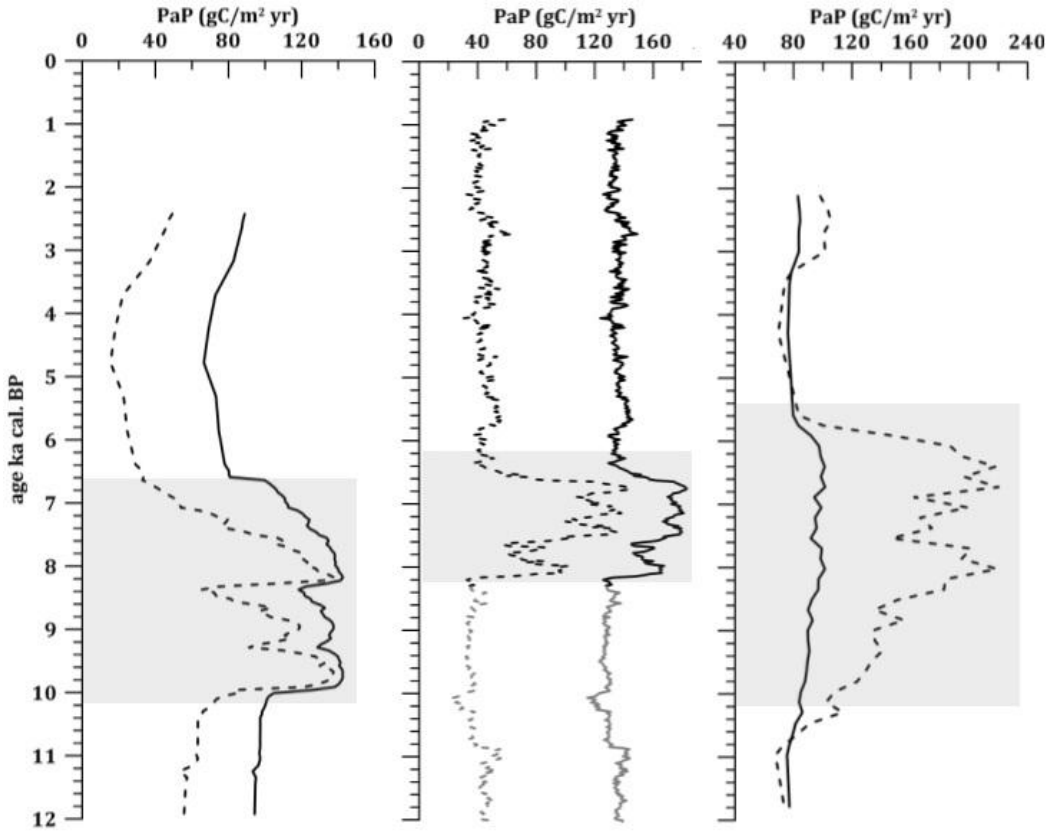

figure 17. Paleoproductivity profiles according to Sarnthein et al. (1992) (solid lines) and Muller & Suess (1979) (dashed lines) for all three cores. The grey shaded areas indicate the sapropel S1 interval. Left MP50PC, middle KN3, right: SL73BC.

4. DISCUSSION

The three cores that have been used in this study all come from the two main areas of eastern Mediterranean deep-water formation. In addition, one core for each area has a high sedimentation rate. Therefore, the cores of this study may provide useful information on deep-water formation and other processes that have occurrred during sapropel S1 formation. The absence of deep-water formation has been reported as one of the main factors of organic matter preservation in the deep Mediterranean basin, during sapropel S1 formation. In addition, there is increasing evidence that conditions were not stable during sapropel S1 formation. Not only the 8.2 cal ka BP interruption, but potentially also other smaller interruptions may have occurred (see introduction). Therefore, the sediments from the selected cores are expected to have recorded even smaller pulses of deep water formation as these are near the source area. In addition, the high sedimentation rates enhance the possibility to document such low amplitude variations during sapropel formation. First the general sapropel features will be assessed for these areas. Subsequently, details of diagnostic elements and elemental ratios will be used to unravel possible variations within the S1 period.

4.1 Sapropel vs non Sapropel

4.1.1 Paleoproductivity and preservation of organic matter

In general, Eastern Mediterranean sediments exhibit low concentrations of organic carbon due to the oligotrophic conditions prevailing in the basin (Bethoux, 1989). The low organic carbon content found in the surface sediments of our cores is in line with this. These organic-lean, marly sediments are interbedded with relatively thin units of organic-rich sediments, the so called sapropels (see Introduction). For sapropel sediments, a clear relationship has been reported between $\%C_{org}$ and waterdepth (Murat & Got, 2000; Mercone et al., 2000; De Lange et al., 2008). The moderate level of $\%C_{org}$ found for sapropel S1 in our cores, corresponds to the relatively shallow depths from which these cores have been collected. In all three cores used in this study the shape of the profiles of TOC (%) and Ba/Al ratios within each core is identical, indicating that postdepositional oxidation did not take place in the upper-most part of the sapropel (Van Santvoort et al., 1996). This is most probably due to high sedimentation rates and thus the presently visible sapropel represents the actual initial sapropelic layer. The Ba/Al ratios vary consistently with the TOC concentrations confirming the strong relation between barite and C_{org} deposition. Ba enrichments especially in the youngest sapropel have been related to marine barite and are thought to represent organic matter fluxes (van Santvoort et al., 1996; Thomson et al., 1999; Martinez – Ruiz et al., 2000). Thus, the elevated concentration of Ba in the sediments underlines the significance of productivity and potentially preservation in the formation of sapropels. The higher levels of productivity can also be attested from the paleoproductivity calculations (table 4, table 5, fig. 16) and C_{org} fluxes in all three studied areas appear elevated (Appendix fig. A6). Despite which equation has been used, during sapropel formation productivity appears to be significantly higher comparing to the background values as well as to the present (fig.16). Unambiguously, in order to achieve this high rate of organic matter accumulation, enhanced preservation is required (Rijk et al., 1999; Nijenhuis & De Lange, 1999). The latter can be attributed merely to rapid burial after deposition but most likely also to reduced oxygen conditions which would prevent decomposition of the organic matter. The anoxic bottom-water conditions have been attested by the high enrichments in redox sensitive elements and trace metals in sapropelic sediments (see discussion below). Notwithstanding, Nijenhuis et al (1998) in order to explain the high accumulation of these elements, showed that the ocean circulation although reduced, must have persisted during this time interval. All information thus points to elevated productivity and preservation to be associated with sapropel formation.

4.1.2 Timing of sapropel S1 formation

As discussed in Introduction and above, in all three cores the current visual sapropel represents the actual initial sapropel layer since the effect of a post depositional oxidation front is negligible. Consequently, the observed timing for the end of sapropel S1 cannot be due to post-depositional oxidation but rather must represent the actual ending of sapropel deposition. The end of sapropel deposition as determined by the TOC and Ba/Al records appears to occur at ~ 6.2 and 6.6 cal ka BP ± 300 yr in the South Aegean and Adriatic Seas respectively, and at ~5.6 cal ka BP (± 500 yr) in the North Aegean Sea. Considering that the uppermost S1 boundary at the North Aegean site has been difficult to detect due to substantial bioturbation (see fig.7), the derived values for the ending of S1 formation are in line with the basin-wide synchronous ending of S1 (de Lange, et al., 2008). The latter authors report 6.1 ± 0.3 cal ka BP and 10.8 ± 0.3 cal ka BP for ending and start of S1 deposition respectively. The value for the onset of S1 formation is identical for the North Aegean and South

Adriatic site, and could not be determined for the South Aegean Sea site. The ages calculated for the ending of S1 deposition are similar for the southern Adriatic and the south Aegean site both being slightly earlier than the reported synchronous S1 formation (6.6 and 6.2 vs 6.1 cal ka BP)), Differences in the duration of sapropel formation have been reported in some other studies, especially in sediments derived from relatively shallow depths (Mercone et al., 2000, Almogi-Labin et al., 2009). Such early ending of sapropel formation could be related to bottom waters to be fully oxygenated in areas of bottom-water formation earlier than elsewhere or to a diminished primary production. However, the age difference for the end of the sapropel S1 between South Aegean and Adriatic Sea sites is within the uncertainties of the age models. Such potential early ending of sapropel S1 formation has been observed only for relatively shallow sediments in areas of deep-water formation. Sample resolution and methodology to derive the ending of sapropel formation may as well contribute to this enigma. In the south Adriatic core, an important re-ventilation event occurs at 7.5 cal ka BP, after which environmental conditions seem to remain oxic/suboxic (as detected from e.g. Mn/Al, Mo/Al and V/Al proxies; see below at: 4.2 Interruptions) until the final ending of S1 formation at 6.6 cal ka BP (as detected from C_{org}% and Ba/Al profiles). It is possible that benthic organisms entered the scene after the 7.5 cal ka BP event, whereas the progressively decreasing %C_{org} and Ba/Al still indicate sapropel productivity/preservation conditions (Jorissen et al., 1993; Rijk et al., 1999). As a consequence, it depends on the diagnostic tools used for detecting the end of S1, which age is assigned to this. It seems in general that reventilation thus re-oxygenation has caused the end of enhanced preservation, whereas surface water primary productivity may still have continued at an enhanced level. Depending on local conditions such as sedimentation rate, water depth, and distance to the area of deep-water formation thus oxygen supply, this may have resulted in still enhanced levels of Ba and Corg, or not.

Table 6. In this table the S1 boundaries and the two interruption events of S1 are given in cal ka BP.

	S.Aegean Sea [a]	***N. Aegean Sea*** [a]	***S. Adriatic Sea*** [a]	***Literature***
top S1	*6.2±0,3*	*5.6±0,5*	*6.6±0,3*	*6.1±0,5* [b]
"7.5 cal ka BP event"	*7.3±0,3*	*7.5±0,5*	*7.3±0,3*	*7.9-7.1* [c] *Aegean Sea 7.3-6.7* [d] *S.Central Mediterranean*
"8.2 cal ka BP event"	*8.2±0,3*	*8.4±0,5*	*8.3±0,3*	*8.2±0,3* [e]
bottom S1	-	*10.2±0,5*	*10.2±0,3*	*10.8±0,4* [b]

(a). this study, (b). de Lange et al. (2008), (c). Geraga et al. (2008), (d). Desprat et al. (2012), (e) Rohling & Palike (2005).

4.1.2 Sedimentary redox conditions

Prior to an evaluation of trace metals as potential redox proxies, the general redox-related processes in the sediments of the three cores need to be assessed. The absence of a distinguishable downward progressing oxidation-front has been discussed above, thus trace element observations within S1 can be considered to represent initial depositional conditions. At the end of S1 formation, water-column conditions are thought to have changed from suboxic, with enhanced dissolved Mn levels, to oxic conditions. Therefore, this major deep-water re-ventilation event has resulted in a distinct Mn/Al peak, coinciding with or just above the end of enhanced Ba/Al levels indicative for the end of S1 formation (e.g. fig.7; De Lange et al., 1989; Van Santvoort et al., 1996; Reitz et al., 2006b; De Lange et al., 2008). The observed post-S1 variability in Mn/Al for the North Aegean and Adriatic cores may reflect non-steady-state changes and concording variability in sedimentary oxygenation. The Mn-peak related to a basin-wide re-ventilation, usually contains substantial amounts of trace elements, Mo in particular (e.g Reitz et al., 2006b). The latter is visible for MP50PC at 6.6-6 cal ka BP (fig. 10). The basin-wide reventilation event at the end of sapropel S1 formation is observed for Adriatic and North Aegean sites but not for the South Aegean site (see pronounced Mn/Al peak at ~ 6.3 cal ka BP; fig. 10). In the former two cores, a clear transition is seen going from low Mn/Al values within S1-indicating suboxic to anoxic sedimentary conditions, to enhanced Mn/Al values that are indicative for oxic/suboxic conditions. In addition, the post-S1 values are similar to, or even higher than, present-day surface sediment values, known to represent oxic bottom water and surficial sediment conditions. For the South Aegean core, the general Mn/Al values are rather constant throughout the core except for the pronounced peak at 7.3 cal ka BP. The latter and detailed variations within S1 for the other cores will be discussed below, under 4.2 Interruptions. At first sight, the absence of a detectable re-ventilation Mn/Al peak at the end of S1 for the South Aegean site seems surprising. However, it needs to be realized that this re-ventilation peak is thought to be mostly water column related. Therefore, a high sedimentation rate of in particular terrestrial material, as is the case for KN3, will

substantially dilute such signal (post-S1 sedimentation rates for North Aegean, Adriatic, and South Aegean sites are respectively. 3, 4.5, and 27 cm/ka (see 3. Age model & Sedimentation rates). In Mediterranean sediments, most of the Mn is present as Mn-oxide and in Al-silicates, and sometimes as $MnCO_3$ (Van Santvoort et al., 1996; Reitz et al., 2006b). The low Mn/Al found within sapropel S1 for the North Aeagen and Adriatic core (~ 80-100 ppm/%) in the presence of sulphides (pyrite), indicates that no Mn-oxides remain. In contrast, the enhanced levels of Mn/Al for the South Aegean (~200 ppm/%) site is indicative for the sustained presence of Mn-oxides, thus suboxic conditions, throughout S1 and until the present. This is in agreement with the suggested absence of fully and persistent anoxic conditions in South Aegean ocean water (Aksu et al., 1995; Mercone et al., 2001; Casford et a., 2003; Abu-Zied et al., 2008; Marino et al., 2009).

As enhanced regeneration of sedimentary phosphate is known to occur only for oxygen-free sedimentary conditions (Slomp et al., 2002; Slomp et al., 2004), the C_{org}/P_{tot} proxy clearly indicates that those conditions for all cores were oxygen-free during S1 formation, thus potentially with enhanced dissolved porewater Mn^{2+} concentrations. The latter concords with observations by Ní Fhlaithearta et al. (2010), who have concluded that an enhanced level of porewater and bottom-water Mn^{2+} has occurred during S1 deposition in the Aegean Sea. The rather low S/Al (~0.04 ppm/%) levels for the South Aegean core, although much higher than for the other two sites, is consistent with such suboxic conditions: The background levels of 0.02-0.04 %/% found for all cores outside S1 are thought to be related to porewater sulphate that upon drying of the samples has become part of the total analysed sediment. At the South Aegean site, the S/Al levels within S1 are only marginally enhanced, indicating a minor sulphide production -if any-, thus no substantial anoxic conditions during sapropel formation. In contrast, the other two sites have considerably enhanced levels of S/Al that are associated with pyrite formation (FeS_2), thus indicating anoxic sulphidic sediment conditions during S1 formation. The enhanced FeS_2 levels do not only coincide with high $\%C_{org}$ but also with Mo/Al and V/Al enrichments (fig. 9, 13 & 15). High levels of C_{org} have resulted in considerable sulphate reduction, thus FeS_2 formation, and enhanced S/Al. In addition, the association of C_{org} and V has resulted in enhanced V/Al, whereas the association of Mo with sulphides has produced coinciding enhanced levels of Mo/Al and S/Al. In summary, the deposition of sapropels coincides with suboxic deep-water conditions and suboxic to anoxic sedimentary conditions. Enrichments in trace metals and redox sensitive elements such as Mo and V are commonly associated with redox conditions in modern and ancient sedimentary records (e.g. Calvert & Pedersen, 1993). These have also been reported for eastern Mediterranean sapropels from Pliocene to Holocene (e.g. Thomson et al., 1995; Nijenhuis et al., 1999; Gallego-Torres et al., 2010). Trace metal enrichments for the sapropel S1 interval are clearly distinguishable in the North Aegean and Adriatic cores but not so much in the South Aegean core.

The presence of trace metals such as Mo and V reflects the redox conditions in the water column and the sediments (fig. 9) (Calvert & Pedersen, 1993). Similarly, high concentrations of Cr, Ni, Zn, Cu and Co in sediments have been linked to low oxygen conditions in the water column and the sediment-water interface (Calvert & Pedersen, 1993; Warning & Brumsack, 2000; Calvert & Pedersen, 2007; Gallego Torres; 2010). Fe and S enrichments have been associated to pyrite formation (FeS_2) which in turn can be used as an indicator of anoxic conditions, whilst during its precipitation trace metals often are incorporated.

The precipitation of Mo and V elements describes different states of anoxia and can be used in order to determine the severity of oxygen depletion during the sapropel formation. V precipitates under moderate suboxic conditions (Emerson & Huested, 1991), whilst Mo fixation requires fully anoxic environments and high dissolved sulfide concentrations (Helz et al., 1996). Mo specifically often shows high concentrations under oxic conditions as well, due to its scavenging by MnO_2 (Nameroff et al., 2002). In marine environments V precipitation is largely associated to organic carbon flux under reduced oxygen condition (Tribovillard et al., 2006; Rutten et al., 1999), and thus V/Al can be considered as a reliable proxy for enhanced organic matter fluxes and sustained suboxic conditions. Similarly, Cu appears enriched under suboxic conditions and its precipitation is associated with organic matter accumulation or Fe – and Mn- oxyhydroxides under more restricted conditions. Ni and Cr in general co-vary with TOC under non-sulfidic anoxic facies whilst under sulfidic conditions its precipitation is related to pyrite formation. Conversely, Co enrichments do not show a strong correlation with TOC and its precipitation is associated more to the presence of sulfides under anoxic conditions (Algeo & Maynard, 2004). Due to the different processes controlling the precipitation of these trace metals, i,e, the water-column inventory, sedimentation rate, diagenetic processes, the co-presence of these elements can describe better the redox state of the bottom water and the sediment.

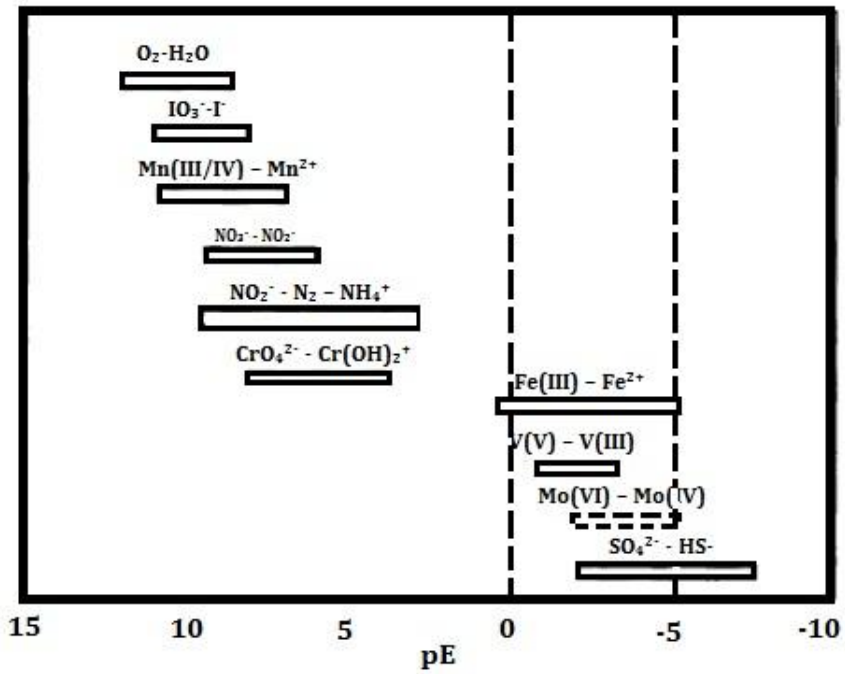

figure 188. Redox couples and predicted pE ranges for seawater (modified from Rue et al., 1997; Mo and V pE ranges after Turner et al., 1981).

In the South Aegean site the continuously relatively high levels of Mn/Al in combination with the low V/Al and Mo/Al indicate the absence of severe or permanent anoxic conditions during deposition of the sapropel S1 (Morford & Emerson, 1999). On the contrary in the South Adriatic Sea core suboxic to anoxic conditions were established already from the beginning of the sapropel formation, although remarkable variations seem to have occurred through time (see discussion below), as it can be attested by the significant enrichments in Mo/Al, V/Al, S/Al and Fe/Al ratios (fig. 13 & 15). In particular, V/Al profiles is tightly coupled with TOC(%) during the formation of sapropel indicating anoxic conditions during the high organic matter accumulation. The North Aegean site records show moderate levels of anoxia especially during S1a; the V/Al ratio implies a progressive development of reduced conditions. V/Al profile coupled with the organic matter content show a moderate enrichment during S1a followed by a distinct high peak during the deposition of S1b, when higher amounts of organic matter were deposited. Fe/Al and S/Al profiles indicate that strictly anoxic conditions may have been established during the S1b interval in North Aegean Sea. In contrast, the Mo/Al profile indicates that sulfidic anoxic conditions were not developed in this site and thus extensive pyrite formation did not take place, observation consistent with the relatively low Fe/Al ratio. Additionally, the co-occurrence of V and Mo in all three studied sites, at least for a small period, indicates euxinic conditions in the sediment/water interface and/or the water column (Tribovillard et al., 2006).

The different oxygen conditions of the water column between the three sites are also confirmed by the anoxia indices V/(V+Ni) and V/Mo. All three sites exhibit values within the slightly dysoxic range (V/Mo>60) (Piper & Calvert, 2009) whilst V/(V+Ni) indicate that only in the South Adriatic Sea dysoxic conditions in the water column have been developed during sapropel S1 deposition (fig. A22 & 23) (Hatch & Leventhal, 1992; Gallego-Torres et al., 2007). The two indices, Ni/Co and V/Cr showed exact opposite conditions prevailing with the former indicating oxic conditions and the latter dysoxic to anoxic conditions. This is probably due to the fact that the total sedimentary Cr and Ni content is not only influenced by redox conditions but also by sediment provenance. High influxes in both elements have been recorded in Aegean Sea draining from Greek and Turkey rivers (Wehausen & Brumsack, 2000; Hamman et al., 2008), whilst Po river and in particular mid-Italian rivers such as Ofanto are major contributors of this elements to the Adriatic Sea (Goudeau et al., 2013, submitted). Accordingly, their content in the South Aegean core is persistently high, thus it is the lack of variability that is consistent with paleoceanographic changes that exclude these elements as redox proxies for this site.

Distinguishable enrichments in other trace elements such as Co and Cu also occur and seem to concur with redox conditions at least to some extent (fig. A9). All these elements exhibit high enrichment factors compared to average shales, not only within the sapropelic sediments but also in the sediments deposited prior and after sapropel deposition (fig. A13-18). Therefore, comparing the elemental ratios to the average shales is not that useful for these particular sites.

Nevertheless, all these elements show higher concentrations during the sapropel interval or just above it and fluctuate either in accordance to C_{org} content or show a strong correlation to Fe/Al profile suggesting that their precipitation is linked to pyrite formation. For the south Aegean Sea site, the profiles of Co/Al and Cu/Al are similar to those of C_{org} and only the latter shows a slight enrichment during sapropel formation. Cu/Al profiles in both North Aegean and South Adriatic Sea sites show great similarities with V/Al profiles and consequently their enrichments appear to be associated to organic carbon fluxes. The Co/Al ratios appear to be relatively enriched, but their variations are more complex. It partly resembles the Mo/Al fluctatuation for the South Adriatic and North Aegean Sea site and thus it may reflect the redox state of the sedimentary record. Additionally, in the North Aegean and Adriatic cores, the Co/Al profiles indicate that their post-S1 enrichment is related to Mn—oxyhydroxides.

Comparing the general environmental conditions for sapropel versus non-sapropel formation as indicated by a range of potential proxies, there is a clear distinction between the South Aegean site and the North Aegean and Adriatic site. This is thought to be related to the enhanced sedimentation rate and concomitant influx of Mn-oxide minerals for the former site. The predominant presence of Mn-oxides together with the moderate presence of C_{org}(%) prevents the sediments of this site to become fully anoxic, i.e. sulphidic. In contrast, the sediments of the North Aegean and Adriatic sites, clearly demonstrate that conditions during S1 formation were mostly anoxic and sulphidic. In any case, such suboxic to anoxic conditions have contributed to the enhanced preservation of organic matter during S1 formation and to the enhanced release of phosphate thus sustaining primary productivity.

In addition to the different redox conditions between sapropel and non-sapropel deposition discussed above, interruptions are observed within the S1 interval. Such variability observed in the redox-related trace element concentrations for the cores of this study concur to a discontinuous suboxic/anoxic environment during sapropel S1 formation. The studied sites are located nearby areas where bottom-water formation occurs, hence are highly sensitive to even small repulses of water formation. These sites are, therefore, very suitable for the study of environmental variability within the S1 formation period.

4.2 Within sapropel S1 variability and interruptions

During S1 deposition additional fluctuations in the TOC(%) concentration and Ba/Al ratios, observed in the cores of this study, indicate variations in productivity and preservation of the organic matter. This variability indicates that the high primary production oscillated through time, whilst the reduced environmental conditions favoring its preservation, as discussed above, also varied. In the South Aegean and Adriatic sediments, abrupt interruptions of high primary production and accumulation of organic matter are accompanied by a dramatic drop in redox proxies such as V/Al and Mo/Al. Such abrupt changes are not so well expressed in the relatively shallow North Aegean core, which sediments have an enhanced bioturbation and a rather low sediment accumulation rate and concomitant sample resolution (sample resolution for N.Aegean, S. Aegean, and Adriatic S1 sediments is approximately 165, 20, and 50 years respectively).

As discussed above in 4.1.2, enhanced levels of Mn/Al usually are associated with more oxic conditions, whereas low Mn/Al such as within S1, indicate reduced, i.e. suboxic to anoxic conditions. In addition, in these high sedimentation rate cores there has been no impact of a downward prograding oxidation front. Consequently, all observed variability can be related to intial water column and sediment environmental, i.e. redox conditions. The continuously rather enhanced levels of Mn/Al in the South Aegean core has been attributed to nearly continuous oxic/suboxic conditions in watercolumn/sediment. The major Mn/Al peak at 7.3 cal ka BP in this core can only be related to an important oxygenation event, involving water column and surface sediment (fig. 18). At exactly the same time interval, a small but distinct Mn/Al peak is also observed in the Adriatic core, pointing to this event to be not only limited to the Aegean but also to extend into the eastern Mediterranean basin. In the Adriatic core MP50PC, a more enhanced Mn/Al peak is observed at 8.3 cal ka BP, which is thought to relate to the 8.2 cal ka BP reventilation event (e.g. Rohling et al 1997; 2002). The latter event has mainly been reported for Aegean sediments; unfortunately, the sediments of this interval have not been recovered in core KN3 of this study (see 3. Age model). This “8.2ka event” (Rohling et al., 1997) has been identified not only in the sedimentary records across the basin but also in on-land records (e.g. Bar-Matthews et al., 2000; 2003; Pross et al., 2009) and connotes the direct response of the basin to Northern Hemisphere climate conditions. The associated climate deterioration is thought to relate to cold and dry air masses reaching the Eastern Mediterranean causing the resumption of the bottom water formation and thus to the oxygen conditions to be (briefly) restored in the basin (see 1.2). Compared to this ‘8.2 cal ka BP event’, the ‘7.5 cal ka BP event’ is not so well represented in the literature. This event has mostly been described as onset of seafloor oxygenation as deduced from the repopulation of the seafloor

with oxic benthic fauna in Adriatic Sea (Jorissen et al., 1993) and from changes in the isotopic composition of planktonic foraminifera and dinoflaggelate cysts assemblages in the central Aegean Sea (de Rijk et al., 1999; Triantafyllou et al., 2009; Geraga et al., 2010). Re-oxygenation of the water column and an increase in sea surface water temperatures have been reported for the southeastern Aegean Sea. The combination of higher temperatures and lower humidity centered at around 7.9-7.3 cal ka BP has been attributed to a weakening of the African monsoon (Gogou et al., 2007; Kouli et al., 2012). The pollen records corroborate the establishment of more dry conditions at 7.9 cal ka BP and 8-7.6 cal ka BP in central Italy and Sicily respectively (Dormoy et al., 2009). Siani et al., (2009 & 2010) observed a climatic deterioration and vertical mixing of the water column which they linked to a cold episode recorded in isotopic composition of stalagmites in a southeastern part of Romania, as well as in speleothems from Central Italy and Northern Sicily (Zancheta et al., 2007). The latter attributed the end of enhanced rainfall around the 7.4 cal ka BP and shifts in isotopic composition of stalagmites to the end of the increased monsoon activity and thus the end of the sapropel formation, like several authors who studied marine cores from the Adriatic Sea (i.e. Arzitegui et al., 2000; Mercone et al., 2001; Giunta et al., 2003). Vegetation turnover has also been reported by Desprat et al. (2012) at the southern central Mediterranean region pointing to a cold and dry episode. Bar-Matthews et al. (2000) reported a major shift in $\delta^{18}O$ values in spelothems from Israel centered at 7 cal ka BP. In the North Aegean Sea a prominent event of climate deterioration has been recorded in pollen records between 7.5-7.2 cal ka BP (Kothoff et al., 2008) and at 7.1 cal ka BP a dry and cold phase has been recognized from changes in deep-sea epifauna (Kuhnt et al., 2007) and correlated to cold episodes in the Northern Hemisphere climate (fig.20). The combination of the lowered humidity and temperature could have been responsible for the resumption of the bottom water formation and thus for the re-establishment of normal oxygen conditions in the deeper water column. The characteristics of this event, that led to the temporal cessation of sapropel S1 deposition, is thought to reflect a cooling event analogous to the 8.2 cal ka BP even. Furthermore, due to its wide spatial distribution, this event is most probably related to an abrupt temporal shift in Northern Hemisphere climate. The slight age offsets of this event between the records can be attributed to age uncertainties involved for each of the age models.

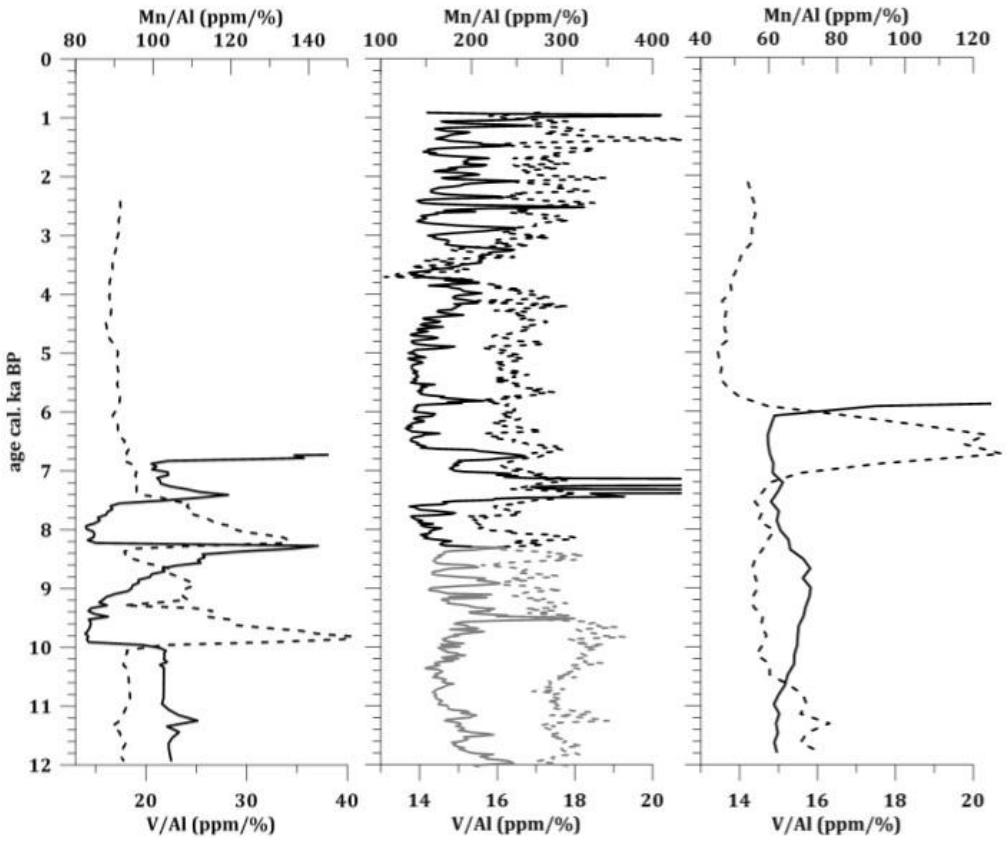

figure 199. Mn/Al (solid lines) in enlarged scale and V/Al (dashed lines) for the MP50PC (left plot), KN3 (middle plot) and SL73BC (right plot)

In the South Adriatic core there is a clear decrease of TOC(%) and Ba/Al ratio at ~7.5 cal ka BP that concurs with a small but distinct increase in Mn/Al, and a rapid drop in Mo/Al and V/Al. All of these consistently point to a reventilation event, thus re-oxygenation of the deep water. In the Adriatic Sea, a disturbance has been detected in several stratigraphic

records at 7.5 cal ka BP but mostly has been considered to reflect a regional cooling and it has not been linked to similar observations from records in other locations of the Mediterranean basin (e.g. Ariztegui et al., 2000). In the South Aegean core a distinct decrease in organic carbon content and Ba/Al can be observed at 7.6 cal ka BP too. This feature is also present at the North Aegean Sea core at ~7.5 cal ka BP but is less well expressed due to the rather low sedimentation rate and potential biomixing. Smaller variations in TOC (%) can be observed in the latter two cores from this time to the end of the sapropel deposition. For the South Adriatic core it is evident, that conditions do not return to a full sapropel setting but rather remain at suboxic to oxic conditions. This observation fits very well with observed re-appearance of benthic organisms in the southern Adriatic from 7.5 cal kal BP onward (Jorissen et al., 1993; see also discussion above)

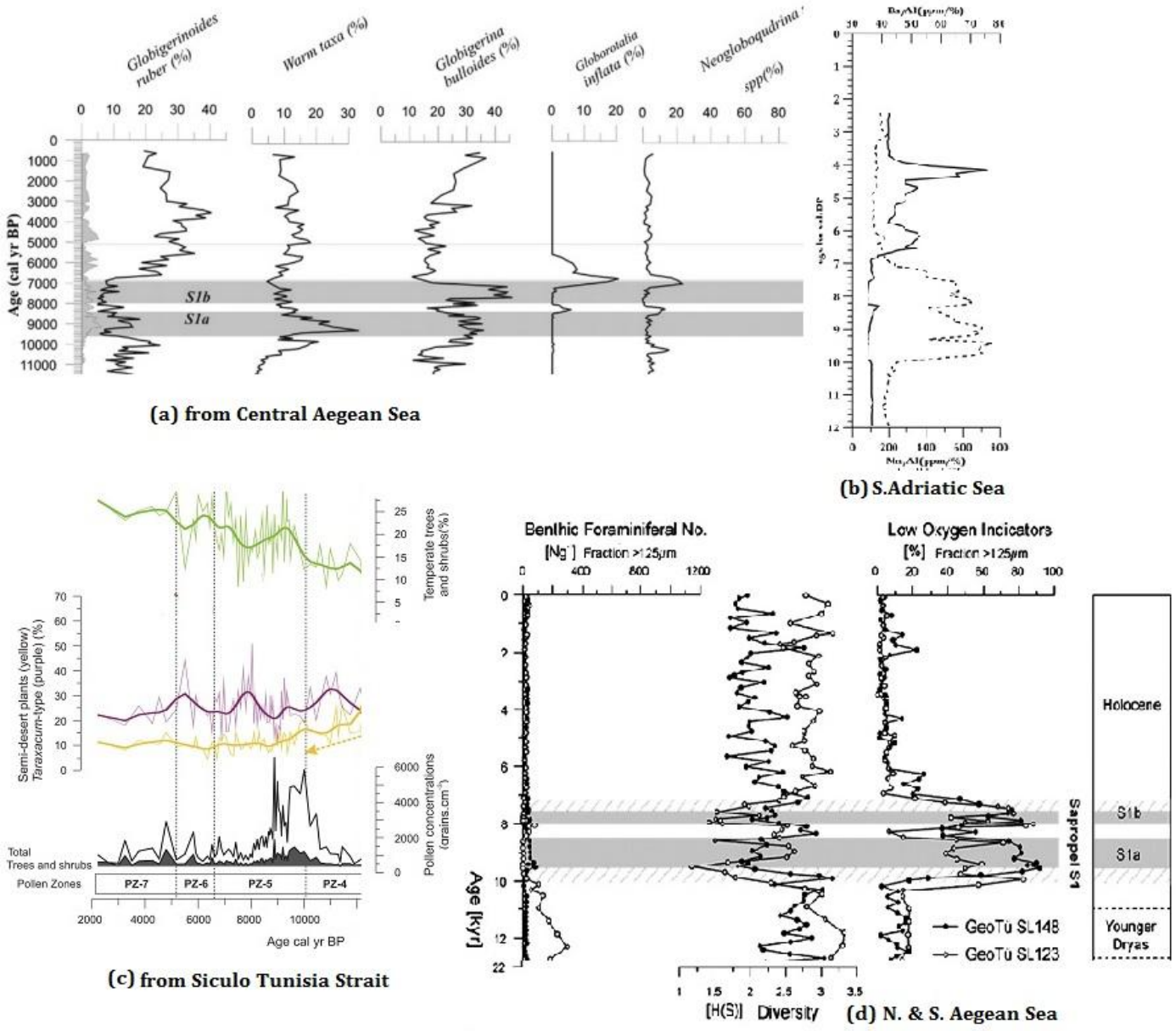

figure 20. Records from literature indicating a cooling event at approximately 7.3 cal ka BP. (a) Geraga et al. (2010), (b) MP50PC from this study, (c) Desprat et al. (2012) and (c) Kuhnt et al. (2007).

In the Adriatic Sea site, a short but pronounced interruption of the sapropel formation seems to have occurred slightly after its start, at ~9.3 cal ka BP. The V/Al profile which shows a strong correlation to organic matter deposition returns to background values, followed by the Ba/Al ratio and altogether suggest the temporal cessation of sapropel formation. However, there is a major discrepancy compared with the other interruptions discussed. Sharp high peaks occur at ~ 9.3 cal ka BP in K/Al, Zr/Al and Na/Al accompanied with low peaks in Mg/Al, Ni/Al and Cr/Al profiles. The relatively thin layer (about 3.5cm) appears to contain substantial amounts of pumice, as observed with a microscope with the highest amounts in the fraction 150-350μm. This is in line with the observed deviations of in particular the Ti/Al and Zr/Al. Caron et al. (2012) recognized five layers of cryptotephra in the 7-9 ka cal BP interval mostly consisting of micro-pumice and one tephra layer originated from the Pomici di Mercato eruption of the Somma – Vesuvius. The latter tephra layer has been dated at ~8.5 cal ka BP (Zancheta et al., 2011) whereas one of the cryptotephra layers is thought to have been deposited at 9.0±0.04 cal ka BP. The latter corresponds to the peak at 230cm (fig. 21). The other reported cryptotephra layers have been recognized at depths 175, 185, 210 and 216-218 cm and correspond to 7.0±0.05, 7.3, 8.1 and 8.27±cal ka BP. The detailed tephrostratigraphic study of the Adriatic Sea eliminates other possible sources for a tephra layer at the study area around this time. Nonetheless, the age difference between the event recognized in MP50PC and the cryptotephra layer is considerable (fig. 21).

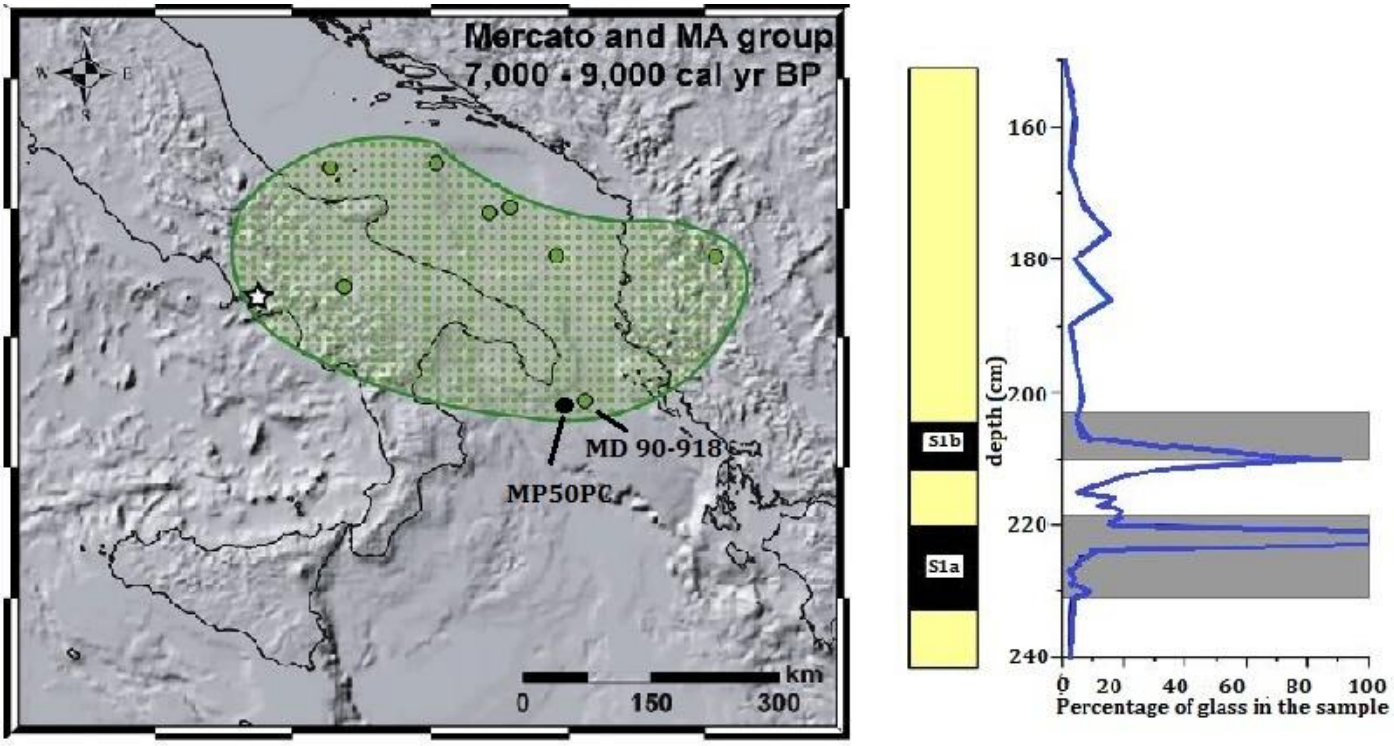

figure 21. Left panel: map of the Adriatic Sea indicating the distribution of Mercato eruption. Right panel: MD 90- 918 core and the percentage of glass. At 223 a tephra layer has been recognixed whilst the peaks below and above that have been attributed to cryptotephra (see text for details) (modified from Caron et al., 2012).

Notwithstanding, the characteristics of this event it cannot be fully excluded that there is a coincidence of two events, the volcanic ash deposit and an unrelated paleoceanographic event. The amount of allochthonous material needed to dilute the $\%C_{org}$, Ba/Al proxies is substantial thus there may have been a coincidental occurrence of events. The occurrence of a 9.3 cal ka BP event is not totally illusive, since an anomaly in $\delta^{18}O$ has been recorded in three Greenland ice cores at 9.3 cal ka BP (Rasmussen et al., 2007). This event appears shorter in duration than that of 8.2 cal ka BP but it is comparable in amplitude. Terrestrial records have also captured a decline in temperature at this time illustrating a climate induced change in the Adriatic Sea centered at 9.4 cal ka BP (Dormoy et al., 2009; Desprat et al., 2012). Due to low sedimentation rate and no recovery for this interval in the other two cores, this observation cannot be verified at a larger spatial scale. Further study is required to assess origin(s) and extent of this event.

4.3 Palaeoceanographic conditions during sapropel formation and their connection to climate variability

The present-day oceanographic setting in the Aegean Sea is regulated mainly by the fresh water flowing from the European rivers and the Marmara Sea. The connection with the latter was re-established at around 9.5ka BP (Aksu et al., 1999), slightly after the initiation of the S1 deposition. A similar regime prevails in Adriatic Sea as well, with high riverine influx and bottom water formation being the governing factors in the processes developing in the basin (Di Bella & Cassieri, 2011).

More humid climate conditions and related enhanced precipitation and riverine influx may lead to increased terrestrial, riverine sediment fluxes, whereas at the same time it results in a reduced aeolian input. Ti/Al and Zr/Al ratios are commonly used as proxies for dust input and usually decrease during sapropel formation. Ti/Al ratios show a small decline in the South Adriatic site and significantly in the North Aegean site. The K/Al and Mg/Al ratios which have been linked to riverine input from the northern mainland rivers show no response to the newly established climate conditions during sapropel deposition in none of the studied sites. This could be adequately explained by the high sedimentation rates which suppress the expression of different fractions and the concentration of these elements appear to be constant in the sediment and indirectly could be linked to the water depth. This could be in particularly the case for the South Aegean Sea. The more humid and warm conditions are also depicted in $\delta^{18}O$ and $\delta^{13}C$ values measured in *Globigerinoides ruber* by shifting to lighter values whilst carbon isotopes of organic matter shift to heavier values, suggesting a higher partition of marine origin organic matter. In contrast to the initial suggestions on the origin of the organic matter in sapropels, the isotopic composition reflects a ratio between terrestrial and marine origin for the two sites from South Aegean and Adriatic Seas. The less negative values in $\delta^{13}C$ of organic matter (~-22.8‰ and ~-23.2‰ for the S.Aegean and Adriatic Sea respectively) indicate a marine origin of organic matter and thus increase in primary production due to the higher availability in nutrients instead of a significant increase of the terrestrial component. Already, a general trend to less negative values can be observed starting from the onset of the Holocene and continuing during the time of sapropel deposition.

The Sr/Ca profiles of this study confirm the overall picture reported by others, namely an increasing level at the onset sapropel S1 (Thomson et al., 2004; Reitz & De Lange, 2006). However, in the South Aegean Sea site, Sr/Ca profile appears to be even more enriched after sapropel S1. The enrichment in Sr/Ca in the sapropelic sediments has been attributed to different processes. A near-coastal provenance related to Halimeda and diagenetic formation related to sulphate reduction have been suggested (Thomson et al., 2005; Reitz & de Lange, 2006). The latter process can be excluded for the South Aegean Site as discussed above, due to the relatively oxygenated bottom water which would not allow extensive sulfate reduction to take place.

The increased primary productivity as discussed above has been clearly initiated by the increased nutrient supply, whilst the weakened ocean circulation allowed the concentration of high amounts of nutrient in the deep water (Meier et al., 2004). The C_{org}/P_{tot} ratio also suggests oxygen-depleted bottom-water which promotes the regeneration of phosphorus to the water column and thus leads to sustained high productivity. The C_{org}/P_{tot} values are significantly lower than those mentioned by Kraal et al., (2006). The latter, however, used sapropels and black shales with significantly higher organic carbon contents. In the North Aegean Sea site, the profiles for C_{org}/P_{tot} and C_{org} seem highly correlated with that of the V/Al ratio. This suggests that regeneration of P is associated with enhanced Corg fluxes and thus with elevated primary productivity.

From this study it appears that the also previously reported "8.2 cal ka BP event" is not the only event that occurred during S1 deposition and that caused the temporal cessation of its formation. The 7.5 cal ka BP, recorded for all three sites of this study, represents a second important interruption that is comparable to the 8.2 cal ka BP event. Sustained severe winter outbreaks of cold and dry air masses are thought to be responsible for both interruptions. The latter are associated with the cooling-induced resumption of deep-water formation thus re-oxygenation of the water column both in the Adriatic (Siani et al., 2010) and the Aegean Sea (e.g Kotthoff et al., 2008; Geraga et al., 2010). The overall cooling of the climate is also reflected in the terrestrial records of the surrounding areas (Dormoy et al., 2009; Desprat et al., 2010). For the south Adriatic core, the 7.5 cal ka BP event is the onset of more continuous oxygenated conditions (see also discussion above). This is clear from a decrease in redox sensitive elements in combination with a slight increase in manganese-oxides that all argue for an increase in oxygen levels from that time onward. Although, the C_{org} content was relatively high at that time, it started decreasing rapidly along with the Ba/Al ratio. This indicates that sapropel formation or preservation diminished shortly after this reventilation event. The 7.5 cal ka BP re-ventilation event

in the south Aegean Sea. is evident but does not lead to a subsequent reduced sapropel formation/preservation for the remainder of the S1 period. The latter may be associated to the extremely high sedimentation rate at this site and the environmental conditions during S1 deposition to be suboxic rather than anoxic throughout (see discussion above). The preservation of organic matter and associated proxies is thus rather related to the high sedimentation rate at this site. In contrast, for the south Adriatic site, the bottom-water redox conditions are an important parameter for the preservation of proxies, thus any change threin will result in a change in preservation.

The sapropel deposition in South Adriatic Sea appears to be under more stable conditions than the ones described in Aegean Sea. The sapropelic layer development in the former can be described as a step-wise process with clear disruptions throughout time but definitely not as a continuous event. Reduced oxygen conditions seem to have been established for longer time periods, nonetheless varying in intensity and duration within this time interval. In South Aegean Sea high frequency variability under nearly oxic water conditions can be distinguished whilst in North Aegean Sea site where dysoxic to anoxic conditions have been developed a low frequency variability is present in all profiles. The water depth in combination with the sedimentation rates appear to control the expression of these fluctuations. Nonetheless, the distinct variations in most of the elemental profiles advocate the high frequency variability in the water column properties during S1 formation. Due to the different hydrological conditions prevailed in each of these sites different diagenetic processes may affect their distribution. In South Aegean Sea Fe/Al ratio appear to be more representative of this variability since it is not associated to pyrite formation, in contrast with the other two studied sites. Spectral analyses showed that high frequency cycles are present although there are no specific cycles present in all records. Cycles with periodicities varying around 210yr and 85-70yr (figure 22, 22 & A24-26) are thought to be related to solar variability (Suess and Gleissberg cycles respectively). Cycles identified in the records of different proxies vary illustrating that different mechanisms are the driving forces to different processes. Even though, the centennial to decennial scale periodicity can be linked at least partially to solar activity (Bond et al., 2001).

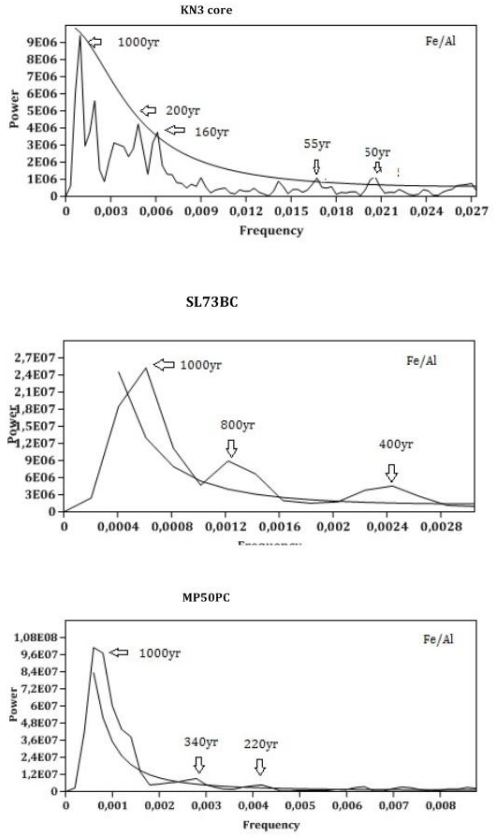

figure 22. Spectral analysis of the Fe/Al ratio from all three cores. The curved lines indicate the 95% confidence interval (Hammer et al., 2001).

5. CONCLUSIONS

The three sites selected for this study are all related to areas where Eastern Mediterranean bottom-water formation is known to occur, namely Adriatic and Aegean Seas. From the high resolution profiles of this study it is also clear that sapropel S1 deposition has not been a stable continuous process especially in such shallow depths.

The sedimentary records show that during most of the time that sapropel S1 formation has been taking place, the sediments in all three sites have been oxygen depleted. In addition, the water column and sediment/water interface conditions have been suboxic to anoxic for North Aegean and Adriatic sites, and rather oxic/suboxic for the South Aegean site.

The onset of sapropel S1 formation is similar for the two sites of this study where it has been recovered, i.e. N.Aegean and S.Adriatic being respectively 10.2 ± 0.5 and 10.2 ± 0.3 ka cal BP, and is consistent with a basin-wide synchronous start of S1 formation reported to be 10.8± 0.4 ka cal BP (de Lange et al., 2008). For the observed end of S1, slightly different ages have been detected in this study, being for N. Aegan, S. Aegean, and S. Adriatic cores, repectively 5.6 ± 0.5; 6.2 ± 0.3; and 6.6 ± 0.3 ka cal BP, compared to that reported for a basin-wide synchronous ending at 6.1 ± 0.5 cal ka BP. For sites located near areas of deepwater formation an earlier ending of sapropel formation could be anticipated but the observations made and uncertainties involved do not permit any firm conclusions to be made. During deposition of sapropel S1, not only the 8.2 cal ka BP event, observed at two sites, but also an additional interruption has been recognized to occur at 7.5 cal ka BP in all three studied sites. Both events have been attributed to a sustained but temporal climate cooling event that has resulted in the resumption of bottom water formation during a short time interval. After the 8.2 cal ka BP event, sapropel formation resumed for all sites, but subsequent to the 7.5 ka cal BP event, sapropel conditions did not fully recover for the south Adriatic site. This observation coincides with reported southern Adriatic bottom water conditions to have remained oxic from 7.5 cal ka BP onward.

A 9.3 cal ka BP interruption observed in the south Adriatic site is most likely associated to a cryptotephra deposit originating from the Somma –Vesuvius, although the expression of a coinciding global cooling event cannot be excluded.

I would like to thank my supervisor Prof. Gert J. de Lange for the great help and support in every step of this study. Also, I would like to thank M.S. (Marie-Louise) Goudeau and F.M. (Rick) Hennekam for their fruitful discussions. This work could not have been carried out without the technical assistance of G.C. (Dineke) van de Meent-Olieman, H.C. (Helen) de Waard, A.E. (Arnold) van Dijk and Ton Zalm. I would also like to thank Prof. Maria Triantaphyllou for providing the samples of the South Aegean Sea core.

6. REFERENCES

Abu-Zied, R. H., Rohling, E. J., Jorissen, F. J., Fontanier, C., Casford, J. S. L. & Cooke, S. (2008). Benthic foraminiferal response to changes in bottom-water oxygenation and organic carbon flux in the eastern Mediterranean during LGM to Recent times. *Marine Micropaleontology*, *67*(1-2), 46–68.

Aksu, A. E., Hiscott, R. N., & Yasar, D. (1999). Oscillating Quaternary water levels of the Marmara Sea and vigorous outflow into the Aegean Sea from the Marmara Sea – Black Sea drainage corridor. *Marine Geology*, *153*, 275–302.

Aksu, A. E., Yahar, D., Mudie, P. J. & Gillespie, H. (1995). Late glacial-Holocene paleoclimatic and paleoceanographic evolution of the Aegean Sea : micropaleontological and stable isotopic evidence. *Marine Micropaleontology*, *25*, 1–28.Algeo, T. J., & Maynard, J. B. (2004). Trace-element behavior and redox facies in core shales of Upper Pennsylvanian Kansas-type cyclothems. *Chemical Geology*, *206*(3-4), 289–318.

Alley, R. B., Mayewski, P. A., Sowers, T., Stuiver, M., Taylor, K. C. & Clark, P. U. (1997). Holocene climatic instability : A prominent, widespread event 8200 yr ago. *Geology*, *25*(6), 483–486.

Almogi-Labin, A., Bar-Matthews, M., Shriki, D., Kolosovsky, E., Paterne, M., Schilman, B., Ayalon, A., Aizenshtat, Z. & Matthews, A. (2009). Climatic variability during the last ~90ka of the southern and northern Levantine Basin as evident from marine records and speleothems. *Quaternary Science Reviews*, *28*(25-26), 2882–2896.

Ariztegui, D., Asioli, A., Lowe, J. J., Trincardi, F., Vigliotti, L., Tamburini, F., Chondrogianni, C., Accorsi, C.A., Bandini Mazzanti, M., Mercuri, A.M., Van der Kaars, S. McKenzie, J.A., Oldfield, F.. (2000). Palaeoclimate and the formation of sapropel S1: inferences from Late Quaternary lacustrine and marine sequences in the central Mediterranean region. Palaeogeography, Palaeoclimatology, Palaeoecology, 158(3-4), 215–240.

Arnaboldi, M. & Meyers, P.A. (2006). Patterns of organic carbon and nitrogen isotopic compositions of latest Pliocene sapropels from six locations across the Mediterranean Sea. *Palaeogeography, Palaeoclimatology, Palaeoecology*, *235*(1-3), 149–167.

Arnaboldi, M. & Meyers, P.A. (2007). Trace element indicators of increased primary production and decreased water-column ventilation during deposition of latest Pliocene sapropels at five locations across the Mediterranean Sea. *Palaeogeography, Palaeoclimatology, Palaeoecology*, *249*(3-4), 425–443.

Artegiani, A., Bregant, D., Paschini, E., Pinardi, N., Raicich, F. & Russo, A. (1997). The Adriatic Sea General Circulation . Part II : Baroclinic Circulation Structure. *Journal of Physical Oceanography*, *27*, 1515–1532.

Asioli, A., Trincardi, F., Lowe, J. J., Ariztegui, D., Langone, L., & Old, F. (2001). Sub-millennial scale climatic oscillations in the central Adriatic during the Lateglacial : palaeoceanographic implications. *Quaternary Science Reviews*, *20*, 1201–1121.

Avramidis, P., Geraga, M., Lazarova, M. & Kontopoulos, N. (2012). Holocene record of environmental changes and palaeoclimatic implications in Alykes Lagoon, Zakynthos Island, western Greece, Mediterranean Sea. *Quaternary International*, *293*, 184–195.

Bar-Matthews, M. I., Ayalon, A., Gilmour, M., Matthews, A., & HAwkesworth, C. J. (2003). Sea – land oxygen isotopic relationships from planktonic foraminifera and speleothems in the Eastern Mediterranean region and their implication for paleorainfall during interglacial intervals. *Geochimica et Cosmochimica Acta*, *67*(17), 3181–3199.

Bar-Matthews, M., Ayalon, A. & Kaufman, A. (2000). Timing and hydrological conditions of Sapropel events in the Eastern Mediterranean, as evident from speleothems, Soreq cave, Israel. *Chemical Geology*, *169*(1-2), 145–156.

Bethoux, J. P. (1989). Oxygen consumption, new production, vertical advection and environmental evolution in the Mediterranean Sea. *Deep - Sea Research*, *36*(5), 769–781.

Béthoux, J.-P. & Pierre, C. (1999). Mediterranean functioning and sapropel formation: respective influences of climate and hydrological changes in the Atlantic and the Mediterranean. *Marine Geology*, *153*(1-4), 29–39.

Béthoux, J.P., Gentili, B., Morin, P., Nicolas, E., Pierre, C. & Ruiz-Pino, D. (1999). The Mediterranean Sea: a miniature ocean for climatic and environmental studies and a key for the climatic functioning of the North Atlantic. *Progress in Oceanography*, *44*(1-3), 131–146.

Bianchi, D., Zavatarelli, M., Pinardi, N., Capozzi, R., Capotondi, L., Corselli, C., & Masina, S. (2006). Simulations of ecosystem response during the sapropel S1 deposition event. *Palaeogeography, Palaeoclimatology, Palaeoecology*, *235*(1-3), 265–287.

Bigg, G. R. (1994). An ocean general circulation model view of the glacial circulation. *Paleoceanography*, 9(5), 705–722.

Boscolo, R. & Bryden, H. (2001). Causes of long-term changes in Aegean sea deep water. *Oceanologica Acta*, *24*(6), 519–527.

Brumsack, H.J. (2006). The trace metal content of recent organic carbon-rich sediments: Implications for Cretaceous black shale formation. *Palaeogeography, Palaeoclimatology, Palaeoecology*, *232*(2-4), 344–361.

Calvert, S. E., & Pedersen, T. F. (2007). Elemental Proxies for Palaeoclimatic and Palaeoceanographic Variability in Marine Sediments : Interpretation and Application. In A. Hillaire-Marcel, C. dv. (*Eds*.), *Proxies in Late Cenozoic Paleoceanography* (vol.1 ed., Vol. 1, pp. 567–644). Elsevier.

Calvert, S. & Pedersen, T. (1993). Geochemistry of Recent oxic and anoxic marine sediments: Implications for the geological record. *Marine Geology*, *113*(1-2), 67–88.

Calvert, S. E. & Fontugne, M. R. (2001). On the late Pleistocene-Holocene sapropel record of climatic and oceanographic variability in the eastern Mediterranean. *Paleoceanography*, *16*(1), 78–94.

Calvert, S. E. (1983). Geochemistry of Pleistocene sapropels and associated sediments from the Eastern Mediterranean. *Oceanologica Acta*, *6*(3), 255–267.

Capotondi, L., Borsetti, A. M. & Morigi, C. (1999). Foraminiferal ecozones , a high resolution proxy for the late Quaternary biochronology in the central Mediterranean Sea. *Marine Geology*, *153*, 253–274.

Capozzi, R. & Negri, A. (2009). Role of sea-level forced sedimentary processes on the distribution of organic carbon-rich marine sediments: A review of the Late Quaternary sapropels in the Mediterranean Sea. *Palaeogeography, Palaeoclimatology, Palaeoecology*, *273*(3-4), 249–257.

Caron, B., Siani, G., Sulpizio, R., Zanchetta, G., Paterne, M., Santacroce, R., Tema, E. & Zanella, E.. (2012). Late Pleistocene to Holocene tephrostratigraphic record from the Northern Ionian Sea. *Marine Geology*, *311-314*, 41–51.

Casford, J. S., Rohling, E.J., Abu-Zied, R. ., Fontanier, C., Jorissen, F. ., Leng, M. ., Schmiedl, G., Thomson, J. (2003). A dynamic concept for eastern Mediterranean circulation and oxygenation during sapropel formation. *Palaeogeography, Palaeoceanography, Palaeoecology*, *190*, 103–119.

Cheddadi, R., & Rossignol-Strick, M. (1995). Improved preservation of organic matter and pollen in eastern Mediterranean sapropels. *Paleoceanography*, *10*(2), 301–309.

Cita, M.B., Vergnaud-Grazzini, C., Robert, C., Chamley, H., Ciaranfi, N. & dÓnofrio, S. (1977). Palaeoclimatic Record of a long Deep Sea Core from the Eastern Mediterranean. *Quaternary Research*, *8*, 205–235.

Cramp, A., & O'Sullivan, G. (1999). Neogene sapropels in the Mediterranean : a review. *Marine Geology*, *153*, 11–28.

De Lange, G.J., Mideelburg, J.J. & Pruysers, P.A. (1989) Middle and Late Quaternary depositional sequences and cycles in the eastern Mediterrranean. *Sedimentology* 36, 151 158.

De Lange, G.J., Van Os, B., Pruysers, P., Middelburg. J.J.,, Castradori, D. Van Santvoort, P., Muller, P.J., Eggenkamp, H. & Prahl F.G. (1993) Possible early diagenetic alteration of palaeo proxies. In: Carbon Cycling in the Glacial Ocean (*Zahn R., Kaminski M.A., Labeyrrie L., and Pedersen T.F., Eds*) NATO Adv. Sci. I 17, 225-258.

De Lange, G. J., Van Santvoort, P. J., Langereis, C., Thomson, J., Corselli, C., Michard, A., Rossignol-Strick, M., Paterne, M. & Anastasakis, G. (1999). Palaeo-environmental variations in eastern Mediterranean sediments: a multidisciplinary approach in a prehistoric setting. *Progress in Oceanography*, *44*(1-3), 369–386.

De Lange, G. J., Thomson, J., Reitz, A., Slomp, C. P., Principato, M. S., Erba, E. & Corselli, C. (2008). Synchronous basin-wide formation and redox-controlled preservation of a Mediterranean sapropel. *Nature*, *1*(September), 606–610.

De Rijk, S., Hayes, A., & Rohling, E. J. (1999). Eastern Mediterranean sapropel S1 interruption : an expression of the onset of climatic deterioration around 7 ka BP. *Marine Geology*, *153*, 337–343.

Desprat, S., Combourieu-Nebout, N., Essallami, L., Sicre, M. a., Dormoy, I., Peyron, O., Siani, G., Bout Toumazeilles, V. & Turon, J.L. (2012). Deglacial and Holocene vegetation and climatic changes at the southernmost tip of the Central Mediterranean from a direct land-sea correlation. *Climate of the Past Discussions*, *8*(6), 5687–5741.

Di Bella, L. & Casieri, S. (2011). Paleoenvironmental reconstruction of Late Quaternary succession by foraminiferal assemblages of three cores from the San Benedetto del Tronto coast (central Adriatic Sea, Italy). *Quaternary International*, *241*(1-2), 169–183.

Dormoy, I., Peyron, O., Combourieu Nebout, N., Goring, S., Kotthoff, U., Magny, M., & Pross, J. (2009). Terrestrial climate variability and seasonality changes in the Mediterranean region between 15 000 and 4000 years BP deduced from marine pollen records. *Climate of the Past*, *5*(4), 615–632.

Emeis, K., Camerlenghi, A., Mckenzie, J. A., Rio, D., Sprovieri, R., & Kiel, U. (1991). The occurrence and significance of Pleistocene and Upper Pliocene sapropels in the Tyrrhenian Sea. *Marine Geology*, *100*, 155–182.

Emeis, K.-C. & Scientific shipboard party (1996). 2. Paleoceanography and sapropel introduction. *In Emeis, K.-C., Robertson, A.H.F. & Richter, C.* (Ed.) *Proceedings of the Ocean Drilling Program*, Initial Reports, 160, 21–28.

Emeis, K.-C., Struck, U., Schulz, H., Rosenberg, R., Bernasconi, S., Erlenkeuser, H., Sakamoto, T., Martinez-Ruiz, F. (2000). Temperature and salinity variations of Mediterranean Sea surface waters over the last 16.000 years from records of planktonic stable oxygen isotopes and alkenone unsaturation ratios. *Palaeogeography, Palaeoceanography, Palaeoecology*, *158*, 259–280.

Facorellis, Y., & Maniatis, Y. (1998). Apparent 14C ages of marine mollusk shells from a Greek island: calculation of the marine reservoir effect in the Aegean Sea. *Radiocarbon*, *40*(2), 963–973.

Fontugne, M. R., & Calvert, S. E. (1992). Late Pleistocene variabitlity of the Carbon isotopic composition of othanic mattern in the Eastern Mediterranean: Monitor of changes in carbon sources and atmopheric CO_2 concentrations. *Paleoceanography*, *7*(1), 1–20.

Fontugne, M.R., Paterne, M., Calvert, S.E., Murat, A., Giochard, F. & Arnold, M. (1989). Adriatic deep water formation during the Holocene: Implication for the reoxygenation of the deep Eastern Mediterranean Sea. *Paleoceanography*, *4*(2), 199–206.

Friedrich, W. L., Kromer, B., Friedrich, M., Heinemeier, J., Pfeiffer, T., & Talamo, S. (2006). Santorini eruption radiocarbon dated to 1627-1600 B.C. *Science*, *312*(5773), 548.

Gallego-Torres, D., Martinez-Ruiz, F., De Lange, G. J., Jimenez-Espejo, F. J., & Ortega-Huertas, M. (2010). Trace-elemental derived paleoceanographic and paleoclimatic conditions for Pleistocene Eastern Mediterranean sapropels. *Palaeogeography, Palaeoclimatology, Palaeoecology*, *293*(1-2), 76–89.

Gallego-Torres, D., Martínez-Ruiz, F., Paytan, a., Jiménez-Espejo, F. J., & Ortega-Huertas, M. (2007). Pliocene–Holocene evolution of depositional conditions in the eastern Mediterranean: Role of anoxia vs. productivity at time of sapropel deposition. *Palaeogeography, Palaeoclimatology, Palaeoecology*, *246*(2-4), 424–439.

Ganssen, G., & Troelstra, S. R. (1987). Paleoenvironmental changes from stable isotopes in planktonic foraminifera from Eastern Mediterranean sapropels. *Marine Geology*, *75*(1-4), 221–230.

Gennari, G., Tamburini, F., Ariztegui, D., Hajdas, I. & Spezzaferri, S. (2009). Geochemical evidence for high-resolution variations during deposition of the Holocene S1 sapropel on the Cretan Ridge, Eastern Mediterranean. *Palaeogeography, Palaeoclimatology, Palaeoecology*, *273*(3-4), 239–248.

Geraga, M., Tsaila-monopolis, S., Ioakim, C., Papatheodorou, G., & Ferentinos, G. (2000). Evaluation of palaeoenvironmental changes during the last 18 , 000 years in the Myrtoon basin , SW Aegean Sea. Palaeogeography, Palaeoceanography, Palaeoecology, 156, 1–17.

Geraga, M., Mylona, G., Tsaila-Monopoli, S., Papatheodorou, G., & Ferentinos, G. (2008). Northeastern Ionian Sea: Palaeoceanographic variability over the last 22 ka. *Journal of Marine Systems*, *74*(1-2), 623–638.

Geraga, M., Ioakim, C., Lykousis, V., Tsaila-Monopolis, S., & Mylona, G. (2010). The high-resolution palaeoclimatic and palaeoceanographic history of the last 24,000years in the central Aegean Sea, Greece. *Palaeogeography, Palaeoclimatology, Palaeoecology*, *287*(1-4), 101–115.

Giunta, S., Negri, a, Morigi, C., Capotondi, L., Combourieu-Nebout, N., Emeis, K. ., Sangiorgi, F., Vigliotti, L. (2003). Coccolithophorid ecostratigraphy and multi-proxy paleoceanographic reconstruction in the Southern Adriatic Sea during the last deglacial time (Core AD91-17). *Palaeogeography, Palaeoclimatology, Palaeoecology*, *190*, 39–59.

Gogou, A., Bouloubassi, I., Lykousis, V., Arnaboldi, M., Gaitani, P., & Meyers, P. A. (2007). Organic geochemical evidence of Late Glacial–Holocene climate instability in the North Aegean Sea. *Palaeogeography, Palaeoclimatology, Palaeoecology*, *256*(1-2), 1–20.

Gvirtzman, G. & Wieder, M. (2001). Climate of the last 53,000 Years in the eastern Mediterranean , based on soil-sequence Stratigraphy in the coastal plain of Israel. *Quaternary Science Reviews*, *20*, 1827–1849.

Hamann, Y., Ehrmann, W., Schmiedl, G., Krüger, S., Stuut, J.-B. & Kuhnt, T. (2008). Sedimentation processes in the Eastern Mediterranean Sea during the Late Glacial and Holocene revealed by end-member modelling of the terrigenous fraction in marine sediments. *Marine Geology*, *248*(1-2), 97–114.

Hammer, Ø., Harper, D.A.T., Ryan, P.D. 2001. PAST: Paleontological statistics software package for education and data analysis. Palaeontologia Electronica 4(1): 9pp.

Hatch, J. R. & Leventhal, J. S. (1992). Relationship between inferred redox potential of the depositional environment and geochemistry of the Upper Pennsylvanian (Missourian) Stark Shale Member of the Dennis Limestone, Wabaunsee County, Kansas, U.S.A. *Chemical Geology*, *99*, 65–82.

Helz, G. R., Miller, C. V., Charnock, J. M., Mosselmans, J. F. W., Pattrick, R. A. D., Garner, C. D., & Vaughan, D. J. (1996). Mechanism of molybdenum removal from the sea and its concentration in black shales : EXAFS evidence. *Geochimica et Cosmochimica Acta*, *60*(19), 3631–3642.

Hilgen, F. J. (1991). Astronomical calibration of Gauss to Matuyama sapropels in the Mediterranean and implication for the Geomagnetic Polarity Time Scale. *Earth and Planetary Science Letters*, *104*(2-4), 226–244.

Hilgen, F. J., Abdul Aziz, H., Krijgsman, W., Raffi, I. & Turco, E. (2003). Integrated stratigraphy and astronomical tuning of the Serravallian and lower Tortonian at Monte dei Corvi (Middle–Upper Miocene, northern Italy). *Palaeogeography, Palaeoclimatology, Palaeoecology*, *199*(3-4), 229–264.

Jenkins, J. A., Williams, D. F., Island, R., Program, M. S. & Carolina, S. (1984). Nile eater as a caise of Eastern Mediterranean sapropel formation: Evidence for and against. *Marine Micropaleontolgy*, *9*, 521–534.

Jilbert T., Reichart G.J., Mason P., and De Lange G.J. (2010). Short-time-scale variability in ventilation and export productivity during the formation of Mediterranean sapropel S1 Paleoceanography 25, PA4232,.

Jorissen, F. J., Asioli, A., Borsetti, A. M., Capotondi, L., Visse, J. P. De, Hilgen, F. J. & Rohling, E. J. (1993). Late Quaternary central Mediterranean biochronology. *Marine Micropaleontology*, *21*, 169–189.

Katsouras, G., Gogou, A., Bouloubassi, I., Emeis, K.-C., Triantaphyllou, M., Roussakis, G. & Lykousis, V. (2010). Organic carbon distribution and isotopic composition in three records from the eastern Mediterranean Sea during the Holocene. *Organic Geochemistry*, *41*(9), 935–939.

Kemp, A. E. D., Pearce, R. B., Koizumi, I., Pike, J. & Pance, S. J. (1999). The role of mat-forming diatoms in the formation of Mediterranean sapropels. *Nature*, *398* (March), 57–61.

Kidd, R. B., Cita, M. B, & Ryan, W. B. F. (1978). Stratigraphy of eastern mediterranean sapropel sequences recovered during dsdp leg 42a and their paleoenvironmental significance. In K. Hsu & L. et al. Montadert (Eds.), *Initial reports DSDP vol.42A* (pp. 421–443). Washington.

Klein, B., Wolfgang, R., Kress, N., Manca, B., Ribera d'Alcala, M Souvermezoglou, E., Theocharis, A., Civitarese, G. & Luchetta, A. (2003). Accelerated oxygen consumption in eastern Mediterranean deep waters following the recent changes in thermohaline circulation. *Journal of Geophysical Research*, *108*(C9), 8107.

Kocak, M., Kubilay, N., Herut, B., & Nimmo, M. (2005). Dry atmospheric fluxes of trace metals (Al, Fe, Mn, Pb, Cd, Zn, Cu) over the Levantine Basin: A refined assessment. *Atmospheric Environment*, *39*(38), 7330–7341.

Kotthoff, U., Pross, J., Müller, U. C., Peyron, O., Schmiedl, G., Schulz, H., & Bordon, A. (2008). Climate dynamics in the borderlands of the Aegean Sea during formation of sapropel S1 deduced from a marine pollen record. *Quaternary Science Reviews*, *27*(7-8), 832–845.

Kouli, K., Gogou, a., Bouloubassi, I., Triantaphyllou, M. V., Ioakim, C., Katsouras, G., Roussakis, G. & Lykousis, V.. (2012). Late postglacial paleoenvironmental change in the northeastern Mediterranean region: Combined palynological and molecular biomarker evidence. *Quaternary International*, *261*, 118–127.

Kraal, P., Slomp, C. P. & De Lange, G. J. (2010). Sedimentary organic carbon to phosphorus ratios as a redox proxy in Quaternary records from the Mediterranean. *Chemical Geology*, *277*, 167–177.

Krom, M., Michard, A, Cliff, R. & Strohle, K. (1999). Sources of sediment to the Ionian Sea and western Levantine basin of the Eastern Mediterranean during S-1 sapropel times. *Marine Geology*, *160*(1-2), 45–61.

Kuhnt, T., Schmiedl, G., Ehrmann, W., Hamann, Y. & Andersen, N. (2008). Stable isotopic composition of Holocene benthic foraminifers from the Eastern Mediterranean Sea: Past changes in productivity and deep water oxygenation. *Palaeogeography, Palaeoclimatology, Palaeoecology*, *268*(1-2), 106–115.

Kuhnt, T., Schmiedl, G., Ehrmann, W., Hamann, Y. & Hemleben, C. (2007). Deep-sea ecosystem variability of the Aegean Sea during the past 22 kyr as revealed by Benthic Foraminifera. *Marine Micropaleontology*, *64*(3-4), 141–162.

Larrasoaña, J. C., Roberts, A. P., Rohling, E. J., Winklhofer, M., & Wehausen, R. (2003). Three million years of monsoon variability over the northern Sahara. *Climate Dynamics*, *21*(7-8), 689–698.

Lascaratos, A., Roether, W., Nittis, K., & Klein, B. (1999). Recent changes in deep water formation and spreading in the eastern Mediterranean Sea: a review. *Progress in Oceanography*, *44*(1-3), 5–36.

Lascaratos, S. (1993). Estimation of deep and intermediate water mass formation rates in the Mediterranean Sea. *Deep - Sea Research*, *40*(6), 1327–1332.

Lourens, L. J., Antonarakou, A., Hilgen, F. J., Hoof, A. A. M. Van, Vergnaud-Grazzini, C., & Zachariasse, W. J. (1996). Evaluation of the Plio-Pleistocene astronomical timescale. *Paleoceanography*, *11*(4), 391–413.

Lourens, L. J., Wehausen, R., & Brumsack, H. J. (2001). Geological constraints on tidal dissipation and dynamical ellipticity of the Earth over the past three million years. *Nature*, *409*(6823), 1029–33.

Lykousis, V. (2001). Subaqueous bedforms on the Cyclades Plateau (NE Mediterranean) — evidence of Cretan Deep Water Formation? *Continental Shelf Research*, *21*(5), 495–507.

Mangini, A., & Schlosser, P. (1986). The formation of Eatern Mediterranean sapropels. *Marine Geology*, *72*, 115–124.

Marino, G. (2008). *Palaeoceanography of the interglacial eastern Mediterranean Sea. Phd thesis.* Utrecht University.

Marino, G., Rohling, E. J., Sangiorgi, F., Hayes, A., Casford, J. L., Lotter, A. F., Kucera, M., et al. (2009). Early and middle Holocene in the Aegean Sea: interplay between high and low latitude climate variability. *Quaternary Science Reviews*, *28*(27-28), 3246–3262.

Martinez-Ruiz, F., Kastner, M., Paytan, A., Ortega-Huertas, M., & Bernasconi, S. M. (2000). Geochemical evidence for enhanced productivity during S1 sapropel deposition in the eastern Mediterranean. *Paleo*, *15*(2), 200–209.

Martinez-Ruiz, F., Paytan, A., Kastner, M., Gonzalez-Donoso, J. M., Linares, D., Bernasconi, S.M., & Limenez-Espejo, F. J. (2003). A comparative study of the geochemical and mineralogical characteristics of the S1 sapropel in the western and eastern Mediterranean. *Palaeogeography, Palaeoclimatology, Palaeoecology*, *190*, 23–37.

Mayewski, P. A. ., Rohling, E. J., Curt Stager, J., Karlén, W., Maasch, K. A., Meeker, L. D., Meyerson, E. A., Gasse, F., van Kreveld, S., Holmgren, K., Lee-Thorp, J., Rosqvist, G., Rack, Fr., Staubwasser, M., Schneider, R. R. & Steig, E. J.. (2004). Holocene climate variability. *Quaternary Research*, 62(3), 243–255.

Mercone, D., Thomson, J., Croudace, I. W, & Rohling, E. J. (2001). High-resolution geochemical and micropalaeontological profling of the most recent eastern Mediterranean sapropel. *Marine Geology*, *177*, 25–44.

Mercone, D., Thomson, J., Croudace, W., Siani, G., Paterne, M. & Troelstra, S. (2000). Duration of S1 , the most recent sapropel in the eastern Mediterranean Sea , as indicated by accelerator mass spectrometry radiocarbon and geochemical evidence. *Paleoceanography*, *15*(3), 336–347.

Meyers, P. A. & Arnaboldi, M. (2008). Paleoceanographic implications of nitrogen and organic carbon isotopic excursions in mid-Pleistocene sapropels from the Tyrrhenian and Levantine Basins, Mediterranean Sea. *Palaeogeography, Palaeoclimatology, Palaeoecology*, *266*(1-2), 112–118.

Meyers, P. A. & Arnaboldi, M. (2005). Trans-Mediterranean comparison of geochemical paleoproductivity proxies in a mid-Pleistocene interrupted sapropel. *Palaeogeography, Palaeoclimatology, Palaeoecology*, *222*(3-4), 313–328.

Meyers, P. A. & Doose, H. (1999). 29. Sources, preservation, and thermal maturity of organic matter in Pliocene-Pleistocene organic-carbon-rich sediments of the Western Mediterranean Sea. In R. Zahn, M. C. Comas, & A. Klaus (Eds.), *Proceedings of the Ocean Drilling Program, Scientifi Results, vol.161* (Vol. 161, pp. 383–390).

Myers, P. G. & Haines, K. (2002). Stability of the Mediterranean's thermohaline circulation under modified surface evaporative fluxes. *Journal of Geophysical Research*, *107*(C3), 7/1–7/10.

Myers, P. G. & Rohling, E. J. (2000). Modeling a 200-Yr Interruption of the Holocene Sapropel S1. *Quaternary Research*, *53*(1), 98–104. doi:10.1006/qres.1999.2100

Myers, P. G., Haines, K. & Rohling, E. J. (1998). Modeling the paleocirculation of the Mediterranean: The last glacial maximum and the Holocene with emphasis on the formation of sapropel S1. *Paleoceanography*, *13*(6), 586–606.

Moller, T., Schulz, H., Hamann, Y., Dellwig, O. & Kucera, M. (2012). Sedimentology and geochemistry of an exceptionally preserved last interglacial sapropel S5 in the Levantine Basin (Mediterranean Sea). *Marine Geology*, *291-294*, 34–48.

Morford J.L. & Emerson, S. (1999). The geochemistry of redox sensitive trace metals in sediments. *Geochimica et Cosmochimica Acta*, *63*(11/12), 1735–1750.

Muerdter, D.R. & Kennett, J. P. (1984). Late Quaternary planktonic foraminiferal biostratigraphy, strait of Sicily, Mediterranean Sea. *Marine Micropaleontology*, *8*, 339–359.

Müller, P.J. & Suess, E. (1979). Productivity, sedimentation rate & sedimentary organic matter in the oceans-I. Organic carbon preservation. Deep – Sea Res. 264. 1347-1362.

Murat, A. & Got, H. (2000). Organic carbon variations of the eastern Mediterranean Holocene sapropel: a key for understanding formation processes. *Palaeogeography, Palaeoclimatology, Palaeoecology*, *158*(3-4), 241–257.

Nameroff, T. J., Balistrieri, L. S. & Murray, J. W. (2002). Suboxic trace metal geochemistry in the eastern tropical North Pacific. *Geochimica et Cosmochimica Acta*, *66*(7), 1139–1158.

Negri, A. & Giunta, S. (2001). Calcareous nannofossil paleoecology in the sapropel S1 of the eastern Ionian sea: paleoceanographic implications. *Palaeogeography, Palaeoclimatology, Palaeoecology*, *169*(1-2), 101–112.

Ní Fhlaithearta, S., Reichart, G.-J., Jorissen, F. J., Fontanier, C., Rohling, E. J., Thomson, J. & De Lange, G. J. (2010). Reconstructing the seafloor environment during sapropel formation using benthic foraminiferal trace metals, stable isotopes, and sediment composition. *Paleoceanography*, *25*(4).

Nijenhuis, I. A, & De Lange, G.J. (2000). Geochemical constraints on Pliocene sapropel formation in the eastern Mediterranean. *Marine Geology*, *163*(1-4), 41–63.

Nijenhuis, I. A., Bosch, H., Sinninghe Damste, J. S., Brumsack, H.-J., & G.J., D. L. (1999). Organic matter and trace element rich sapropels and black shales : a geochemical comparison. *Earth and Planetary Science Letters*, *169*, 277–290.

Nolet, G. J. & Corliss, B. H. (1990). Benthic foraminiferal evidence for reduced deep-water circulation during sapropel deposition in the eastern Mediterranean. *Marine Geology*, *94*(1-2), 109–130.

Passier, H. F., De Lange, G. J. & Dekkers, M. J. (2001). Magnetic properties and geochemistry of the active oxidation front and the youngest sapropel in the eastern Mediterranean Sea. *Geophysical Journal International*, *145*(3).

Passier, H. F., Middelburg, J. J., De Lange, G. J. & Bottcher, M. E. (1999). Modes of sapropel formation in the eastern Mediterranean : some constraints based on pyrite properties. *Marine Geology*, *153*, 199–219.

Passier, H. F., Middelburg, J. J., Van Os, B.J.H. & De Lange, G.J. (1996). Diagenetic pyritisation under eastern Mediterranean caused by downward sulphide diffusion sapropels. *Geochimica et Cosmochimica Acta*, *60*(5), 751–763.

Paytan, A., Martinez-Ruiz, F., Eagle, M., Ivy, A. & Wankel, S. D. (2004). Using sulfur isotope to elucidate the origin of barite associated with high organic matter accumulation events in marine sediments. *Geological Society Of America Bulletin*, *379*, 151–160. Peyron, O., Goring, S., Dormoy, I., Kotthoff, U., Pross, J., De Beaulieu, J.-L., Drescher-Schneider, R., Vanniere, B. & Magny, M.l. (2011). Holocene seasonality changes in the central Mediterranean region reconstructed from the pollen sequences of Lake Accesa (Italy) and Tenaghi Philippon (Greece). *The Holocene*, 21(1), 131–146.

Peyron, O., Goring, S., Dormoy, I., Kotthoff, U., Pross, J., de Beaulieu, J.-L., Drescher-Schneider, R. Vanniere, B. & Magny, M. (2011). Holocene seasonality changes in the central Mediterranean region reconstructed from the pollen sequences of Lake Accesa (Italy) and Tenaghi Philippon (Greece). *The Holocene*, *21*(1), 131–146.

Pinardi, N. & Masetti, E. (2000). Variability of the large scale general circulation of the Mediterranean Sea from observations and modelling: a review. *Palaeogeography, Palaeoclimatology, Palaeoecology*, *158*(3-4), 153–173.

Principato, M. S., Crudeli, D., Ziveri, P., Slomp, C. P., Corselli, C., Erba, E. & De Lange, G.J. (2006). Phyto- and zooplankton paleofluxes during the deposition of sapropel S1 (eastern Mediterranean): Biogenic carbonate preservation and paleoecological implications. *Palaeogeography, Palaeoclimatology, Palaeoecology*, *235*(1-3), 8–27.

Pross, J., Kotthoff, U., Muller, U. C., Peyron, O., Dormoy, I., Schmiedl, G., Kalaitzidis, S. & Smith, A.M. (2009). Massive perturbation in terrestrial ecosystems of the Eastern Mediterranean region associated with the 8.2 kyr B.P. climatic event. *Geology*, *37*(10), 887–890.

Pruysers, P. A., De Lange, G. J. & Middelburg, J.J. (1991). Geochemistry of eastern Mediterranean sediments:Primary sediment composition and diagenetic alterations. *Marine Geology*, *100*, 137–154.

Pruysers, P. A., De Lange, G. J., Middelburg, J. J. & Hydes, D.J. (1993). The diagenetic formation of metal-rich layers in sapropel-containing sediments in the eastern Mediterranean. *Geochimica et Cosmochimica Acta*, *57*(3), 527–536.

Rasmussen, S. O., Vinther, B. M., Clausen, H. B. & Andersen, K. K. (2007). Early Holocene climate oscillations recorded in three Greenland ice cores. *Quaternary Science Reviews*, *26*(15-16), 1907–1914.

Reed, D. C., Slomp, C. P. & de Lange, G. J. (2011). A quantitative reconstruction of organic matter and nutrient diagenesis in Mediterranean Sea sediments over the Holocene. *Geochimica et Cosmochimica Acta*, *75*(19), 5540–5558.

Reimer, P.J. & McCormac, F. G. (2002). Marine Radiocarbon reservoir correction for the Mediterranean and aegean Seas. *Radiocarbon*, *44*(1), 159–166.

Reitz, A. (2005). *Diagenetic and Paleoceanographic variations with emphasis on the eastern Mediterranean sapropel S1*. (*phd thesis*) Utrecht University.

Reitz, A., Thomson, J., De Lange, G. J., Green, D. R. H., Slomp, C. P. & Gebhardt, A. C. (2006a). Effects of the Santorini (Thera) eruption on manganese behavior in Holocene sediments of the eastern Mediterranean. *Earth and Planetary Science Letters*, *241*(1-2), 188–201.

Reitz, A., Thomson, J., De Lange, G.J., Hensen, C. (2006b). Source and development of large manganese enrichments above eastern Mediterranean sapropel S1. *Paleoceanography*, 21, PA3007.

Reitz, A., De Lange, G.J. (2006). Abundant Sr-rich aragonite in eastern Mediterranean sapropel S1: Diagenetic vs. detrital/biogenic origin. *Palaeogeography. Palaeoclimatology. Palaeoecology*, 235, 135-148,.

Rinna, J., Warning, B., Meyers, P.A. Brumsack, H.-J. & Rullkotter, J. (2002). Combined organic and inorganic geochemical reconstruction of paleodepositional conditions of a Pliocene sapropel from the eastern Mediterranean Sea. *Geochimica et Cosmochimica Acta*, *66*(11), 1969–1986.

Robinson, A. R., Hecht, A., Michelato, A., Roether, W., Theocharis, A., Unliiata, U., Pinardi, N., Bergamasco, A., Bishop, J., Brenner, S., Christianidis, S., Gacic, M.J., Georgopoulos, D., Golnaraghi, M., Hausmann, M., Junghaus, H., Lascaratos, A., Latif, M.A., Leslie, W.G., Lozano, C.J., Oğuz, T., Özsoy, E., Papageorgiou, E., Paschini, E., Rozentroub, Z., Sansone, E., Schlitzer, R., Spezie, G., Tziperman, E., Zodiatis, G., Gerges, L ., Athanassiadou, M. & Osman, M. (1992). General circulation of the Eastern Mediterranean. *Earth-Science Reviews*, 32, 285–309.

Robinson, R. S., Kienast, M., Luiza Albuquerque, A., Altabet, M., Contreras, S., De Pol Holz, R., Dubois, N., Roger, F., Galbraith, E., Hsu, T.C., Ivanochko T., Jaccard, S.l., Kao, S.Ji., Kiefer, T., Kienast, S., Lehmann, M., Martinez, P., McCarthy, M., Möbius, J., Pedersen, T., Quan, T. M., Ryabenko, E., Schmittner, A., Schneider, R., Schneider-Mor, A., Shigemitsu, M., Sinclair, D., Somes, C., Studer, A., Thunell, R. & Yang, J.Y. (2012). A review of nitrogen isotopic alteration in marine sediments. *Paleoceanography*, 27(4), PA4203.

Rohling, E., Mayewski, P.A., Abu-Zied, R., Casford, J. & Hayes, A. (2002). Holocene atmosphere-ocean interactions: records from Greenland and the Aegean Sea. *Climate Dynamics*, *18*(7), 587–593.

Rohling, E.J, Abu-Zied, R., Casford, J.S.L., Hayes, A. & Hoogakker, B. A. A. (2008). The Mediterranean Sea : Present and Past. *In J. Woodward (Ed.), Physical Geography of the Mediterranean Basin* (pp. 1–24). Oxford University Press.

Rohling, E.J. & Gieskes, W.C. (1989). Late Quaternary changes in Mediterranean Intermediate Water density and formation rate. *Paleoceanography*, *4*(5), 531–545.

Rohling, E.J. & Hilgen, F.J. (1991). The eastern Mediterranean climate at times of sapropel formation : a review. *Geologie en Mijnbouw*, *70*, 253–264.

Rohling, E.J. & Palike, H. (2005). Centennial-scale climate cooling with a sudden cold event around 8.200 years ago. *Nature*, *434*(April), 975–979.

Rohling, E.J. (1991). Shoaling of the Eastern Mediterranean pycnocline due to reduction of excess evaporation:implications for sapropel formation. *Paleoceanography*, *6*(6), 747–753.

Rohling, E.J. (1994). Review and new aspects concerning the formation of eastern Mediterranean sapropels. *Marine Geology*, *122*(1-2), 1–28.

Rohling, E.J., De Rijk, S., Myers, P. G. & Haines, K. (2000). Palaeoceanography and numerical modelling: the Mediterranean Sea at times of sapropel formation. *Geological Society, London, Special Publications*, *181*(1), 135–149.

Rohling, E.J., Jorissen, F.J. & de Stigter. H. C. (1997). 200 Year Interruption of Holocene sapropel formation in the Adriatic Sea. *Journal of Micropalaeontology*, *16*, 97–108.

Ross, D. A. & Uchupi, E. (1979). Shallow structure and sedimentation in the Southeastern Mediterranean Sea. *Sedimentary Geology*, *23*, 1–18.

Rossignol-strick, M. (1999). The Holocene climatic optimum and pollen records of sapropel 1 in the eastern Mediterranean, 9000 — 6000 BP. *Quaternary Science Reviews*, *18*, 515–530.

Rossignol-Strick. (1985). Mediterranean quaternary sapropels, an immediate response of the african monsoon to variation of insolation. *Palaeogeography, Palaeoceanography, Palaeoecology*, *49*, 237–263.

Rue, E. L., Smith, G. J., Cutter, G. a., & Bruland, K. W. (1997). The response of trace element redox couples to suboxic conditions in the water column. *Deep Sea Research Part I: Oceanographic Research Papers*, *44*(1), 113–134.

Rutten, A., De Lange, G. J., Hayes, A., Rohling, E. J., De Jong, A. F. & Van der Borg, K. (1999). Deposition of sapropel S1 sediments in oxic pelagic and anoxic brine environments in the eastern Mediterranean: differences in diagenesis and preservation. *Marine Geology*, *153*(1-4), 319–335.

Sachs, J. P., & Repeta, D. J. (1999). Oligotrophy and Nitrogen Fixation During Eastern Mediterranean Sapropel Events. *Science*, *286*(5449), 2485–2488.

Sarmiento, J. L. & Herbert, T. (1988). Mediterranean nutrient balance and episodes of anoxia. *Global Biogeochemical Cycles*, *2*(4), 427–444.

Schlitzer, R., Roether, W., Oster, H., Junghans, H.-G., Hausmann, M., Johannsen, H. & Michelato, A. (1991). Chlorofluoromethane and oxygen in the Eastern Mediterranean. *Deep Sea Research Part A. Oceanographic Research Papers*, 38(12), 1531–1551.

Schmiedl, G., Kuhnt, T., Ehrmann, W., Emeis, K.-C., Hamann, Y., Kotthoff, U., Dulski, P. & Pross, J. (2010). Climatic forcing of eastern Mediterranean deep-water formation and benthic ecosystems during the past 22 000 years. *Quaternary Science Reviews*, *29*(23-24), 3006–3020.

Siani, G., Magny, M., Paterne, M., Debret, M. & Fontugne, M. (2013). Paleohydrology reconstruction and Holocene climate variability in the South Adriatic Sea. *Climate of the Past*, *9*(1), 499–515.

Siani, G., Paterne, M., & Colin, C. (2010). Late glacial to Holocene planktic foraminifera bioevents and climatic record in the South Adriatic Sea. *Journal of Quaternary Science*, *25*(5).

Siani, G., Paterne, M., Michel, E., Sulpizio, R., Sbrana, A., Arnold, M. & Haddad, G. (2001). Mediterranean Sea surface radiocarbon reservoir age changes since the last glacial maximum. *Science (New York, N.Y.)*, *294*(5548), 1917–20.

Slomp, C.P., Thomson, J. & De Lange, G.J. (2002). Enhanced regeneration of phosphorus during formation of the most recent eastern Mediterranean sapropel (S1). *Geochemica et Cosmochimica Acta*, *66*(7), 1171–1184.

Slomp, C. P., Thomson, J. & De Lange, G. J. (2004). Controls on phosphorus regeneration and burial during formation of eastern Mediterranean sapropels. *Marine Geology*, *203*(1-2), 141–159.

Stratford, K. & Haines, K. (2002). Modelling nutrient cycling during the eastern Mediterranean transient event 1987 – 1995 and beyond. *Geophysical Research Letters*, *29*(3), 0–3.

Stratford, K., Williams, R.G. & Myers, P. G. (2000). Impact of the circulation on sapropel formation in the eastern Mediterranean. *Global and Planetary Change*, *14*(2), 683–695.

Struck, U., Emeis, K.-C., Voss, M., Krom, M. D. & Rau, G. H. (2001). Biological productivity during sapropel S5 formation in the Eastern Mediterranean Sea : Evidence from stable isotopes of nitrogen and carbon. *Geochimica et Cosmochimica Acta*, *65*(19), 3249–3266.

Stuiver, M., Reimer, P., Bard, E., Beck, J. W., Burr, G. S., Hughen, K., Kromer, B., McCormac, G., Van der Plicht, J. & Spurk, M. (1998). INTCAL98 Radiocarbon age calibration, 24,000-0 cal BP. *Radiocarbon*, 40(3), 1041–1083.

Stuiver, M., Ver, U. I. & Reimer, P. J. (1993). Extended 14C data base amd revised calib 3.0 14C asge calibration program. *Radiocarbon*, *35*(1), 215–230.

Sutherland, H. E., Calvert, S. E. & Morris, R. J. (1984). Geochemical studies of the recent sapropel and associated sediment from the hellenic outer ridge, eastern Mediterranean Sea. I:Mineralogy and chemical composition. *Marine Geology*, *56*, 79–92.

Ten Haven, H., Baas, M., Deleeuw, J., Schenck, P. & Brinkhuis, H. (1987). Late Quaternary Mediterranean sapropels II. Organic geochemistry and palynology of S1 sapropels and associated sediments. *Chemical Geology*, *64*(1-2), 149–167.

Theocharis, A., Balopoulos, E., Kioroglou, S., Kontoyiannis, H. & Iona, A. (1999). A synthesis of the circulation and hydrography of the South Aegean Sea and the Straits of the Cretan Arc (March 1994–January 1995). *Progress in Oceanography*, *44*(4), 469–509.

Theocharis, A., Georgopoulos, D., Lascaratos, A. & Nittis, K. (1993). Water masses and circulation in the central region of the Eastern Mediterranean: Eastern Ionian, South Aegean and Northwest Levantine, 1986–1987. *Deep Sea Research Part II: Topical Studies in Oceanography*, *40*(6), 1121–1142.

Thomson, J., Crudeli, D., De Lange, G. J., Slomp, C. P., Corselli, C., & Calvert, S. E. (2004). Florisphaera profunda and the origin and diagenesis of carbonate phases in eastern Mediterranean sapropel units. *Paleoceanography*, *19*(3),

Thomson, J., Higgs, N. C., Wilson, T. R. S., Croudace, I. W., De Lange, G. J. & Van Santvoort, P.J.M. (1995). Redistribution and geochemical behaviour of redox-sensitive elements around S1 , the most recent eastern Mediterranean sapropel. *Geochimica et Cosmochimica Acta*, *59*(17), 3487–3501.

Thomson, J., Mercone, D., De Lange, G.J. & van Santvoort, P. J. (1999). Review of recent advances in the interpretation of eastern Mediterranean sapropel S1 from geochemical evidence. *Marine Geology*, *153*(1-4), 77–89.

Thunell, R. C. & Williams, D. F. (1989). Glacial-Holocene salinity changes in the Mediterranean Sea: hydrographic and depositional effects. *Nature*, *338*, 493–496.

Thunell, R. C., Williams, D. F. & Belyea, P. R. (1984). Anoxic events in the Mediterranean Sea in relation to the evolution of late Neogene climates. *Marine Geology*, *59*(1-4), 105–134.

Thunell, R. C., Williams, D. F. & Kennett, J. P. (1977). Late Quaternary Paleoclimatology, Stratigraphy and sapropel history in Eastern Mediterranean deep-sea sediments. *Marine Geology*, *2*, 371–388.

Triantaphyllou, M. V., Ziveri, P., Gogou, a., Marino, G., Lykousis, V., Bouloubassi, I., Emeis, K.-C., Kouli, K. Dimiza, M., Rosell-Melé, A., Papanikolaou, M., Katsouras, G. & Nunez, N. (2009). Late Glacial–Holocene climate variability at the south-eastern margin of the Aegean Sea. Marine Geology, 266(1-4), 182–197.

Tribovillard, N., Algeo, T. J., Lyons, T., & Riboulleau, A. (2006). Trace metals as paleoredox and paleoproductivity proxies: An update. *Chemical Geology*, *232*(1-2), 12–32.

Tsimplis, M., Velegrakis, A., Drakopoulos, P., Theocharis, A. & Collins, M. . (1999). Cretan deep water outflow into the Eastern Mediterranean. *Progress in Oceanography*, *44*(4), 531–551.

Tuenter, E., Weber, S.L., Hilgen, F.J. & Lourens, L.J. (2003). The response of the African summer monsoon to remote and local forcing due to precession and obliquity. *Global and Planetary Change*, *36*(4), 219–235.

Turley, C.M. (1999). The changing Mediterranean Sea — a sensitive ecosystem? *Progress in Oceanography*, *44*(1-3), 387–400.

Turner, D. R., Whitfield, M., & Dickson, A. G. (1981). The equilibrium speciation of dissolved components in freshwater and seawater at WC and 1 atm pressure. *Geochimica et Cosmochimica Acta*, *45*, 855–881.

Van Os, B.J.H., Middelburg, J.J. & De Lange, G.J. (1991). Possible diagenetic mobilization of barium in sapropelic sediment from the eastern Mediterranean. *Marine Geology*, *100*, 125–136.

Van Santvoort, P.J.M., De Lange, G.J., Thomson, J., Cussen, H., Wilson, T.R.S., Krom, M.D. & Ströhle. K.. (1996). Active post-depositional oxidation of the most recent sapropel (S1) in sediments of the eastern Mediterranean Sea. *Geochimica et Cosmochimica Acta*, *60*(21), 4007–4024.

Vergnaud Grazzin, C., Devaux, M. & Znaidi, J. (1986). Stable isotope änomalies"in Mediterranean Pleistocene records. *Marine Micropaleontology*, *10*, 35–69.

Warning, B., & Brumsack, H.J. (2000). Trace metal signatures of eastern Mediterranean sapropels. *Palaeogeography, Palaeoclimatology, Palaeoecology*, *158*(3-4), 293–309.

Wedepohl, B. K. H. (1971). Environmental influences on the chemical composition of shales and clays. In H. C. Ahrens, L.H., Press, F., Runcorn, S.K., Urey (Ed.), *Physics and Chemistry of the Earth.* Oxford,: Pergamon,.

Wehausen, R. & Brumsack, H.J. (1999). Cyclic variations in the chemical composition of eastern Mediterranean Pliocene sediments: a key for understanding sapropel formation. *Marine Geology*, *153*(1-4), 161–176.

Wehausen, R. & Brumsack, H.-J. (2000). Chemical cycles in Pliocene sapropel-bearing and sapropel-barren eastern Mediterranean sediments. *Palaeogeography, Palaeoclimatology, Palaeoecology*, *158*(3-4), 325–352.

Williams, D.F. & Thunell, R. C. (1979). Faunal and oxygen isotopic evidence for surface water salinity changes during sapropel formation in the Eastern Mediterranean. *Sedimentary Geology*, *23*, 81–93.

Zanchetta, G., Sulpizio, R., Roberts, N., Cioni, R., Eastwood, W. J., Siani, G., Caron, B.,Paterne, M. & Santacroce, R. (2011). Tephrostratigraphy, chronology and climatic events of the Mediterranean basin during the Holocene: An overview. *The Holocene*, *21*(1), 33–52.

Zanchetta, G., Drysdale, R. N., Hellstrom, J. C., Fallick, a. E., Isola, I., Gagan, M. K. & Pareschi, M. T. (2007). Enhanced rainfall in the Western Mediterranean during deposition of sapropel S1: stalagmite evidence from Corchia cave (Central Italy). *Quaternary Science Reviews*, *26*(3-4), 279–286.

Zervakis, V., Georgopoulos, D. & Drakopoulos, P. G. (2000). The role of the North Aegean in triggering the recent Eastern Mediterranean climatic changes the North Aegean the North Aegean. *Journal of Geophysical Research*, *105*(Cll).

Zonneveld, K. A. F., Versteegh, G. J. M. & De Lange, G. J. (2001). Palaeoproductivity and post-depositional aerobic organic matter decay reflected by dinoflagellate cyst assemblages of the Eastern Mediterranean S1 sapropel ABC26. *Marine Geology*, *172*, 181–195.

Zonneveld, K.A.F. (1996). Paleoclimatic reconstruction of the last deglaciation (18-8ka B.P.) in the Adriatic Sea region; a land - sea correlation based on palynological evidence. *Palaeogeography, Palaeoclimatology, Palaeoecology*, *122*(95), 89–106.

7. APPENDIX

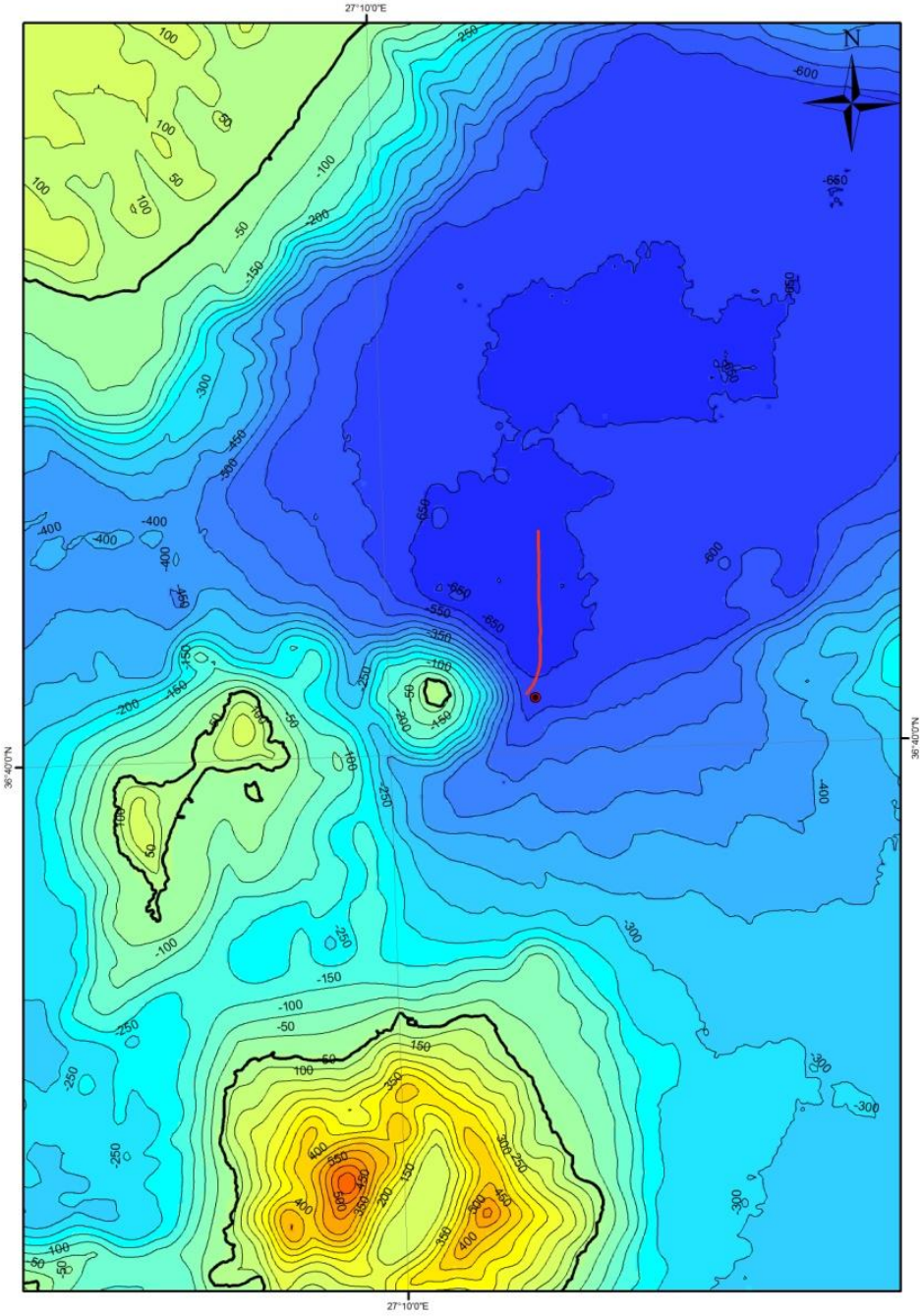

figure A1. Bathymetric map of the South Aegean Sea. The red circle indicates where KN3 was collected and the red line the seismic profile shown in figure A223 (V.Anagnostopoulos pers. communication).

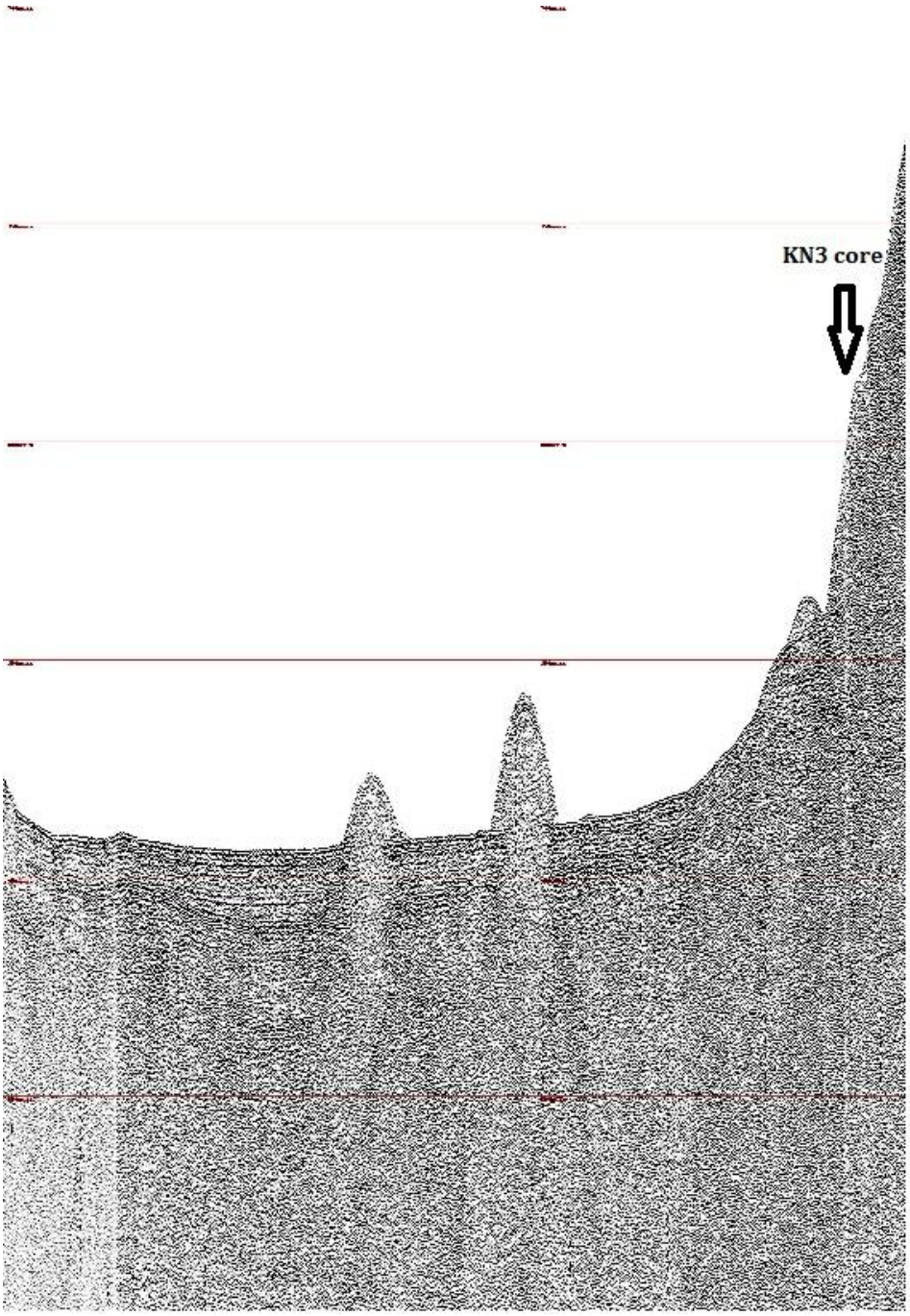

figure A223. Seismic profile in South Aegean Sea (red line in figure). (V.Anagnostopoulos pers. communication).

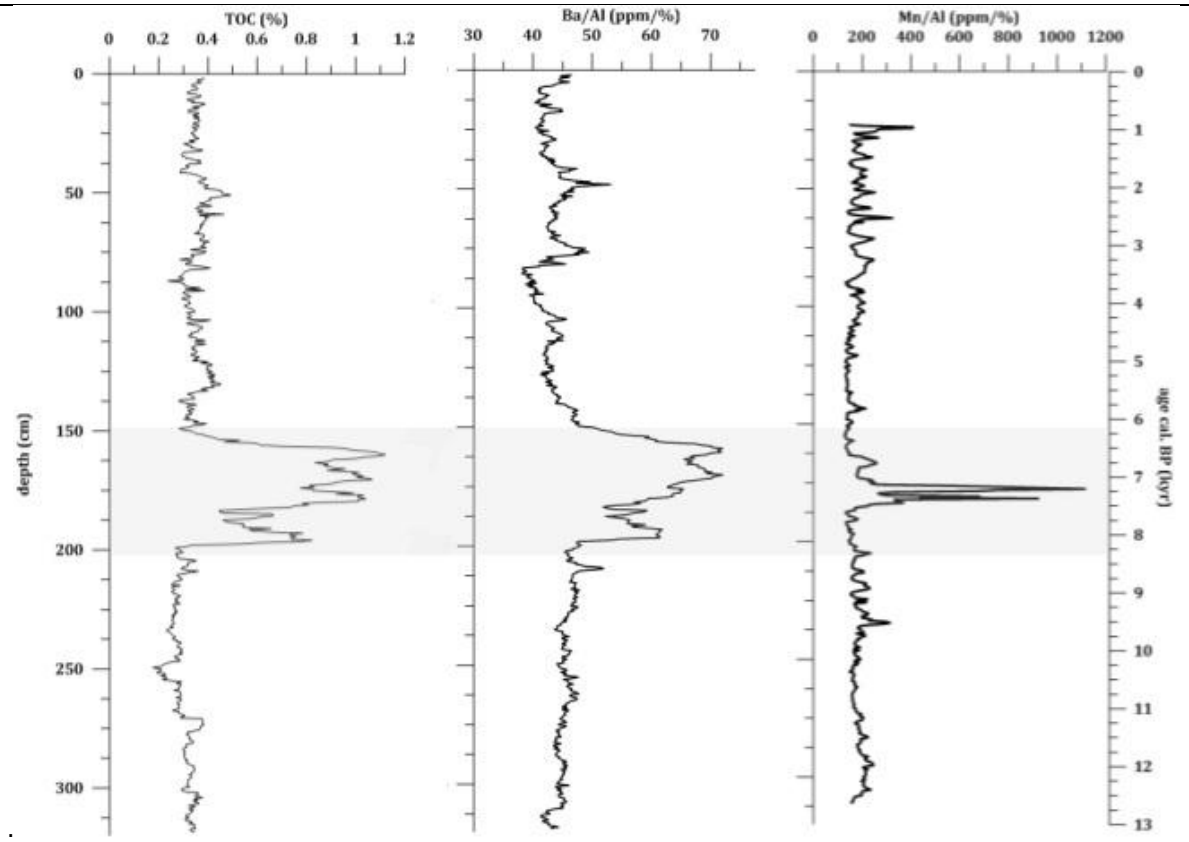

figure A3. KN3 core. TOC (%), Ba/Al and Mn/Al (ppm/%) profiles vs depth. As it can be observed only the sapropel S1b can be detected in the sediments.

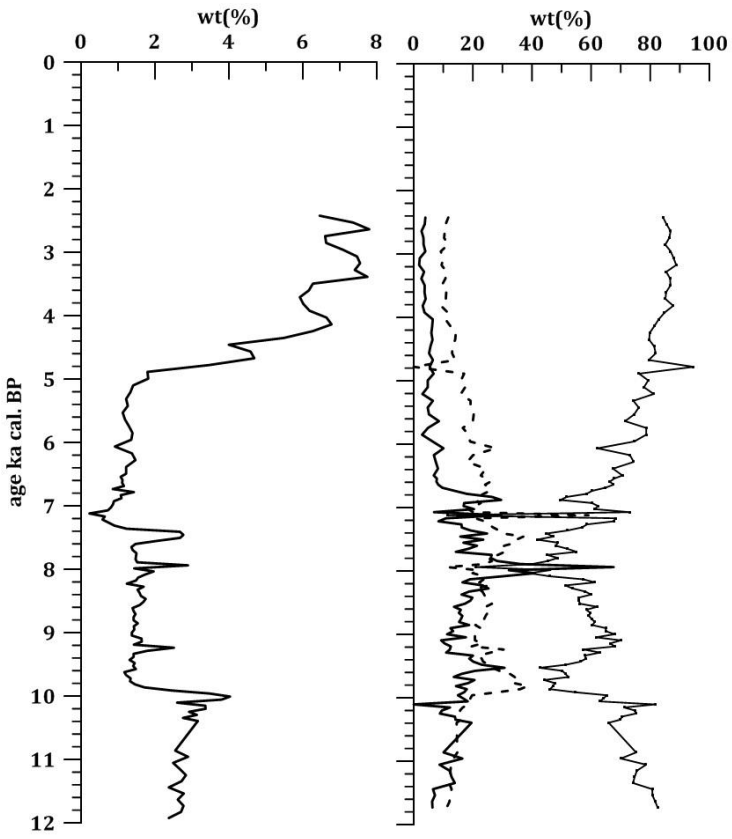

figure A4. MP50PC left plot: wt(%) micropaleontological content of the fractions >355µm, 355-150µm and 150-63µm, right plot: wt(%) of >350µm (black line), 350-150µm (dashed line), 150-63µm (grey line) fractions.

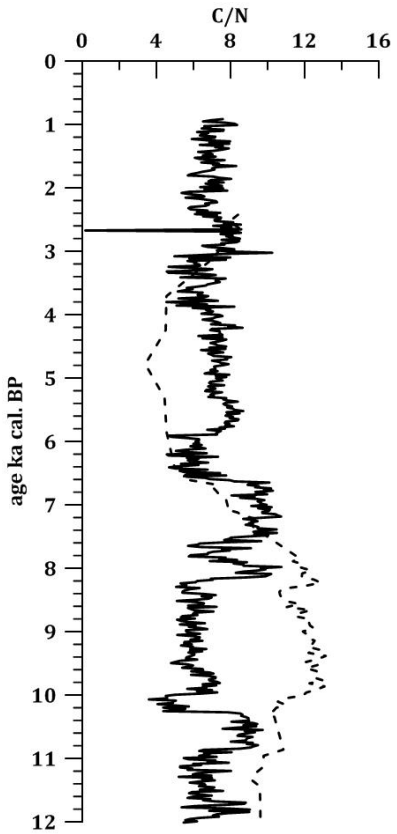

figure A5 C/N ratios versus age (yr) (cal BP) are plotted for the last 11ka BP for KN3 core (thick line) and MP50PC (thin line).

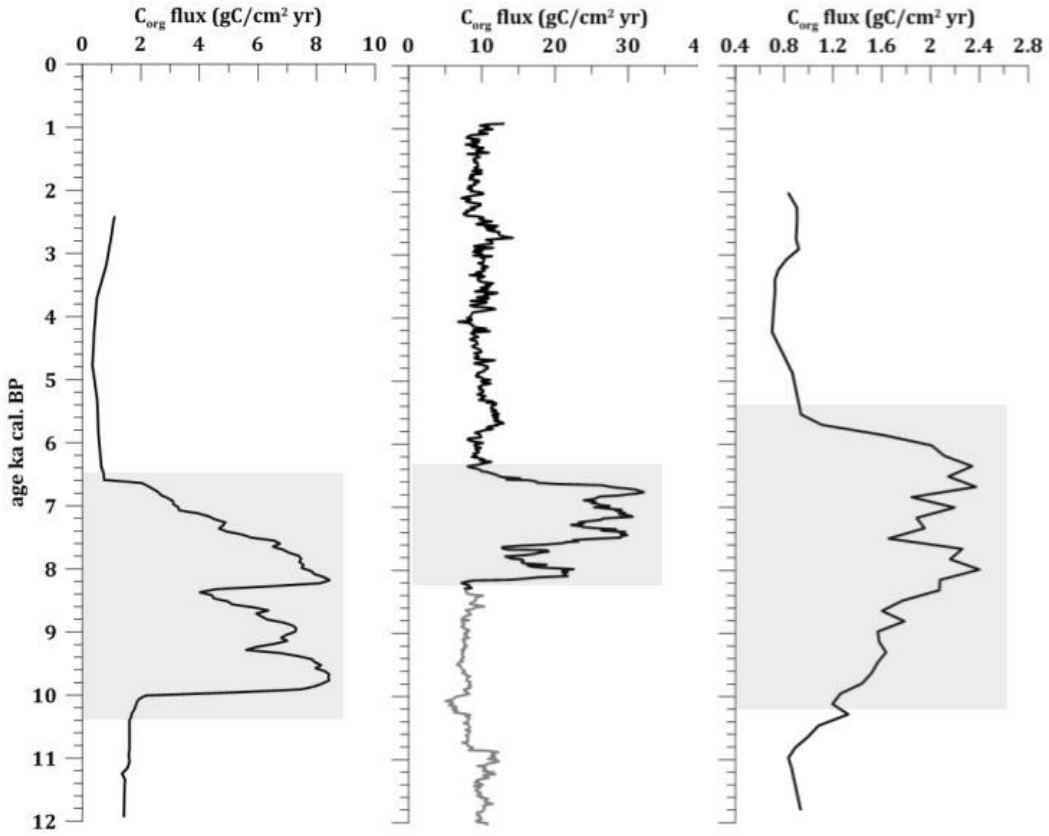

figure A6. Corg fluxes are plotted for the last 12 ka BP for the three cores. The grey shaded areas indicte the sapropel S1 interval. Left MP50PC, middle KN3, right: SL73BC.

Elemental Concentrations

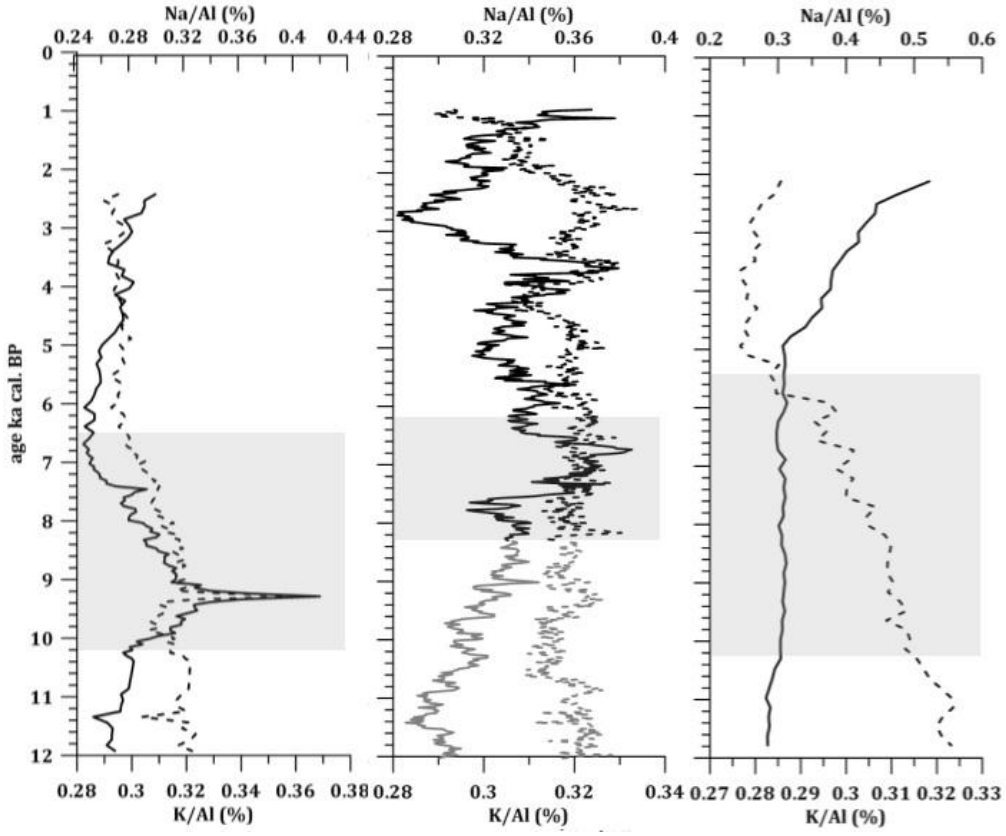

figure A7. Na/Al (solid lines)l and K/Al (dashed linesl, (%)profiles of the last 12kaBP for the the three cores. The grey shaded area indicates the sapropel S1 interval. Left MP50PC, middle KN3, right: SL73BC.

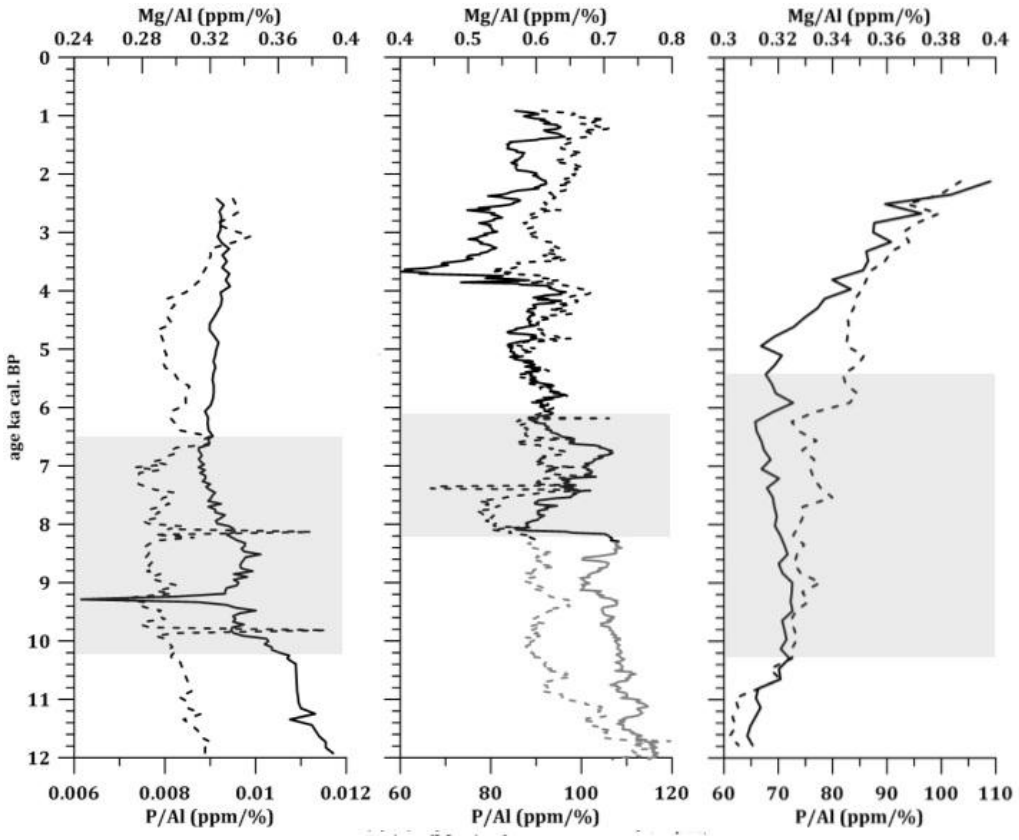

figure A8. Na/Al (%) (solid lines) and P/Al (ppm/%) (dashed lines) profiles of the last 12kaBP for the three cores. The grey shaded area indicates the sapropel S1 interval. Left MP50PC, middle KN3, right: SL73BC.

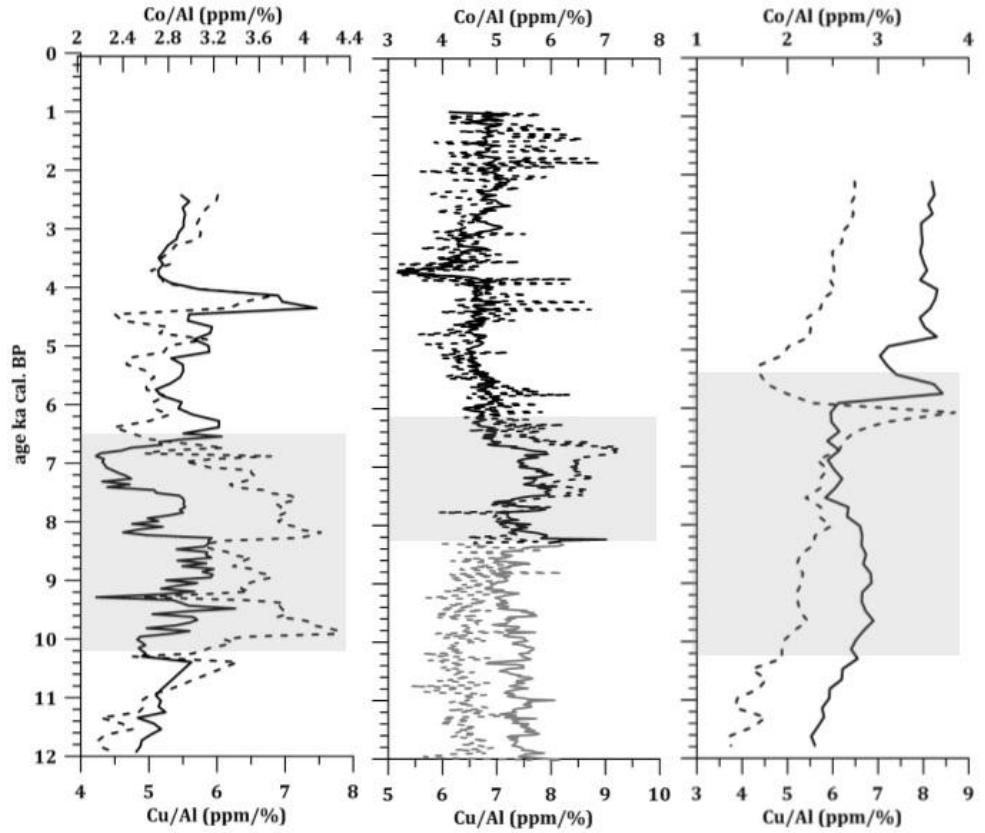

figure A9. Co/Al (solid lines) and Cu/Al (dashed lines) (ppm/%) profiles for the last 12ka BP for the three cores. The grey shaded area indicates the sapropel S1 interval. Left MP50PC, middle KN3, right: SL73BC.

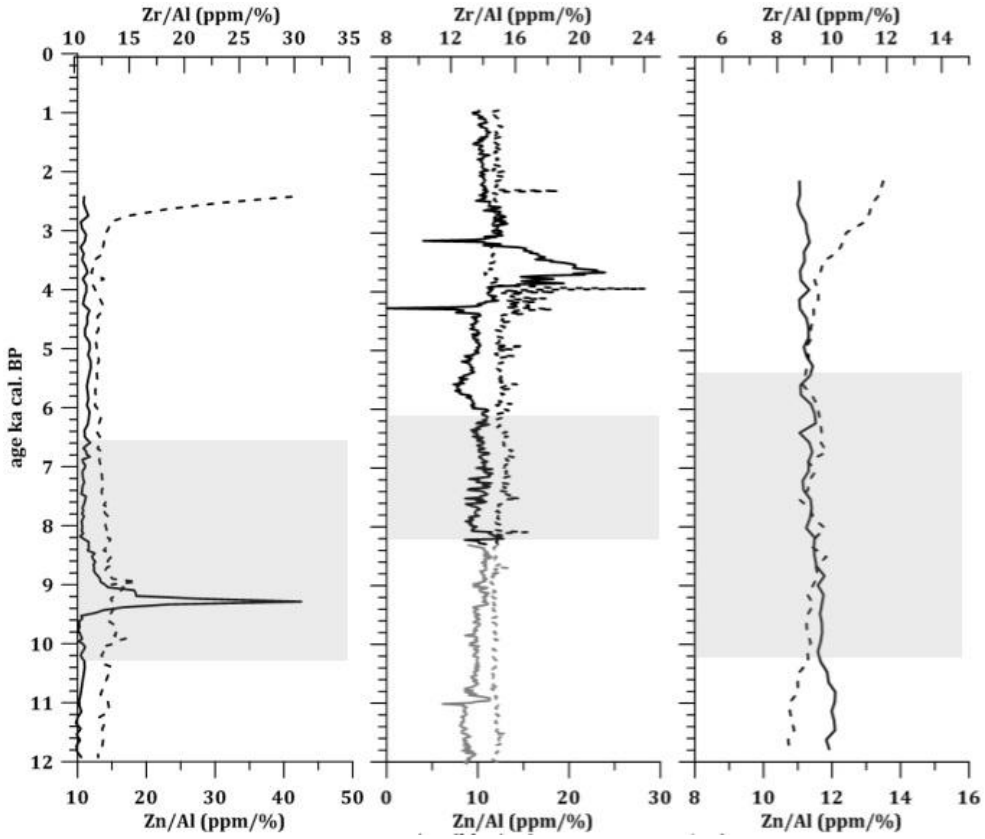

figure A10. Zn/Al (solid lines) and Zr/Al (dashed lines) (ppm/%) profiles for the last 12 ka for the three cores. The grey shaded area indicates the sapropel S1 interval. Left MP50PC, middle KN3, right: SL73BC.

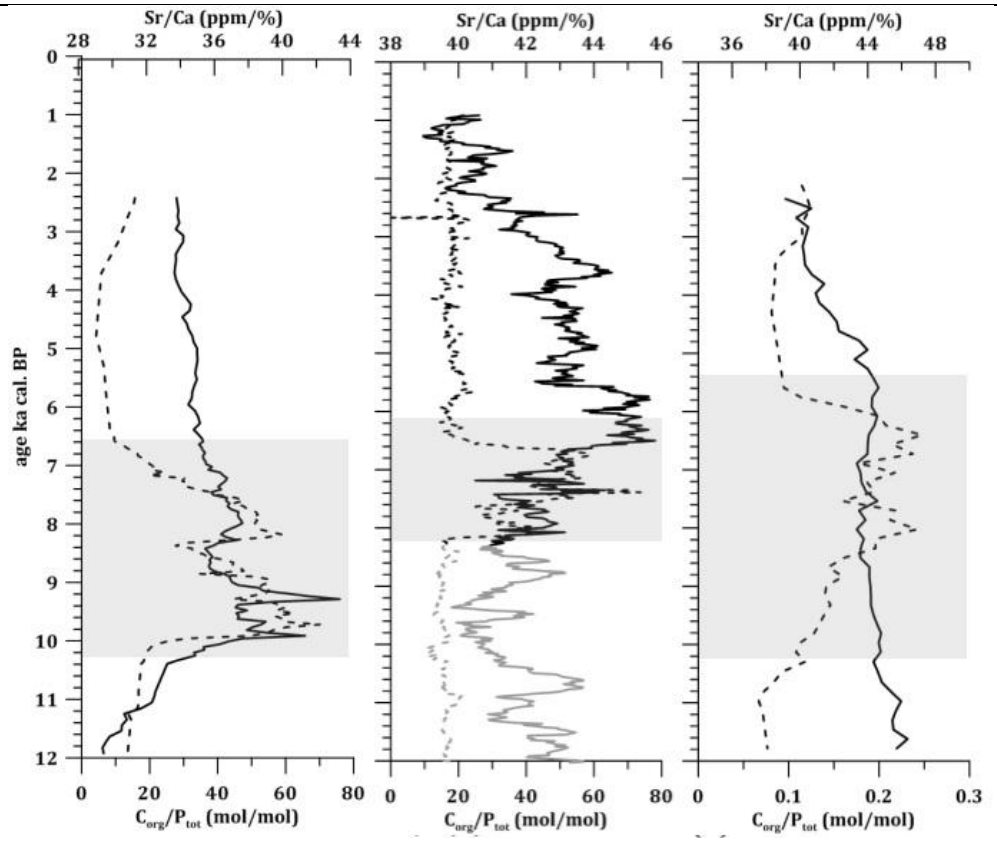

figure A11 Sr/Ca (ppm/%) (solid lines) and C_{org}/P_{tot} (dashed lines) (mol/mol) for the last 12ka for the three cores. The grey shaded area indicates the sapropel S1 interval. Left MP50PC, middle KN3, right: SL73BC.

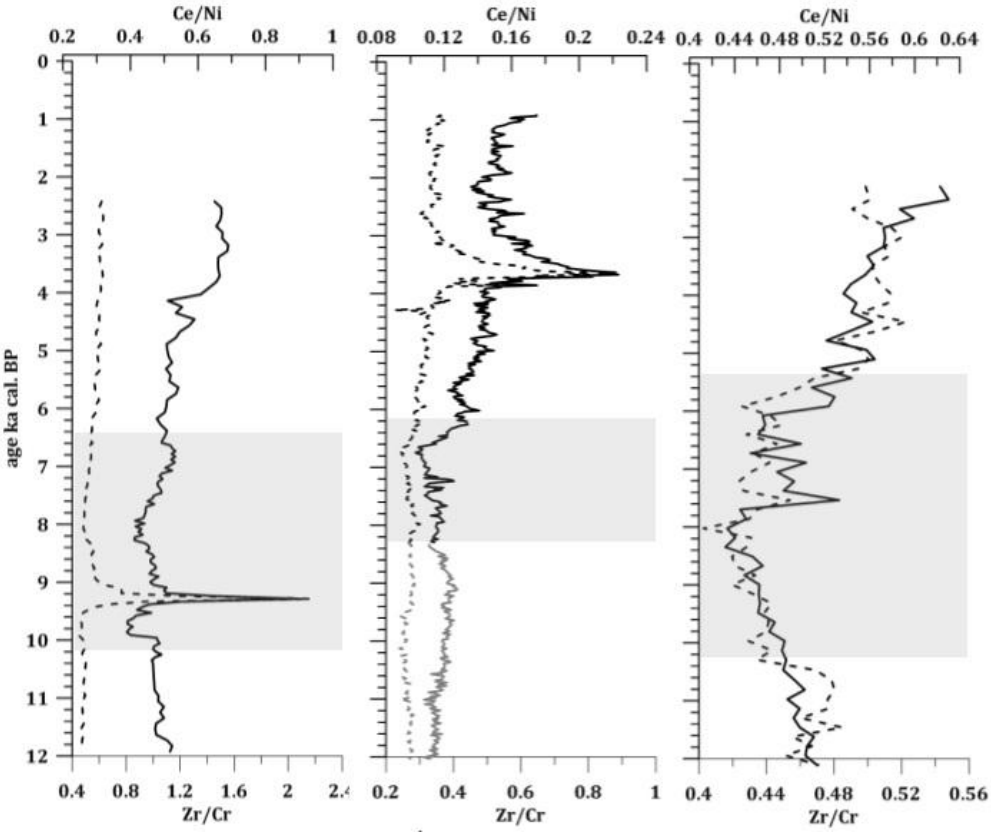

figure A12. Ce/Ni (solid lines) and Zr/Cr (dashed lines) for the last 12ka for the three cores. The grey shaded area indicates the sapropel S1 interval. Left MP50PC, middle KN3, right: SL73BC.

Enrichment Factors

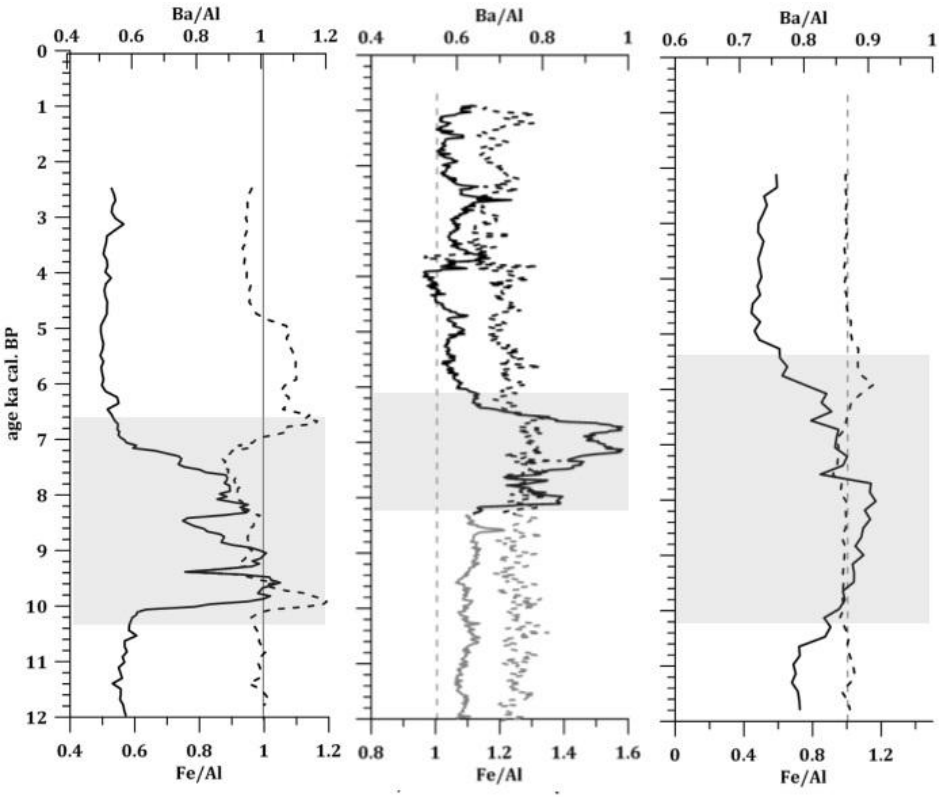

figure A13. Enrichment factors for Ba/Al (ppm/%) (solid lines) and Fe/Al (%) (dashed lines) for the last 12ka for the three cores. Accordingly the black and the dashed vertical lines indicate the EF=1 compared to the average shale composition. Left MP50PC, middle KN3, right: SL73BC.

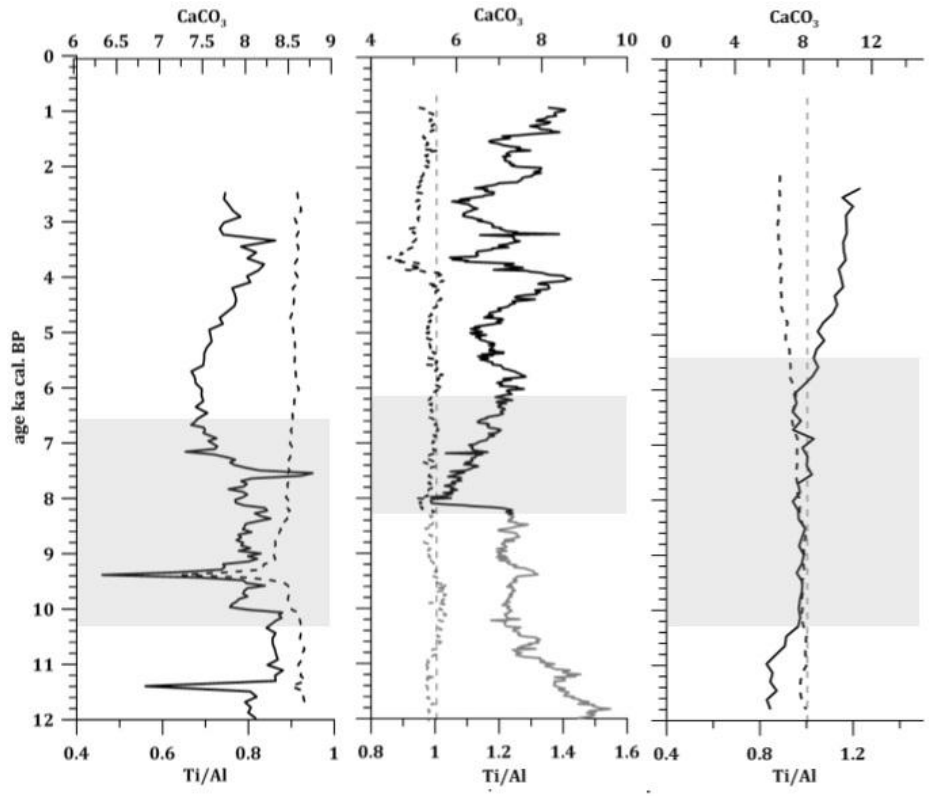

figure A14. Enrichment factors for $CaCO_3$ (%) (solid lines) and Ti/Al (ppm/%) (dashed lines) for the last 12ka for the three cores. Accordingly the black and the dashed vertical lines indicate the EF=1 compared to the average shale composition. Left MP50PC, middle KN3, right: SL73BC .

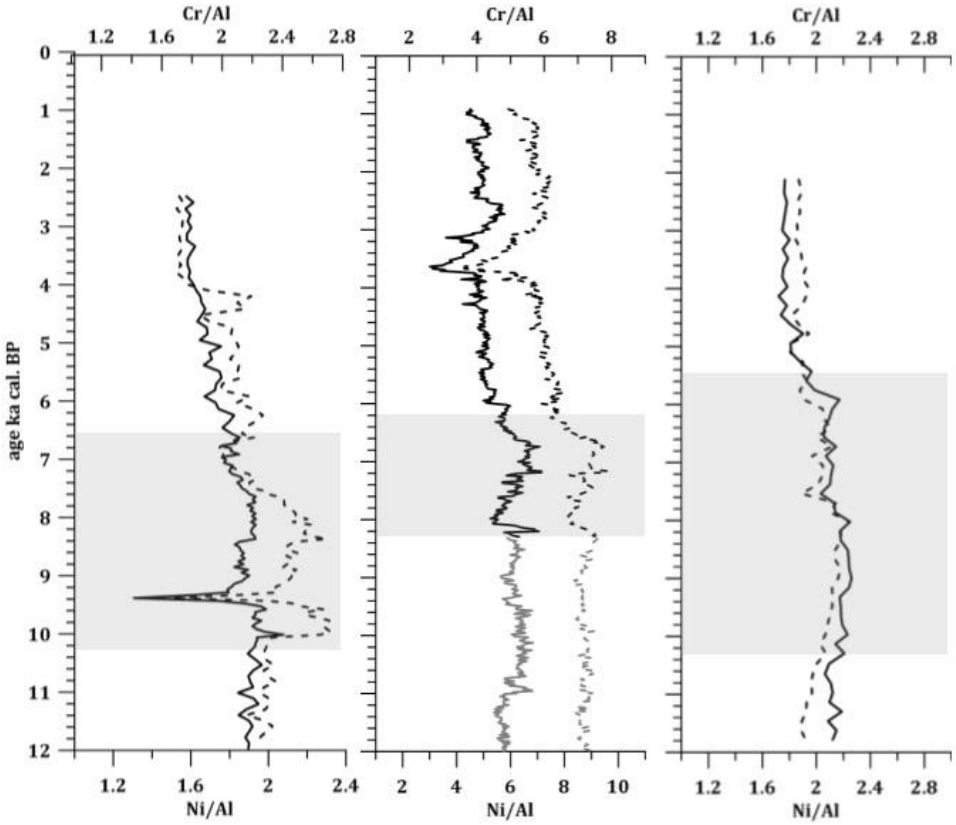

figure A15. Enrichment factors for Cr/Al (solid lines) and Ni/Al (dashed lines) (ppm/%) for the last 12ka for the three cores. Accordingly the black and the dashed vertical lines indicate the EF=1 compared to the average shale composition. Left MP50PC, middle KN3, right: SL73BC.

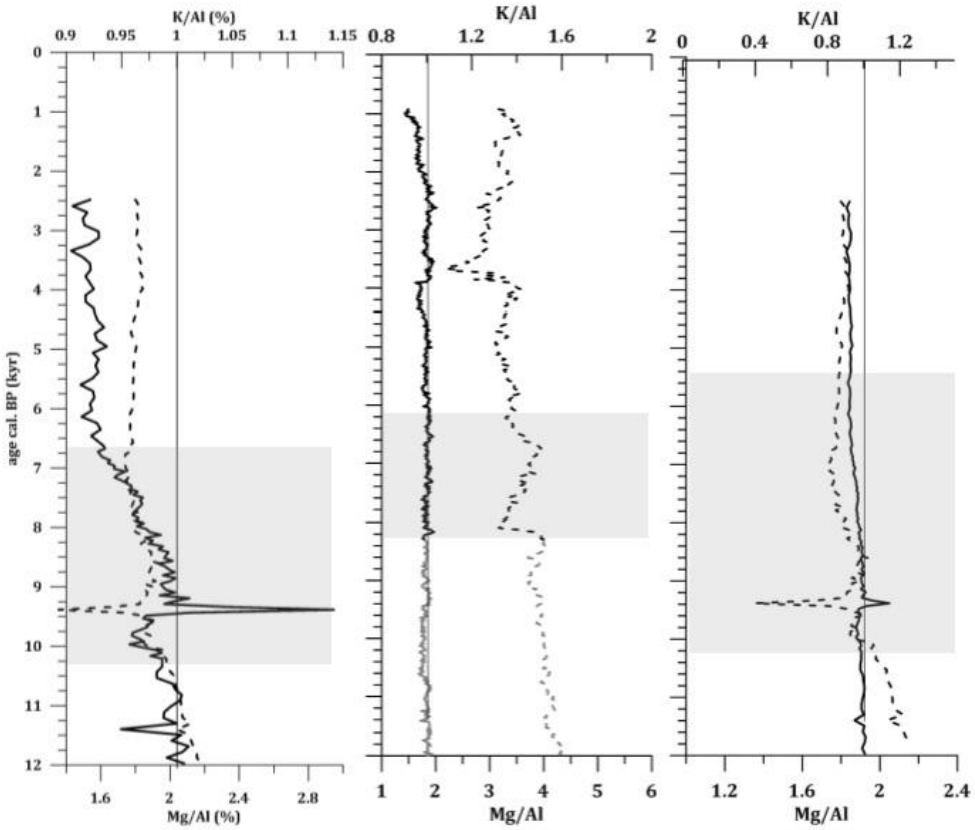

figure A16. Enrichment factors for K/Al (solid lines) (%) and Mg/Al (dashed lines) (%) for the last 12ka BP for the three cores. Accordingly the black and the dashed vertical lines indicate the EF=1 compared to the average shale composition. Left MP50PC, middle KN3, right: SL73BC.

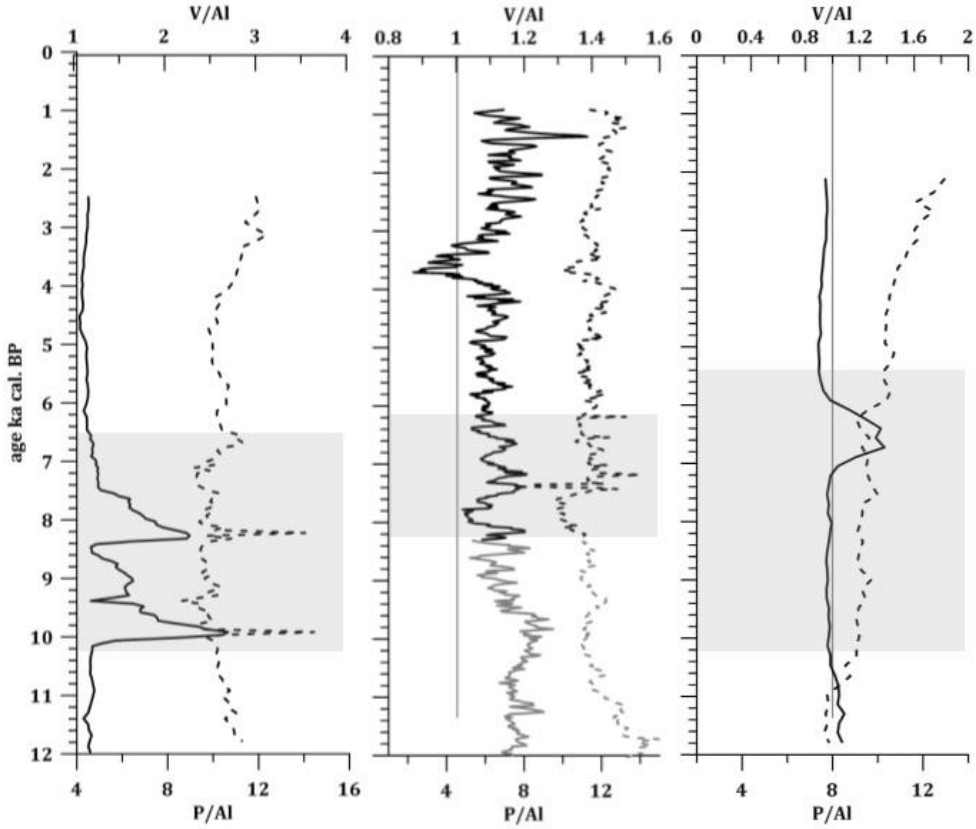

figure A17. Enrichment factors for V/Al (ppm/%) (solid lines) and P/Al (%) (dashed lines) for the last 12ka for the three cores. Accordingly the black and the dashed vertical lines indicate the EF=1 compared to the average shale composition. Left MP50PC, middle KN3, right: SL73BC.

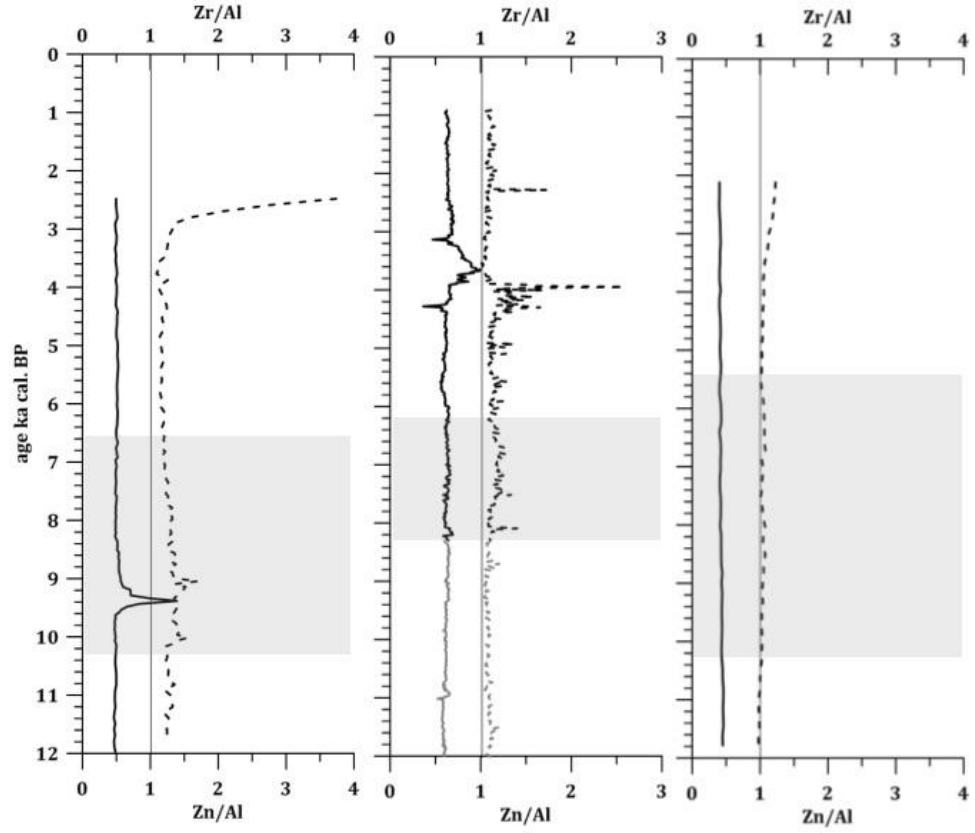

figure A18. Enrichment factors for V/Al (ppm/%) (solid lines) and P/Al (%) (dashed lines) for the last 12ka for the three cores. Left MP50PC, middle KN3, right: SL73BC.

Fluxes

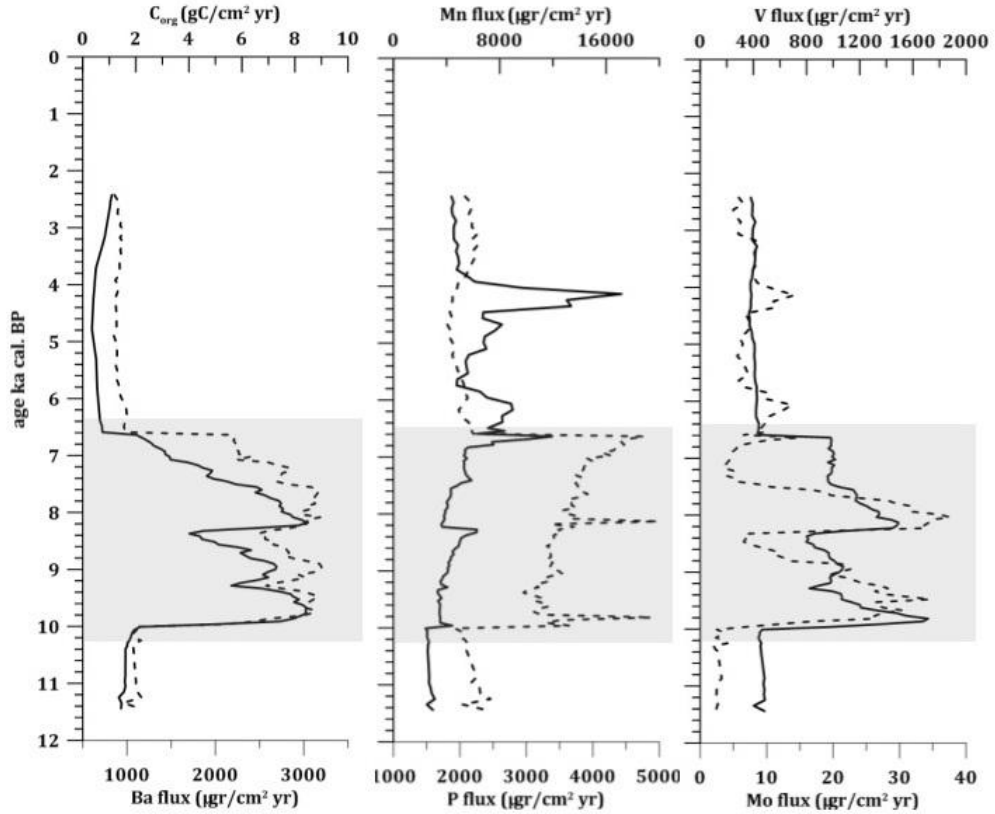

figure A19. MP50PC. Fluxes of Corg (gC/cm² yr), Mn, V, Ti, K, Fe (solid lines) and Ba, Al, Mo, Zr, Mg and S (dashed lines) (µgr/cm² yr).

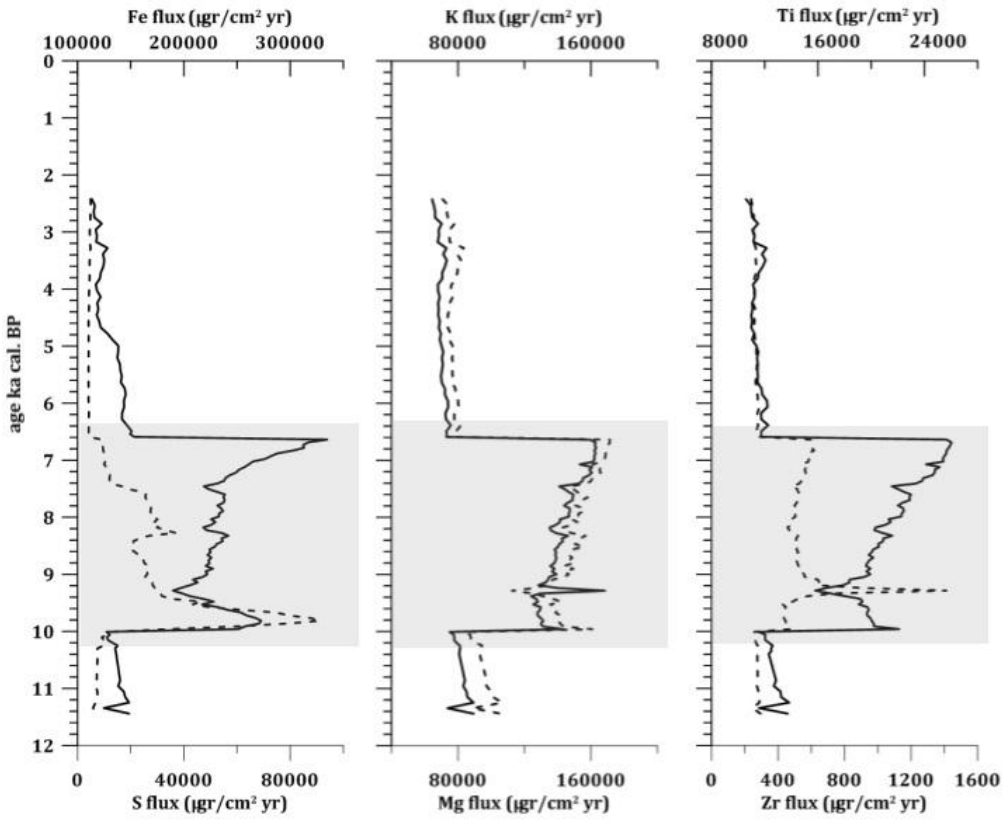

figure A20. . MP50PC. Fluxes of Fe, K and Ti (solid lines) and S, Mg and Zr (dashed lines) (µgr/cm² yr).

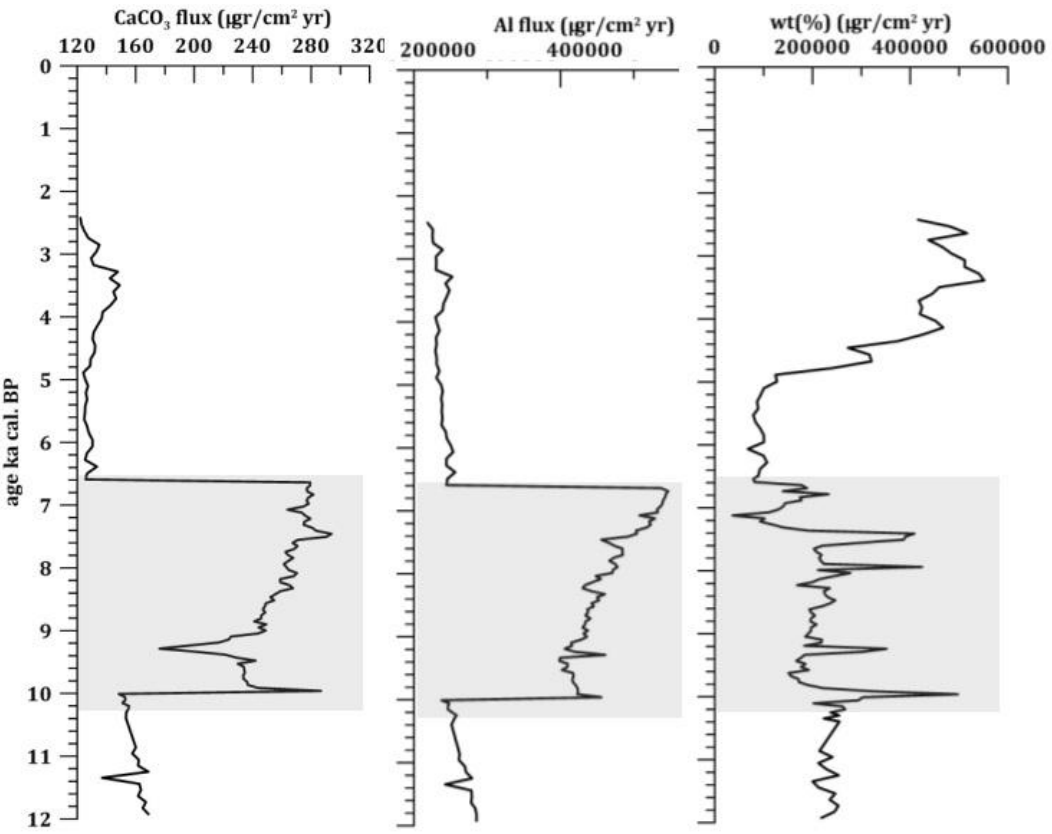

figure A21 MP50PC. Fluxes of CaCO3, Al and wt (%) micropaleontological fraction >63μm (μgr/cm² yr)..

Anoxia indices

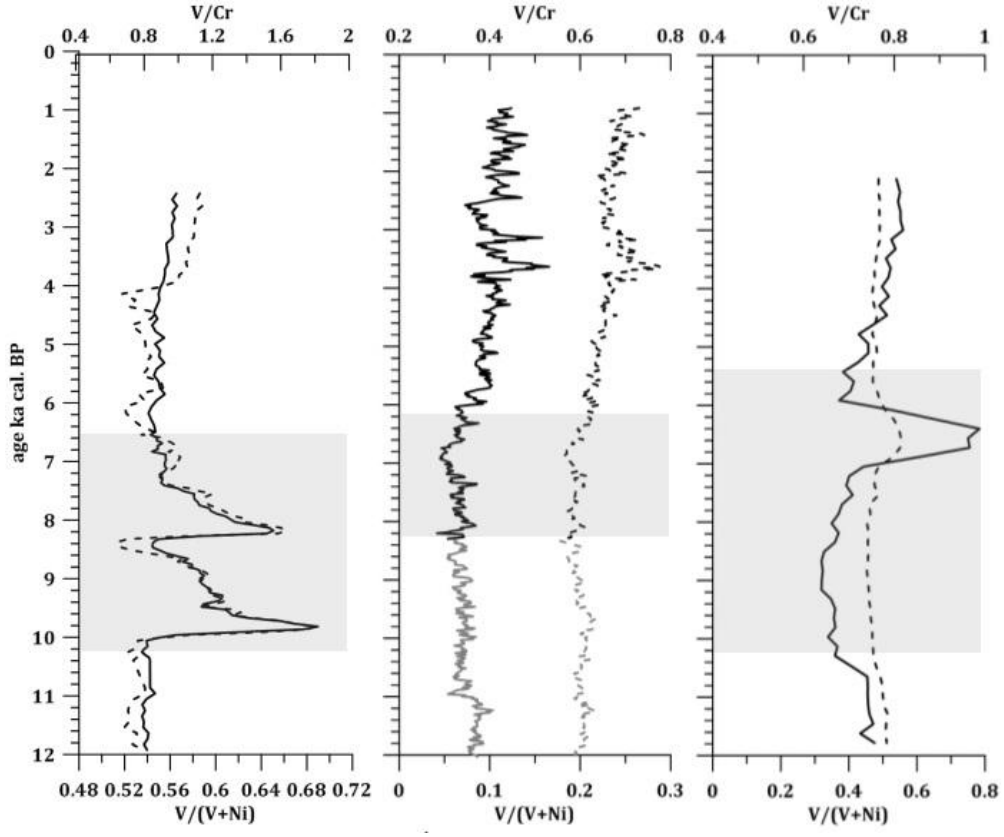

figure A22. The anoxia indices (Gallego – Torres et al., 2007) V/Cr (solid lines) and V/(V+Ni) (dashed lines) are plotted against time (cal kyr) for the last 12 ka for the three cores. The grey shaded area indicates the sapropel S1 interval. Left MP50PC, middle KN3, right: SL73BC.

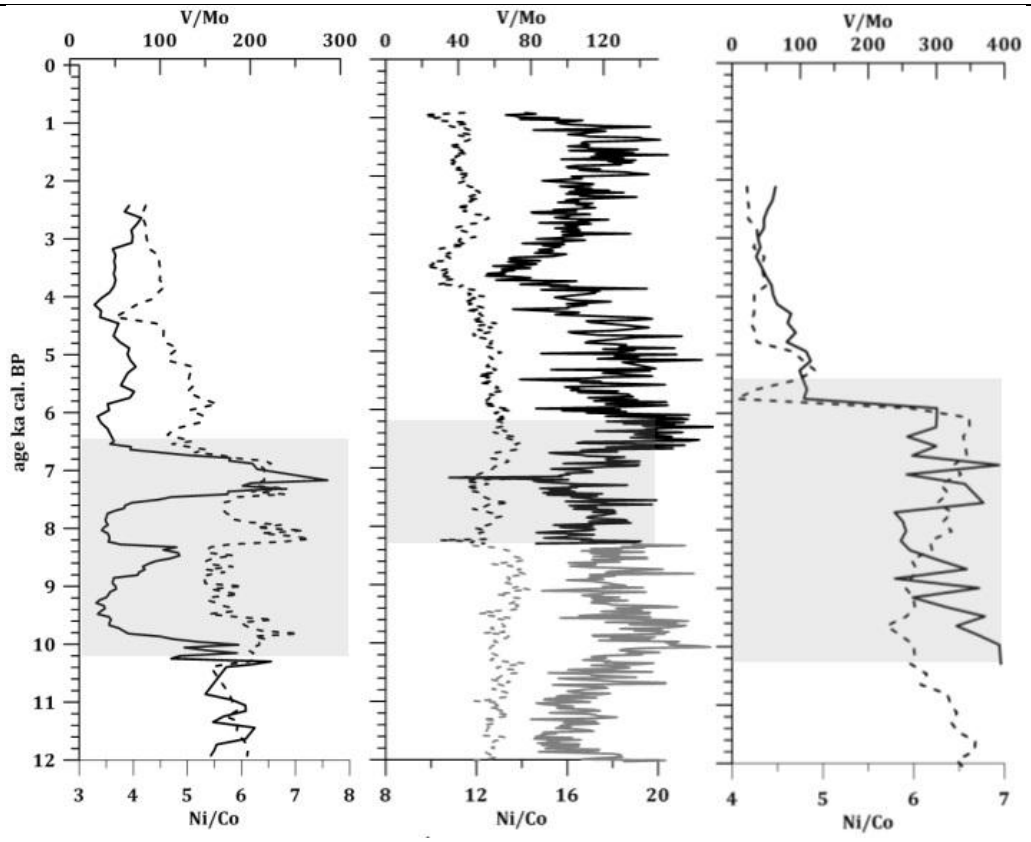

figure A23. The anoxia indices (Gallego – Torres et al., 2007) V/Mo (solid lines) and Ni/Co (dashed lines) are plotted against time (cal kyr) for the last 12 ka for the three cores. The grey shaded area indicates the sapropel S1 interval. Left MP50PC, middle KN3, right: SL73BC.

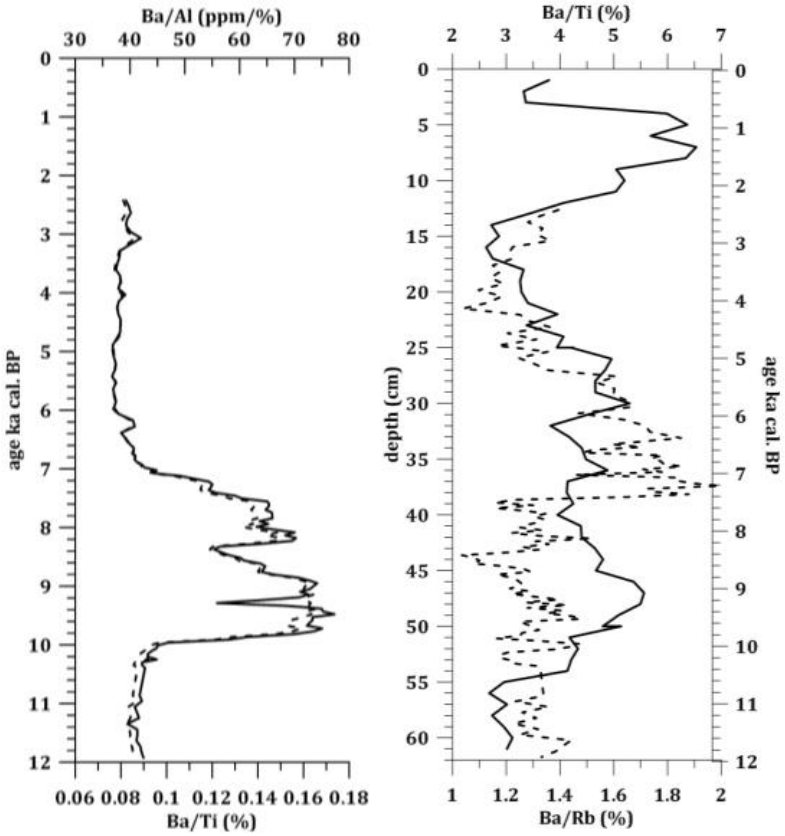

figure A24. Left panel: Ba/Al (ppm/%) (solid lines), Ba/Ti (%) (dashed lines) for MP50PC core (ICP results). Right panel: Ba/Ti (%) (solid lines), Ba/Rb (%) (dashed lines) for MP50PC (XRF data).

.

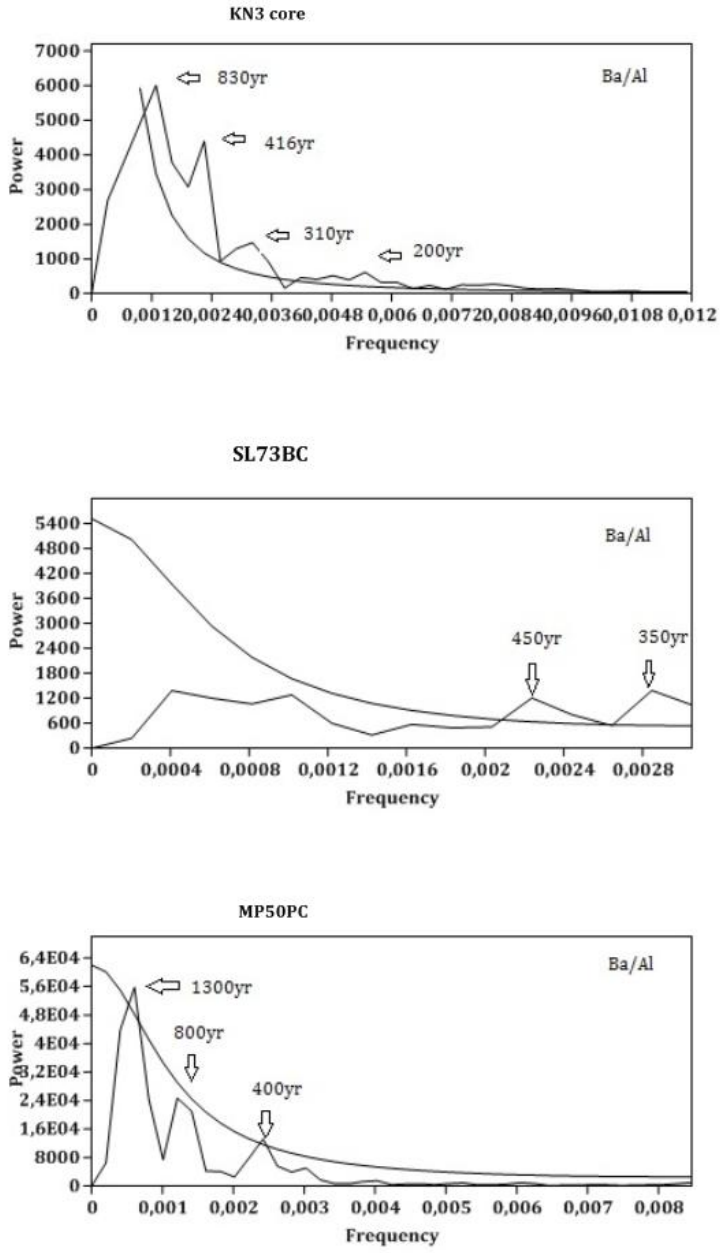

figure A24. Spectral analysis of the Ba/Al ratios from all three cores for the sapropel S1 interval. The curved lines indicate the 95% confidence interval.

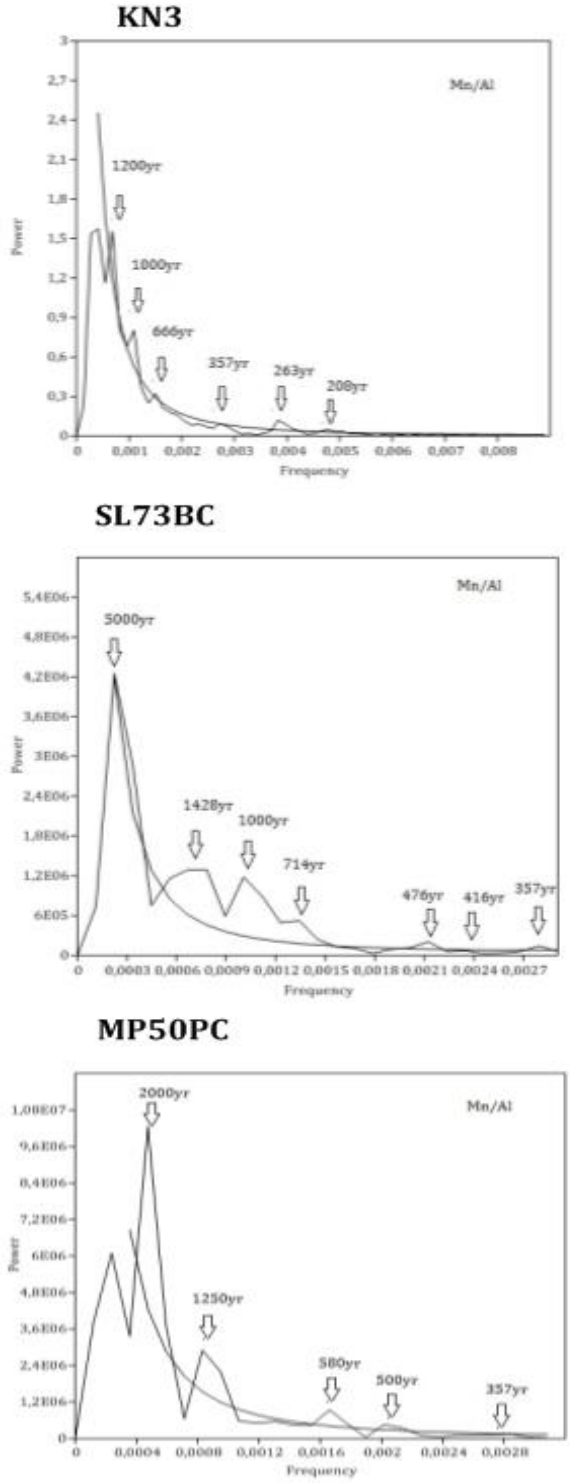

figure A25. Spectral analysis of the Mn/Al ratios from all three cores for the post sapropel S1 interval. The curved lines indicate the 95% confidence interval.

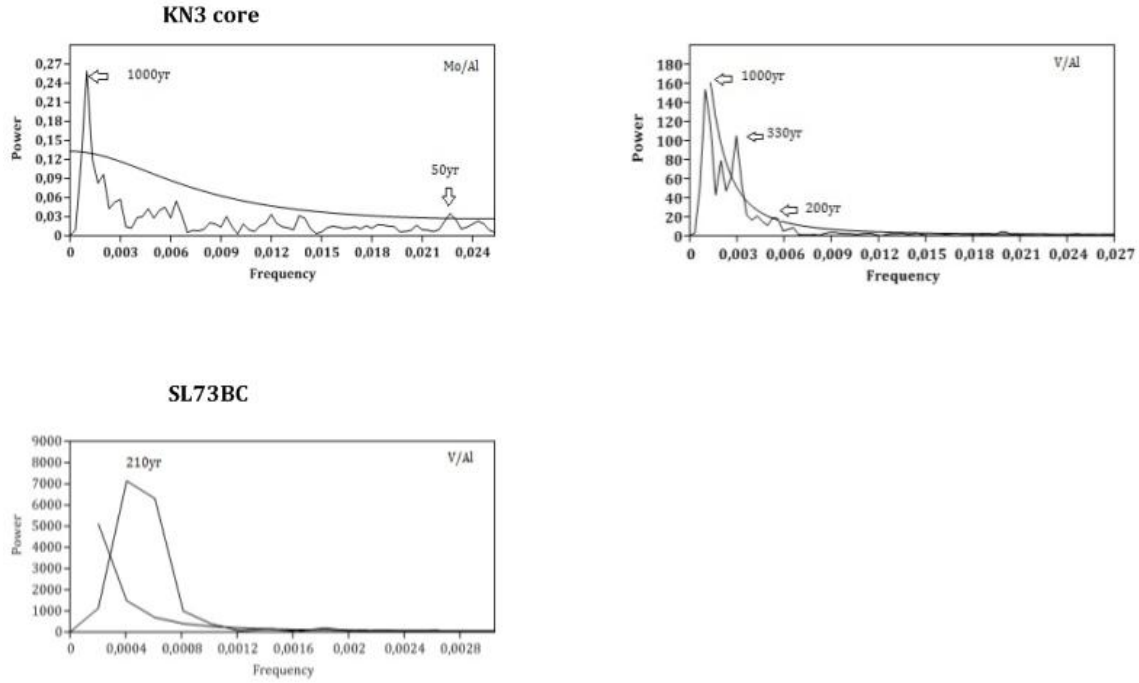

figure A26. Spectral analysis of the V/Al and Mo/Al ratios fromKN3 core and V/Al from SL73BC . The curved lines indicate the 95% confidence interval.